Flavour physics and CP violation: looking forward to the LHC

R. Fleischer
CERN, Geneva, Switzerland

Abstract
The starting point of these lectures is an introduction to the weak interactions of quarks and the Standard-Model description of CP violation, where the central rôle is played by the Cabibbo–Kobayashi–Maskawa matrix and the corresponding unitarity triangles. Since the B-meson system governs the stage of (quark) flavour physics and CP violation, it is our main focus: we shall classify B-meson decays, introduce the theoretical tools to deal with them, investigate the requirements for non-vanishing CP-violating asymmetries, and discuss the main strategies to explore CP violation and the preferred avenues for physics beyond the Standard Model to enter. This formalism allows us then to discuss important benchmark modes, where we shall also address the question of how much space for new-physics effects in the B studies at the LHC is left by the recent experimental results from the B factories and the Tevatron.

1 Introduction

The history of CP violation, i.e. the non-invariance of the weak interactions with respect to a combined charge-conjugation (C) and parity (P) transformation, goes back to the year 1964, where this phenomenon was discovered through the observation of $K_{\rm L} \to \pi^+\pi^-$ decays [1]. This surprising effect is a manifestation of *indirect* CP violation, which arises from the fact that the mass eigenstates $K_{\rm L,S}$ of the neutral kaon system, which shows K^0–$\bar{K}^0$ mixing, are not eigenstates of the CP operator. In particular, the $K_{\rm L}$ state is governed by the CP-odd eigenstate, but has also a tiny admixture of the CP-even eigenstate, which may decay through CP-conserving interactions into the $\pi^+\pi^-$ final state. These CP-violating effects are described by the following observable:

$$\varepsilon_K = (2.280 \pm 0.013) \times 10^{-3} \times e^{i\pi/4}. \tag{1}$$

On the other hand, CP-violating effects may also arise directly at the decay-amplitude level, thereby yielding *direct* CP violation. This phenomenon, which leads to a non-vanishing value of a quantity ${\rm Re}(\varepsilon'_K/\varepsilon_K)$, was eventually established in 1999 through the NA48 (CERN) and KTeV (FNAL) Collaborations [2]; the final results of the corresponding measurements are given by

$${\rm Re}(\varepsilon'_K/\varepsilon_K) = \begin{cases} (14.7 \pm 2.2) \times 10^{-4} & \text{(NA48 [3])} \\ (20.7 \pm 2.8) \times 10^{-4} & \text{(KTeV [4]).} \end{cases} \tag{2}$$

In this decade, there have been huge experimental efforts to further explore CP violation and the quark-flavour sector of the Standard Model (SM). In these studies, the main actor is the B-meson system, where we distinguish between charged and neutral B mesons, which are characterized by the following valence-quark contents:

$$\begin{array}{llll} B^+ \sim u\bar{b}, & B_c^+ \sim c\bar{b}, & B_d^0 \sim d\bar{b}, & B_s^0 \sim s\bar{b}, \\ B^- \sim \bar{u}b, & B_c^- \sim \bar{c}b, & \bar{B}_d^0 \sim \bar{d}b, & \bar{B}_s^0 \sim \bar{s}b. \end{array} \tag{3}$$

In contrast to the charged B mesons, their neutral counterparts B_q ($q \in \{d, s\}$) show — in analogy to K^0–$\bar{K}^0$ mixing — the phenomenon of B_q^0–$\bar{B}_q^0$ mixing. Decays of B mesons are studied at two kinds of experimental facilities. The first are the 'B factories' at SLAC and KEK with the BaBar and Belle

experiments, respectively. These machines are asymmetric e^+e^- colliders that have now produced altogether $\mathcal{O}(10^9)$ $B\bar{B}$ pairs, establishing CP violation in the B system through the 'golden' $B^0_d \to J/\psi K_{\rm S}$ channel in 2001 [5], and leading to many other interesting results. There are currently discussions of a 'super-B factory', with an increase of luminosity by two orders of magnitude with respect to the current machines [6]. Since the B factories are operated at the $\Upsilon(4S)$ resonance, only $B^0_d\bar{B}^0_d$ and $B^+_u B^-_u$ pairs are produced. On the other hand, hadron colliders produce, in addition to B_d and B_u, also B_s mesons,[1] as well as B_c and Λ_b hadrons, and the Tevatron experiments CDF and D0 have reported first $B_{(s)}$-decay results. The physics potential of the B_s-meson system can be fully exploited at the LHC, starting operation in the summer of 2008. Here the general-purpose experiments ATLAS and CMS can also address some B-physics topics. However, these studies are the main target of the dedicated LHCb experiment [8], which will allow us to enter a new territory in the exploration of CP violation. Concerning the kaon system, there are plans to measure the 'rare' kaon decays $K^+ \to \pi^+\nu\bar{\nu}$ and $K_{\rm L} \to \pi^0\nu\bar{\nu}$, which are absent at the tree level in the SM and exhibt extremely tiny branching ratios at the 10^{-10} level, at CERN and J-PARC (for a recent overview, see Ref. [9]).

The main interest in the study of CP violation and flavour physics in general is due to the fact that 'new physics' (NP) typically leads to new patterns in the flavour sector [10]. This is actually the case in several specific extensions of the SM, such as supersymmetry (SUSY) scenarios, left–right-symmetric models, models with extra Z' bosons, scenarios with extra dimensions, or 'little Higgs' models. Moreover, also the evidence for non-zero neutrino masses points towards an origin lying beyond the SM [11], raising questions of having CP violation in the neutrino sector and about connections between lepton- and quark-flavour physics.

Interestingly, CP violation offers also a link to cosmology. One of the key features of our Universe is the cosmological baryon asymmetry of $\mathcal{O}(10^{-10})$ [12]. As was pointed out by Sakharov [13], the necessary conditions for the generation of such an asymmetry include also the requirement that elementary interactions violate CP (and C). Model calculations of the baryon asymmetry indicate, however, that the CP violation present in the SM seems to be too small to generate the observed asymmetry [14]. On the one hand, the required new sources of CP violation could be associated with very high energy scales, as in 'leptogenesis', where new CP-violating effects appear in decays of heavy Majorana neutrinos [15]. On the other hand, new sources of CP violation could also be accessible in the laboratory, as they arise naturally when going beyond the SM, as we have noted above.

Before searching for NP at flavour factories, it is essential to understand first the picture of flavour physics and CP violation arising in the framework of the SM, where the Cabibbo–Kobayashi–Maskawa (CKM) matrix — the quark-mixing matrix — plays the central rôle [16, 17]. The corresponding phenomenology is extremely rich [18]. In general, the key problem for the theoretical interpretation of experimental results is related to strong interactions, i.e. to 'hadronic' uncertainties. A famous example is the observable ${\rm Re}(\varepsilon'_K/\varepsilon_K)$, where we have to deal with a subtle interplay between different contributions which largely cancel [19]. Although the non-vanishing value of this quantity has unambiguously ruled out 'superweak' models of CP violation [20], it currently does not allow a stringent test of the SM.

In the B-meson system, there are various strategies to eliminate the hadronic uncertainties in the exploration of CP violation. Moreover, we may also search for relations and/or correlations that hold in the SM but could well be spoiled by NP contributions. These topics will be the focus of this lecture, which is organized as follows: in Section 2, we discuss the quark mixing in the SM by having a closer look at the CKM matrix and the associated unitarity triangles. In Section 3, we make first contact with weak decays of B mesons, and introduce the theoretical tool of low-energy effective Hamiltonians that is used for the analysis of non-leptonic B-meson decays, representing the key players for the exploration of CP violation. We shall discuss the challenges in these studies, and classify the main strategies to deal with them. Here we shall encounter two major avenues: the use of amplitude relations and the study of CP violation through neutral B decays. In Section 4, we illustrate the former kind of methods, whereas

[1] Recently, data were taken by Belle at $\Upsilon(5S)$, allowing also access to B_s decays [7].

we discuss the features of neutral B_q mesons and B_q^0–$\bar{B}_q^0$ mixing ($q \in \{d, s\}$) in Section 5. In Section 6, we address the question of how NP could enter the B-physics landscape, while we turn to puzzling patterns in the current B-factory data in Section 7. Finally, in Section 8, we have a detailed look at the key targets of the B-physics programme at the LHC, which is characterized by high statistics and the complementarity to the studies at the e^+e^- B factories. The conclusions and a brief outlook are given in Section 9.

For more detailed discussions and textbooks dealing with flavour physics and CP violation, the reader is referred to Refs. [21–24], alternative lecture notes can be found in Refs. [25–27], and a selection of more compact recent reviews is given in Refs. [28–30].

2 CP violation in the Standard Model

2.1 Weak interactions of quarks and the quark-mixing matrix

In the framework of the Standard Model of electroweak interactions [31, 32], which is based on the spontaneously broken gauge group

$$SU(2)_{\rm L} \times U(1)_{\rm Y} \stackrel{\rm SSB}{\longrightarrow} U(1)_{\rm em}, \tag{4}$$

CP-violating effects may originate from the charged-current interactions of quarks, having the structure

$$D \to U W^-. \tag{5}$$

Here $D \in \{d, s, b\}$ and $U \in \{u, c, t\}$ denote down- and up-type quark flavours, respectively, whereas the W^- is the usual $SU(2)_{\rm L}$ gauge boson. From a phenomenological point of view, it is convenient to collect the generic 'coupling strengths' V_{UD} of the charged-current processes in (5) in the form of the following matrix:

$$\hat{V}_{\rm CKM} = \begin{pmatrix} V_{ud} & V_{us} & V_{ub} \\ V_{cd} & V_{cs} & V_{cb} \\ V_{td} & V_{ts} & V_{tb} \end{pmatrix}, \tag{6}$$

which is referred to as the Cabibbo–Kobayashi–Maskawa (CKM) matrix [16, 17].

From a theoretical point of view, this matrix connects the electroweak states (d', s', b') of the down, strange and bottom quarks with their mass eigenstates (d, s, b) through the following unitary transformation [32]:

$$\begin{pmatrix} d' \\ s' \\ b' \end{pmatrix} = \begin{pmatrix} V_{ud} & V_{us} & V_{ub} \\ V_{cd} & V_{cs} & V_{cb} \\ V_{td} & V_{ts} & V_{tb} \end{pmatrix} \cdot \begin{pmatrix} d \\ s \\ b \end{pmatrix}. \tag{7}$$

Consequently, $\hat{V}_{\rm CKM}$ is actually a *unitary* matrix. This feature ensures the absence of flavour-changing neutral-current (FCNC) processes at the tree level in the SM, and is hence at the basis of the famous Glashow–Iliopoulos–Maiani (GIM) mechanism [33]. We shall return to the unitarity of the CKM matrix in Subsection 2.6, discussing the 'unitarity triangles'. If we express the non-leptonic charged-current interaction Lagrangian in terms of the mass eigenstates appearing in (7), we arrive at

$$\mathcal{L}_{\rm int}^{\rm CC} = -\frac{g_2}{\sqrt{2}} \left(\begin{array}{ccc} \bar{u}_{\rm L}, & \bar{c}_{\rm L}, & \bar{t}_{\rm L} \end{array} \right) \gamma^\mu \hat{V}_{\rm CKM} \begin{pmatrix} d_{\rm L} \\ s_{\rm L} \\ b_{\rm L} \end{pmatrix} W_\mu^\dagger \; + \; \text{h.c.}, \tag{8}$$

where the gauge coupling g_2 is related to the gauge group $SU(2)_{\rm L}$, and the $W_\mu^{(\dagger)}$ field corresponds to the charged W bosons. Looking at the interaction vertices following from (8), we observe that the elements of the CKM matrix describe in fact the generic strengths of the associated charged-current processes, as we have noted above.

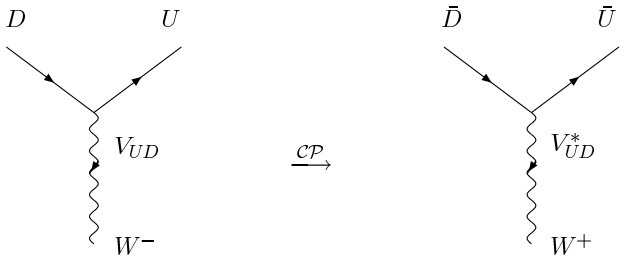

Fig. 1: CP-conjugate charged-current quark-level interaction processes in the SM

In Fig. 1, we show the $D \to UW^-$ vertex and its CP conjugate. Since the corresponding CP transformation involves the replacement

$$V_{UD} \xrightarrow{\mathcal{CP}} V^*_{UD}, \tag{9}$$

CP violation could — in principle — be accommodated in the SM through complex phases in the CKM matrix. The crucial question in this context is, of course, whether we may actually have physical complex phases in that matrix.

2.2 Phase structure of the CKM matrix

We have the freedom of redefining the up- and down-type quark fields in the following way:

$$U \to \exp(i\xi_U)U, \quad D \to \exp(i\xi_D)D. \tag{10}$$

If we perform such transformations in (8), the invariance of the charged-current interaction Lagrangian implies the following phase transformations of the CKM matrix elements:

$$V_{UD} \to \exp(i\xi_U)V_{UD}\exp(-i\xi_D). \tag{11}$$

Using these transformations to eliminate unphysical phases, it can be shown that the parametrization of the general $N \times N$ quark-mixing matrix, where N denotes the number of fermion generations, involves the following parameters:

$$\underbrace{\frac{1}{2}N(N-1)}_{\text{Euler angles}} + \underbrace{\frac{1}{2}(N-1)(N-2)}_{\text{complex phases}} = (N-1)^2. \tag{12}$$

If we apply this expression to the case of $N = 2$ generations, we observe that only one rotation angle — the Cabibbo angle $\theta_{\rm C}$ [16] — is required for the parametrization of the 2×2 quark-mixing matrix, which can be written in the following form:

$$\hat{V}_{\rm C} = \begin{pmatrix} \cos\theta_{\rm C} & \sin\theta_{\rm C} \\ -\sin\theta_{\rm C} & \cos\theta_{\rm C} \end{pmatrix}, \tag{13}$$

where $\sin\theta_{\rm C} = 0.22$ can be determined from $K \to \pi\ell\bar{\nu}$ decays. On the other hand, in the case of $N = 3$ generations, the parametrization of the corresponding 3×3 quark-mixing matrix involves three Euler-type angles and a single *complex* phase. This complex phase allows us to accommodate CP violation in the SM, as was pointed out by Kobayashi and Maskawa in 1973 [17]. The corresponding picture is referred to as the Kobayashi–Maskawa (KM) mechanism of CP violation.

In the 'standard parametrization' advocated by the Particle Data Group (PDG) [34], the three-generation CKM matrix takes the following form:

$$\hat{V}_{\rm CKM} = \begin{pmatrix} c_{12}c_{13} & s_{12}c_{13} & s_{13}e^{-i\delta_{13}} \\ -s_{12}c_{23} - c_{12}s_{23}s_{13}e^{i\delta_{13}} & c_{12}c_{23} - s_{12}s_{23}s_{13}e^{i\delta_{13}} & s_{23}c_{13} \\ s_{12}s_{23} - c_{12}c_{23}s_{13}e^{i\delta_{13}} & -c_{12}s_{23} - s_{12}c_{23}s_{13}e^{i\delta_{13}} & c_{23}c_{13} \end{pmatrix}, \tag{14}$$

where $c_{ij} \equiv \cos\theta_{ij}$ and $s_{ij} \equiv \sin\theta_{ij}$. Performing appropriate redefinitions of the quark-field phases, the real angles θ_{12}, θ_{23} and θ_{13} can all be made to lie in the first quadrant. The advantage of this parametrization is that the generation labels $i, j = 1, 2, 3$ are introduced in such a way that the mixing between two chosen generations vanishes if the corresponding mixing angle θ_{ij} is set to zero. In particular, for $\theta_{23} = \theta_{13} = 0$, the third generation decouples, and the 2×2 submatrix describing the mixing between the first and second generations takes the same form as (13).

Let us finally note that physical observables, for instance CP-violating asymmetries, *cannot* depend on the chosen parametrization of the CKM matrix, i.e., they have to be invariant under the phase transformations specified in (11).

2.3 Further requirements for CP violation

As we have just seen, in order to be able to accommodate CP violation within the framework of the SM through a complex phase in the CKM matrix, at least three generations are required. However, this feature is not sufficient for observable CP-violating effects. To this end, further conditions have to be satisfied, which can be summarized as follows [35, 36]:

$$(m_t^2 - m_c^2)(m_t^2 - m_u^2)(m_c^2 - m_u^2)(m_b^2 - m_s^2)(m_b^2 - m_d^2)(m_s^2 - m_d^2) \times J_{\rm CP} \neq 0\,, \tag{15}$$

where

$$J_{\rm CP} = |{\rm Im}(V_{i\alpha} V_{j\beta} V_{i\beta}^* V_{j\alpha}^*)| \quad (i \neq j,\, \alpha \neq \beta)\,. \tag{16}$$

The mass factors in (15) are related to the fact that the CP-violating phase of the CKM matrix could be eliminated through an appropriate unitary transformation of the quark fields if any two quarks with the same charge had the same mass. Consequently, the origin of CP violation is closely related to the 'flavour problem' in elementary particle physics, and cannot be understood in a deeper way, unless we have fundamental insights into the hierarchy of quark masses and the number of fermion generations.

The second element of (15), the 'Jarlskog parameter' $J_{\rm CP}$ [35], can be interpreted as a measure of the strength of CP violation in the SM. It does not depend on the chosen quark-field parametrization, i.e. it is invariant under (11), and the unitarity of the CKM matrix implies that all combinations $|{\rm Im}(V_{i\alpha} V_{j\beta} V_{i\beta}^* V_{j\alpha}^*)|$ are equal to one another. Using the standard parametrization of the CKM matrix introduced in (14), we obtain

$$J_{\rm CP} = s_{12} s_{13} s_{23} c_{12} c_{23} c_{13}^2 \sin\delta_{13}\,. \tag{17}$$

The experimental information on the CKM parameters implies $J_{\rm CP} = \mathcal{O}(10^{-5})$, so that CP-violating phenomena are hard to observe.

2.4 Experimental information on $|V_{\rm CKM}|$

In order to determine the magnitudes $|V_{ij}|$ of the elements of the CKM matrix, we may use the following tree-level processes:

- Nuclear beta decays, neutron decays $\Rightarrow |V_{ud}|$.
- $K \to \pi \ell \bar{\nu}$ decays $\Rightarrow |V_{us}|$.
- ν production of charm off valence d quarks $\Rightarrow |V_{cd}|$.
- Charm-tagged W decays (as well as ν production and semileptonic D decays) $\Rightarrow |V_{cs}|$.
- Exclusive and inclusive $b \to c \ell \bar{\nu}$ decays $\Rightarrow |V_{cb}|$.
- Exclusive and inclusive $b \to u \ell \bar{\nu}$ decays $\Rightarrow |V_{ub}|$.
- $\bar{t} \to \bar{b} \ell \bar{\nu}$ processes $\Rightarrow$ (crude direct determination of) $|V_{tb}|$.

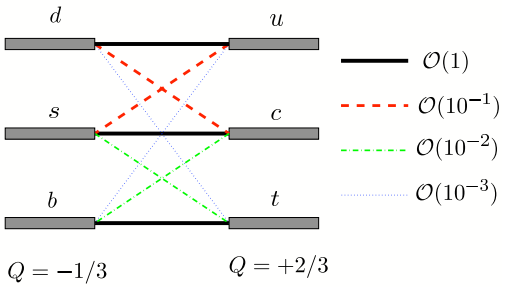

Fig. 2: Hierarchy of the quark transitions mediated through charged-current processes

If we use the corresponding experimental information, together with the CKM unitarity condition, and assume that there are only three generations, the following 90% C.L. limits for the $|V_{ij}|$ emerge [34, 37]:

$$|\hat{V}_{\rm CKM}| = \begin{pmatrix} 0.9739\text{–}0.9751 & 0.221\text{–}0.227 & 0.0029\text{–}0.0045 \\ 0.221\text{–}0.227 & 0.9730\text{–}0.9744 & 0.039\text{–}0.044 \\ 0.0048\text{–}0.014 & 0.037\text{–}0.043 & 0.9990\text{–}0.9992 \end{pmatrix}. \tag{18}$$

In Fig. 2, we have illustrated the resulting hierarchy of the strengths of the charged-current quark-level processes: transitions within the same generation are governed by CKM matrix elements of $\mathcal{O}(1)$, those between the first and the second generation are suppressed by CKM factors of $\mathcal{O}(10^{-1})$, those between the second and the third generation are suppressed by $\mathcal{O}(10^{-2})$, and the transitions between the first and the third generation are even suppressed by CKM factors of $\mathcal{O}(10^{-3})$. In the standard parametrization (14), this hierarchy is reflected by

$$s_{12} = 0.22 \gg s_{23} = \mathcal{O}(10^{-2}) \gg s_{13} = \mathcal{O}(10^{-3}). \tag{19}$$

2.5 Wolfenstein parametrization of the CKM matrix

For phenomenological applications, it would be useful to have a parametrization of the CKM matrix available that makes the hierarchy arising in (18) — and illustrated in Fig. 2 — explicit [38]. In order to derive such a parametrization, we introduce a set of new parameters, λ, A, ρ and η, by imposing the following relations [39]:

$$s_{12} \equiv \lambda = 0.22, \quad s_{23} \equiv A\lambda^2, \quad s_{13}e^{-i\delta_{13}} \equiv A\lambda^3(\rho - i\eta). \tag{20}$$

If we now go back to the standard parametrization (14), we obtain an *exact* parametrization of the CKM matrix as a function of λ (and A, ρ, η), allowing us to expand each CKM element in powers of the small parameter λ. If we neglect terms of $\mathcal{O}(\lambda^4)$, we arrive at the famous 'Wolfenstein parametrization' [38]:

$$\hat{V}_{\rm CKM} = \begin{pmatrix} 1 - \frac{1}{2}\lambda^2 & \lambda & A\lambda^3(\rho - i\eta) \\ -\lambda & 1 - \frac{1}{2}\lambda^2 & A\lambda^2 \\ A\lambda^3(1 - \rho - i\eta) & -A\lambda^2 & 1 \end{pmatrix} + \mathcal{O}(\lambda^4), \tag{21}$$

which makes the hierarchical structure of the CKM matrix very transparent and is an important tool for phenomenological considerations, as we shall see throughout this lecture.

For several applications, next-to-leading order corrections in λ play an important rôle. Using the exact parametrization following from (14) and (20), they can be calculated straightforwardly by expanding each CKM element to the desired accuracy in λ [39, 40]:

$$V_{ud} = 1 - \frac{1}{2}\lambda^2 - \frac{1}{8}\lambda^4 + \mathcal{O}(\lambda^6), \quad V_{us} = \lambda + \mathcal{O}(\lambda^7), \quad V_{ub} = A\lambda^3(\rho - i\,\eta),$$

$$V_{cd} = -\lambda + \frac{1}{2}A^2\lambda^5\left[1 - 2(\rho + i\eta)\right] + \mathcal{O}(\lambda^7),$$
$$V_{cs} = 1 - \frac{1}{2}\lambda^2 - \frac{1}{8}\lambda^4(1 + 4A^2) + \mathcal{O}(\lambda^6), \tag{22}$$
$$V_{cb} = A\lambda^2 + \mathcal{O}(\lambda^8), \quad V_{td} = A\lambda^3\left[1 - (\rho + i\eta)\left(1 - \frac{1}{2}\lambda^2\right)\right] + \mathcal{O}(\lambda^7),$$
$$V_{ts} = -A\lambda^2 + \frac{1}{2}A(1 - 2\rho)\lambda^4 - i\eta A\lambda^4 + \mathcal{O}(\lambda^6), \quad V_{tb} = 1 - \frac{1}{2}A^2\lambda^4 + \mathcal{O}(\lambda^6).$$

It should be noted that

$$V_{ub} \equiv A\lambda^3(\rho - i\eta) \tag{23}$$

receives *by definition* no power corrections in λ within this prescription. If we follow Ref. [39] and introduce the generalized Wolfenstein parameters

$$\bar{\rho} \equiv \rho\left(1 - \frac{1}{2}\lambda^2\right), \quad \bar{\eta} \equiv \eta\left(1 - \frac{1}{2}\lambda^2\right), \tag{24}$$

we may simply write, up to corrections of $\mathcal{O}(\lambda^7)$,

$$V_{td} = A\lambda^3(1 - \bar{\rho} - i\,\bar{\eta}). \tag{25}$$

Moreover, we have to an excellent accuracy

$$V_{us} = \lambda \quad \text{and} \quad V_{cb} = A\lambda^2, \tag{26}$$

as these quantities receive only corrections at the λ^7 and λ^8 levels, respectively. In comparison with other generalizations of the Wolfenstein parametrization found in the literature, the advantage of (22) is the absence of relevant corrections to V_{us} and V_{cb}, and that V_{ub} and V_{td} take forms similar to those in (21). As far as the Jarlskog parameter introduced in (16) is concerned, we obtain the simple expression

$$J_{\rm CP} = \lambda^6 A^2\eta, \tag{27}$$

which should be compared with (17).

2.6 Unitarity triangles of the CKM matrix

The unitarity of the CKM matrix, which is described by

$$\hat{V}_{\rm CKM}^{\dagger} \cdot \hat{V}_{\rm CKM} = \hat{1} = \hat{V}_{\rm CKM} \cdot \hat{V}_{\rm CKM}^{\dagger}, \tag{28}$$

leads to a set of 12 equations, consisting of 6 normalization and 6 orthogonality relations. The latter can be represented as 6 triangles in the complex plane [41], all having the same area, $2A_\Delta = J_{\rm CP}$ [42]. Let us now have a closer look at these relations: those describing the orthogonality of different columns of the CKM matrix are given by

$$\underbrace{V_{ud}V_{us}^*}_{\mathcal{O}(\lambda)} + \underbrace{V_{cd}V_{cs}^*}_{\mathcal{O}(\lambda)} + \underbrace{V_{td}V_{ts}^*}_{\mathcal{O}(\lambda^5)} = 0 \tag{29}$$
$$\underbrace{V_{us}V_{ub}^*}_{\mathcal{O}(\lambda^4)} + \underbrace{V_{cs}V_{cb}^*}_{\mathcal{O}(\lambda^2)} + \underbrace{V_{ts}V_{tb}^*}_{\mathcal{O}(\lambda^2)} = 0 \tag{30}$$
$$\underbrace{V_{ud}V_{ub}^*}_{(\rho+i\eta)A\lambda^3} + \underbrace{V_{cd}V_{cb}^*}_{-A\lambda^3} + \underbrace{V_{td}V_{tb}^*}_{(1-\rho-i\eta)A\lambda^3} = 0, \tag{31}$$

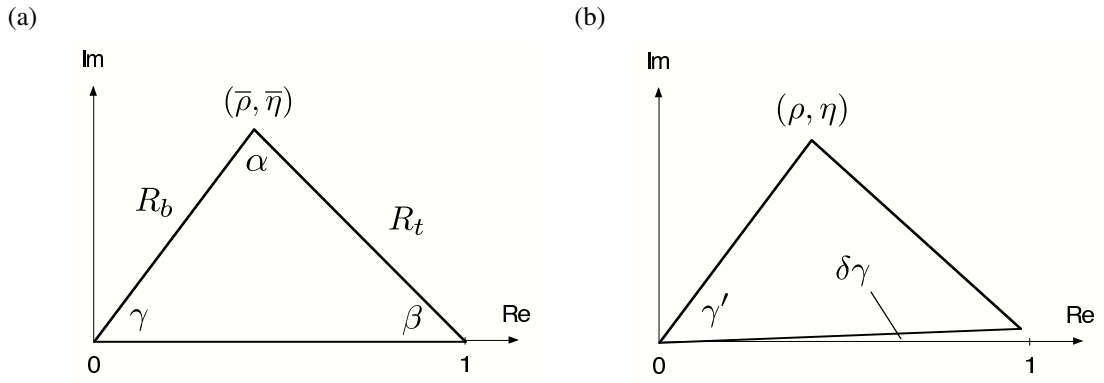

Fig. 3: The two non-squashed unitarity triangles of the CKM matrix, as explained in the text: (a) and (b) correspond to the orthogonality relations (31) and (34), respectively. In Asia, the notation $\phi_1 \equiv \beta$, $\phi_2 \equiv \alpha$ and $\phi_3 \equiv \gamma$ is used for the angles of the triangle shown in (a).

whereas those associated with the orthogonality of different rows take the following form:

$$\underbrace{V_{ud}^* V_{cd}}_{\mathcal{O}(\lambda)} + \underbrace{V_{us}^* V_{cs}}_{\mathcal{O}(\lambda)} + \underbrace{V_{ub}^* V_{cb}}_{\mathcal{O}(\lambda^5)} = 0 \tag{32}$$

$$\underbrace{V_{cd}^* V_{td}}_{\mathcal{O}(\lambda^4)} + \underbrace{V_{cs}^* V_{ts}}_{\mathcal{O}(\lambda^2)} + \underbrace{V_{cb}^* V_{tb}}_{\mathcal{O}(\lambda^2)} = 0 \tag{33}$$

$$\underbrace{V_{ud}^* V_{td}}_{(1-\rho-i\eta)A\lambda^3} + \underbrace{V_{us}^* V_{ts}}_{-A\lambda^3} + \underbrace{V_{ub}^* V_{tb}}_{(\rho+i\eta)A\lambda^3} = 0. \tag{34}$$

Here we have also indicated the structures that arise if we apply the Wolfenstein parametrization by keeping just the leading, non-vanishing terms. We observe that only in (31) and (34), which describe the orthogonality of the first and third columns and of the first and third rows, respectively, are all three sides of comparable magnitude, $\mathcal{O}(\lambda^3)$, while in the remaining relations, one side is suppressed with respect to the others by factors of $\mathcal{O}(\lambda^2)$ or $\mathcal{O}(\lambda^4)$. Consequently, we have to deal with only *two* non-squashed unitarity triangles in the complex plane. However, as we have already indicated in (31) and (34), the corresponding orthogonality relations agree with each other at the λ^3 level, yielding

$$\left[(\rho + i\eta) + (-1) + (1 - \rho - i\eta)\right] A\lambda^3 = 0. \tag{35}$$

Consequently, they describe the same triangle, which is usually referred to as *the* unitarity triangle of the CKM matrix [42, 43].

Concerning the B-decay studies in the LHC era, we have to take the next-to-leading-order terms of the Wolfenstein expansion into account, and have to distinguish between the unitarity triangles following from (31) and (34). Let us first have a closer look at the former relation. Including terms of $\mathcal{O}(\lambda^5)$, we obtain the following generalization of (35):

$$\left[(\bar{\rho} + i\bar{\eta}) + (-1) + (1 - \bar{\rho} - i\bar{\eta})\right] A\lambda^3 + \mathcal{O}(\lambda^7) = 0, \tag{36}$$

where $\bar{\rho}$ and $\bar{\eta}$ are as defined in (24). If we divide this relation by the overall normalization factor $A\lambda^3$, and introduce

$$R_b \equiv \sqrt{\overline{\rho}^2 + \overline{\eta}^2} = \left(1 - \frac{\lambda^2}{2}\right) \frac{1}{\lambda} \left|\frac{V_{ub}}{V_{cb}}\right| \tag{37}$$

$$R_t \equiv \sqrt{(1 - \overline{\rho})^2 + \overline{\eta}^2} = \frac{1}{\lambda} \left|\frac{V_{td}}{V_{cb}}\right|, \tag{38}$$

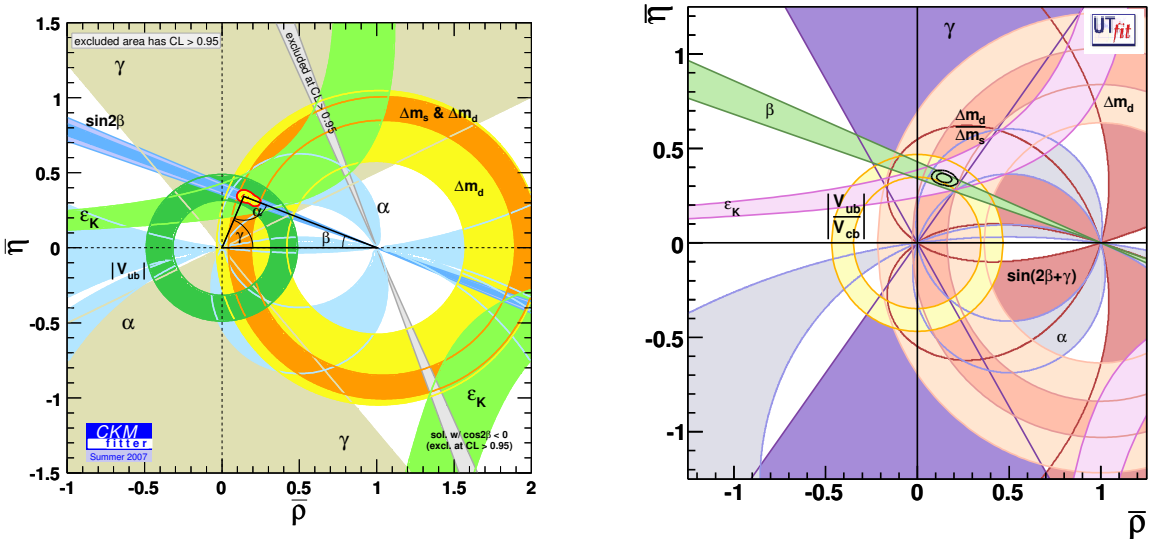

Fig. 4: Analyses of the CKMfitter (left panel) and UTfit (right panel) Collaborations [44, 45]

we arrive at the unitarity triangle illustrated in Fig. 3 (a). It is a straightforward generalization of the leading-order case described by (35): instead of (ρ, η), the apex is now simply given by $(\bar{\rho}, \bar{\eta})$ [39]. The two UT sides R_b and R_t as well as the UT angles will show up at several places throughout this lecture. Moreover, the relations

$$V_{ub} = A\lambda^3 \left(\frac{R_b}{1-\lambda^2/2}\right) e^{-i\gamma}, \quad V_{td} = A\lambda^3 R_t e^{-i\beta} \tag{39}$$

are also useful for phenomenological applications, since they make the dependences of γ and β explicit; they correspond to the phase convention chosen both in the standard parametrization (14) and in the generalized Wolfenstein parametrization (22). Finally, if we take also (20) into account, we obtain

$$\delta_{13} = \gamma. \tag{40}$$

Let us now turn to (34). Here we arrive at an expression that is more complicated than (36):

$$\left[\left\{1 - \frac{\lambda^2}{2} - (1-\lambda^2)\rho - i(1-\lambda^2)\eta\right\} + \left\{-1 + \left(\frac{1}{2} - \rho\right)\lambda^2 - i\eta\lambda^2\right\} + \{\rho + i\eta\}\right] A\lambda^3 + \mathcal{O}(\lambda^7) = 0. \tag{41}$$

If we divide again by $A\lambda^3$, we obtain the unitarity triangle sketched in Fig. 3 (b), where the apex is given by (ρ, η) and *not* by $(\bar{\rho}, \bar{\eta})$. On the other hand, we encounter a tiny angle

$$\delta\gamma \equiv \lambda^2\eta = \mathcal{O}(1^\circ) \tag{42}$$

between real axis and basis of the triangle, which satisfies

$$\gamma = \gamma' + \delta\gamma, \tag{43}$$

where γ coincides with the corresponding angle in Fig. 3 (a).

Whenever referring to a 'unitarity triangle' (UT) in the following discussion, we mean the one illustrated in Fig. 3 (a), which is the generic generalization of the leading-order case described by (35). The UT is a central target for the experimental testing of the SM description of CP violation. Interestingly, also the tiny angle $\delta\gamma$ can be probed directly through certain CP-violating effects that can be explored at the LHCb experiment, as we shall see in Section 8.

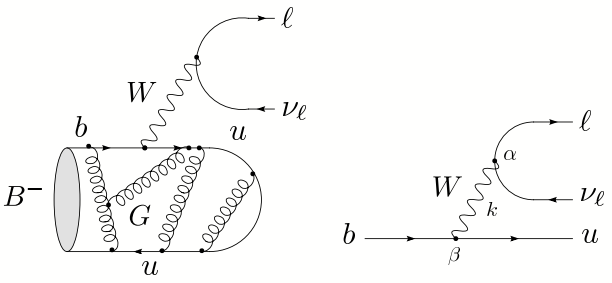

Fig. 5: Feynman diagrams contributing to the leptonic decay $B^- \to \ell\bar{\nu}_\ell$

2.7 The determination of the unitarity triangle

The next obvious question is how the UT can be determined. There are two conceptually different avenues that we may follow to this end:

(i) In the 'CKM fits', theory is used to convert experimental data into contours in the $\bar{\rho}$–$\bar{\eta}$ plane. In particular, semileptonic $b \to u\ell\bar{\nu}_\ell$, $c\ell\bar{\nu}_\ell$ decays and B_q^0–$\bar{B}_q^0$ mixing ($q \in \{d, s\}$) allow us to determine the UT sides R_b and R_t, respectively, i.e. to fix two circles in the $\bar{\rho}$–$\bar{\eta}$ plane. Furthermore, the indirect CP violation in the neutral kaon system described by ε_K can be transformed into a hyperbola.

(ii) Theoretical considerations allow us to convert measurements of CP-violating effects in B-meson decays into direct information on the UT angles. The most prominent example is the determination of $\sin 2\beta$ through CP violation in $B_d^0 \to J/\psi K_{\rm S}$ decays, but several other strategies have been proposed and can be confronted with the experimental data.

The goal is to 'overconstrain' the UT as much as possible. Additional contours can be fixed in the $\bar{\rho}$–$\bar{\eta}$ plane through the measurement of rare decays [21].

In Fig. 4, we show examples of the comprehensive analyses of the UT that are being performed — and continuously updated — by the 'CKM Fitter Group' [44] and the 'UTfit Collaboration' [45]. In these figures, we can see the circles that are determined through the semileptonic B decays and the ε_K hyperbolas. Moreover, the straight lines following from the direct measurement of $\sin 2\beta$ with the help of $B_d^0 \to J/\psi K_{\rm S}$ modes are also shown. We observe that the global consistency is very good. However, on looking closer, we also see that the average for $(\sin 2\beta)_{\psi K_{\rm S}}$ is now on the lower side, so that the situation in the $\bar{\rho}$–$\bar{\eta}$ plane is no longer fully 'perfect'. Furthermore, as we shall discuss in detail in Section 7, there are certain puzzling patterns in the B-factory data, and various key aspects have not yet been addressed experimentally and are hence still essentially unexplored. Consequently, still a lot of space is left for the detection of possible, unambiguous inconsistencies with respect to the SM picture of CP violation and quark-flavour physics. Since weak decays of B mesons play a key rôle in this adventure, let us next have a closer look at them.

3 Weak decays of B mesons

The B-meson system consists of charged and neutral B mesons, which are characterized by the valence quark contents in (3). The characteristic feature of the neutral B_q ($q \in \{d, s\}$) mesons is the phenomenon of B_q^0–$\bar{B}_q^0$ mixing, which will be discussed in Section 5. As far as the weak decays of B mesons are concerned, we distinguish between leptonic, semileptonic, and non-leptonic transitions.

3.1 Leptonic decays

The simplest B-meson decay class is given by leptonic decays of the kind $B^- \to \ell\bar{\nu}_\ell$, as illustrated in Fig. 5. If we evaluate the corresponding Feynman diagram, we arrive at the following transition

amplitude:

$$T_{fi} = -\frac{g_2^2}{8} V_{ub} \underbrace{[\bar{u}_\ell \gamma^\alpha (1-\gamma_5) v_\nu]}_{\text{Dirac spinors}} \left[\frac{g_{\alpha\beta}}{k^2 - M_W^2}\right] \underbrace{\langle 0|\bar{u}\gamma^\beta(1-\gamma_5)b|B^-\rangle}_{\text{hadronic ME}}, \tag{44}$$

where g_2 is the $SU(2)_{\rm L}$ gauge coupling, V_{ub} the corresponding element of the CKM matrix, α and β are Lorentz indices, and M_W denotes the mass of the W gauge boson. Since the four-momentum k that is carried by the W satisfies $k^2 = M_B^2 \ll M_W^2$, we may write

$$\frac{g_{\alpha\beta}}{k^2 - M_W^2} \quad \longrightarrow \quad -\frac{g_{\alpha\beta}}{M_W^2} \equiv -\left(\frac{8 G_{\rm F}}{\sqrt{2} g_2^2}\right) g_{\alpha\beta}, \tag{45}$$

where $G_{\rm F}$ is Fermi's constant. Consequently, we may 'integrate out' the W boson in (44), which yields

$$T_{fi} = \frac{G_{\rm F}}{\sqrt{2}} V_{ub} \, [\bar{u}_\ell \gamma^\alpha (1-\gamma_5) v_\nu] \, \langle 0|\bar{u}\gamma_\alpha(1-\gamma_5)b|B^-\rangle. \tag{46}$$

In this simple expression, *all* the hadronic physics is encoded in the *hadronic matrix element*

$$\langle 0|\bar{u}\gamma_\alpha(1-\gamma_5)b|B^-\rangle,$$

i.e. there are no other strong-interaction QCD effects (for a detailed discussion of QCD, see Ref. [46]). Since the B^- meson is a pseudoscalar particle, we have

$$\langle 0|\overline{u}\gamma_\alpha b|B^-\rangle = 0, \tag{47}$$

and may write

$$\langle 0|\bar{u}\gamma_\alpha\gamma_5 b|B^-(q)\rangle = i f_B q_\alpha, \tag{48}$$

where f_B is the B-meson *decay constant*, which is an important input for phenomenological studies. In order to determine this quantity, which is a very challenging task, non-perturbative techniques, such as QCD sum-rule analyses [47] or lattice studies, where a numerical evaluation of the QCD path integral is performed with the help of a space-time lattice [48–50], are required. If we use (46) with (47) and (48), and perform the corresponding phase-space integrations, we obtain the following decay rate:

$$\Gamma(B^- \to \ell\bar{\nu}_\ell) = \frac{G_{\rm F}^2}{8\pi} M_B m_\ell^2 \left(1 - \frac{m_\ell^2}{M_B^2}\right)^2 f_B^2 |V_{ub}|^2, \tag{49}$$

where M_B and m_ℓ denote the masses of the B^- and ℓ, respectively. Because of the tiny value of $|V_{ub}| \propto \lambda^3$ and a helicity-suppression mechanism, we obtain unfortunately very small branching ratios of $\mathcal{O}(10^{-10})$ and $\mathcal{O}(10^{-7})$ for $\ell = e$ and $\ell = \mu$, respectively [51].

The helicity suppression is not effective for $\ell = \tau$, but — because of the required τ reconstruction — these modes are also very challenging from an experimental point of view. Nevertheless, the Belle experiment has recently reported the first evidence for the purely leptonic decay $B^- \to \tau^-\bar{\nu}_\tau$, with the following branching ratio [52]:

$$\text{BR}(B^- \to \tau^-\bar{\nu}_\tau) = \left[1.79^{+0.56}_{-0.49}\,(\text{stat})\,^{+0.46}_{-0.51}\,(\text{syst})\right] \times 10^{-4}, \tag{50}$$

which corresponds to a significance of about 3.5 standard deviations. On the other hand, BaBar gives an upper limit of $\text{BR}(B^- \to \tau^-\bar{\nu}_\tau) < 1.8 \times 10^{-4}$ (90% C.L.), as well as the following value [53]:

$$\text{BR}(B^- \to \tau^-\bar{\nu}_\tau) = \left[0.88^{+0.68}_{-0.67}\,(\text{stat}) \pm 0.11\,(\text{syst})\right] \times 10^{-4}. \tag{51}$$

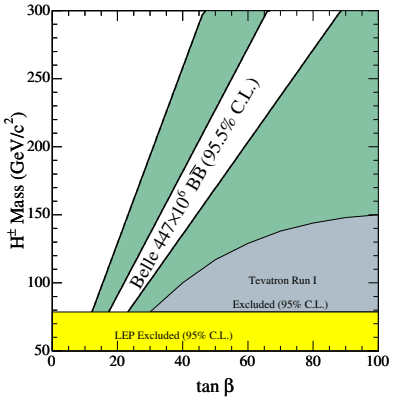

Fig. 6: Constrains on the charged Higgs parameter space [55]

Using the SM expression for this branching ratio and the measured values of $G_{\rm F}$, M_B, m_τ and the B-meson lifetime, the product of the B-meson decay constant f_B and the magnitude of the CKM matrix element $|V_{ub}|$ is obtained as

$$f_B|V_{ub}| = \left[10.1^{+1.6}_{-1.4}\,({\rm stat})\,^{+1.3}_{-1.4}\,({\rm syst})\right] \times 10^{-4}\,{\rm GeV} \tag{52}$$

from the Belle result. The determination of this quantity is very interesting, as knowledge of $|V_{ub}|$ (see Subsection 3.2) allows us to extract f_B, thereby providing tests of non-perturbative calculations of this important parameter. On the other hand, when going beyond the SM, the $B^- \to \tau^-\bar{\nu}_\tau$ decay is a sensitive probe of effects from charged Higgs bosons; the corresponding Feynman diagram can easily be obtained from Fig. 5 by replacing the W boson through a charged Higgs H. The SM expression for the branching ratio is then simply modified by the following factor [54]:

$$r_H = \left[1 - \left(\frac{M_B}{M_H}\tan\beta\right)^2\right]^2 \stackrel{\rm Belle}{\longrightarrow} 1.13 \pm 0.53, \tag{53}$$

where $\tan\beta \equiv v_2/v_1$ is defined through the ratio of vacuum expectation values and does *not* involve the UT angle β. Using information on f_B and $|V_{ub}|$, constraints on the charged Higgs parameter space can be obtained from the measured $B^- \to \tau^-\bar{\nu}_\tau$ branching ratio, as shown in Fig. 6.

Before discussing the determination of $|V_{ub}|$ from semileptonic B decays in the next subsection, let us have a look at the leptonic D-meson decay $D^+ \to \mu^+\nu$. It is governed by the CKM factor

$$|V_{cd}| = |V_{us}| + \mathcal{O}(\lambda^5) = \lambda[1 + \mathcal{O}(\lambda^4)], \tag{54}$$

whereas $B^- \to \mu^-\bar{\nu}$ involves $|V_{ub}| = \lambda^3 R_b$. Consequently, we win a factor of $\mathcal{O}(\lambda^4)$ in the decay rate, so that $D^+ \to \mu^+\nu$ is accessible at the CLEO-c experiment [56]. Since the corresponding CKM factor is well known, the decay constant f_{D^+} defined in analogy to (48) can be extracted, allowing another interesting testing ground for lattice QCD calculations. Thanks to recent progress in these techniques [57], the 'quenched' approximation, which had to be applied for many many years and ignores quark loops, is no longer required for the calculation of f_{D^+}. In the summer of 2005, there was a first show-down between the corresponding theoretical prediction and experiment: the lattice result of $f_{D^+} = (201 \pm 3 \pm 17)$MeV was reported [58], while CLEO-c announced the measurement of $f_{D^+} = (222.6 \pm 16.7^{+2.8}_{-3.4})$ MeV [59]. Both numbers agree well within the uncertainties. For a review of recent developments and other results on decay constants of pseudoscalar mesons, see Ref. [60].

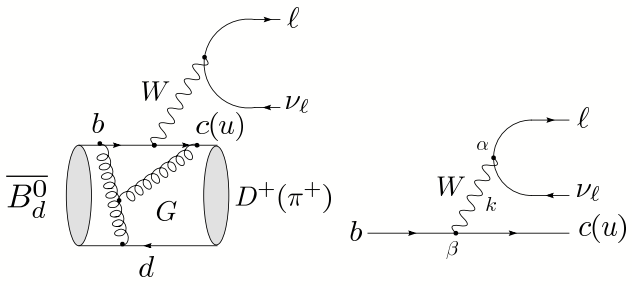

Fig. 7: Feynman diagrams contributing to semileptonic $\bar{B}_d^0 \to D^+(\pi^+)\ell\bar{\nu}_\ell$ decays

3.2 Semileptonic decays

3.2.1 General structure

Semileptonic B-meson decays of the kind shown in Fig. 7 have a structure that is more complicated than the one of the leptonic transitions. If we evaluate the corresponding Feynman diagram for the $b \to c$ case, we obtain

$$T_{fi} = -\frac{g_2^2}{8} V_{cb} \underbrace{[\bar{u}_\ell \gamma^\alpha (1-\gamma_5) v_\nu]}_{\text{Dirac spinors}} \left[\frac{g_{\alpha\beta}}{k^2 - M_W^2}\right] \underbrace{\langle D^+ | \bar{c}\gamma^\beta (1-\gamma_5) b | \bar{B}_d^0 \rangle}_{\text{hadronic ME}}. \tag{55}$$

Because of $k^2 \sim M_B^2 \ll M_W^2$, we may again — as in (44) — integrate out the W boson with the help of (45), which yields

$$T_{fi} = \frac{G_{\rm F}}{\sqrt{2}} V_{cb} \, [\bar{u}_\ell \gamma^\alpha (1-\gamma_5) v_\nu] \, \langle D^+ | \bar{c}\gamma_\alpha (1-\gamma_5) b | \bar{B}_d^0 \rangle, \tag{56}$$

where *all* the hadronic physics is encoded in the hadronic matrix element

$$\langle D^+ | \bar{c}\gamma_\alpha (1-\gamma_5) b | \bar{B}_d^0 \rangle,$$

i.e. there are *no* other QCD effects. Since the $\bar{B}_d^0$ and D^+ are pseudoscalar mesons, we have

$$\langle D^+ | \bar{c}\gamma_\alpha \gamma_5 b | \bar{B}_d^0 \rangle = 0, \tag{57}$$

and may write

$$\langle D^+(k) | \bar{c}\gamma_\alpha b | \bar{B}_d^0(p) \rangle = F_1(q^2) \left[(p+k)_\alpha - \left(\frac{M_B^2 - M_D^2}{q^2}\right) q_\alpha\right] + F_0(q^2) \left(\frac{M_B^2 - M_D^2}{q^2}\right) q_\alpha, \tag{58}$$

where $q \equiv p - k$, and the $F_{1,0}(q^2)$ denote the *form factors* of the $\bar{B} \to D$ transitions. Consequently, in contrast to the simple case of the leptonic transitions, semileptonic decays involve *two* hadronic form factors instead of the decay constant f_B. In order to calculate these parameters, which depend on the momentum transfer q, again non-perturbative techniques (QCD sum rules, lattice, etc.) are required.

3.2.2 Aspects of the heavy-quark effective theory

If the mass m_Q of a quark Q is much larger than the QCD scale parameter $\Lambda_{\rm QCD} = \mathcal{O}(100\,\text{MeV})$, it is referred to as a 'heavy' quark. Since the bottom and charm quarks have masses at the level of 5 GeV and 1 GeV, respectively, they belong to this important category. As far as the extremely heavy top quark, with $m_t \sim 170\,\text{GeV}$ is concerned, it decays unfortunately through weak interactions before a hadron can be formed. Let us now consider a heavy quark that is bound inside a hadron, i.e. a bottom or a charm

quark. The heavy quark then moves almost with the hadron's four velocity v and is almost on-shell, so that

$$p_Q^\mu = m_Q v^\mu + k^\mu, \tag{59}$$

where $v^2 = 1$ and $k \ll m_Q$ is the 'residual' momentum. Owing to the interactions of the heavy quark with the light degrees of freedom of the hadron, the residual momentum may only change by $\Delta k \sim \Lambda_{\rm QCD}$, and $\Delta v \to 0$ for $\Lambda_{\rm QCD}/m_Q \to 0$.

It is now instructive to have a look at the elastic scattering process $\bar{B}(v) \to \bar{B}(v')$ in the limit of $\Lambda_{\rm QCD}/m_b \to 0$, which is characterized by the following matrix element:

$$\frac{1}{M_B}\langle \bar{B}(v')|\bar{b}_{v'}\gamma_\alpha b_v|\bar{B}(v)\rangle = \xi(v'\cdot v)(v+v')_\alpha. \tag{60}$$

Since the contraction of this matrix element with $(v-v')^\alpha$ has to vanish because of $\not{v} b_v = b_v$ and $\overline{b}_v \not{v}' = \overline{b}_{v'}$, no $(v-v')_\alpha$ term arises in the parametrization in (60). On the other hand, the $1/M_B$ factor is related to the normalization of states, i.e. the right-hand side of

$$\left(\frac{1}{\sqrt{M_B}}\langle \bar{B}(p')|\right)\left(|\bar{B}(p)\rangle\frac{1}{\sqrt{M_B}}\right) = 2v^0(2\pi)^3\delta^3(\vec{p}-\vec{p}') \tag{61}$$

does not depend on M_B. Finally, current conservation implies the following normalization condition:

$$\xi(v'\cdot v = 1) = 1, \tag{62}$$

where the 'Isgur–Wise' function $\xi(v'\cdot v)$ does *not* depend on the flavour of the heavy quark (heavy-quark symmetry) [61]. Consequently, for $\Lambda_{\rm QCD}/m_{b,c} \to 0$, we may write

$$\frac{1}{\sqrt{M_D M_B}}\langle D(v')|\bar{c}_{v'}\gamma_\alpha b_v|\bar{B}(v)\rangle = \xi(v'\cdot v)(v+v')_\alpha, \tag{63}$$

and observe that this transition amplitude is governed — in the heavy-quark limit — by *one* hadronic form factor $\xi(v'\cdot v)$, which satisfies $\xi(1) = 1$. If we now compare (63) with (58), we obtain

$$F_1(q^2) = \frac{M_D + M_B}{2\sqrt{M_D M_B}}\xi(w) \tag{64}$$

$$F_0(q^2) = \frac{2\sqrt{M_D M_B}}{M_D + M_B}\left[\frac{1+w}{2}\right]\xi(w), \tag{65}$$

with

$$w \equiv v_D \cdot v_B = \frac{M_D^2 + M_B^2 - q^2}{2M_D M_B}. \tag{66}$$

Similar relations hold for the $\bar{B} \to D^*$ form factors because of the heavy-quark spin symmetry, since the D^* is related to the D by a rotation of the heavy-quark spin. A detailed discussion of these interesting features and the associated 'heavy-quark effective theory' (HQET) is beyond the scope of this lecture. For a detailed overview, we refer the reader to Ref. [62], where a comprehensive list of original references can also be found. For a more phenomenological discussion, Ref. [63] is very useful.

3.2.3 Applications

An important application of the formalism sketched above is the extraction of the CKM element $|V_{cb}|$. To this end, $\bar{B} \to D^* \ell \bar{\nu}$ decays are particularly promising. The corresponding rate can be written as

$$\frac{{\rm d}\Gamma}{{\rm d}w} = G_{\rm F}^2 K(M_B, M_{D^*}, w) F(w)^2 |V_{cb}|^2, \tag{67}$$

where $K(M_B, M_{D^*}, w)$ is a known kinematic function, and $F(w)$ agrees with the Isgur–Wise function, up to perturbative QCD corrections and $\Lambda_{\rm QCD}/m_{b,c}$ terms. The form factor $F(w)$ is a non-perturbative quantity. However, it satisfies the following normalization condition:

$$F(1) = \eta_A(\alpha_s)\left[1 + \frac{0}{m_c} + \frac{0}{m_b} + \mathcal{O}(\Lambda^2_{\rm QCD}/m^2_{b,c})\right], \tag{68}$$

where $\eta_A(\alpha_s)$ is a perturbatively calculable short-distance QCD factor, and the $\Lambda_{\rm QCD}/m_{b,c}$ corrections *vanish* [62, 64]. The important latter feature is an implication of Luke's theorem [65]. Consequently, if we extract $F(w)|V_{cb}|$ from a measurement of (67) as a function of w and extrapolate to the 'zero-recoil point' $w = 1$ (where the rate vanishes), we may determine $|V_{cb}|$. In the case of $\bar{B} \to D\ell\bar{\nu}$ decays, we have $\mathcal{O}(\Lambda_{\rm QCD}/m_{b,c})$ corrections to the corresponding rate $\mathrm{d}\Gamma/\mathrm{d}w$ at $w = 1$. In order to determine $|V_{cb}|$, inclusive $B \to X_c\ell\bar{\nu}$ decays offer also very attractive avenues. As becomes obvious from (26) and the considerations in Subsection 2.6, $|V_{cb}|$ fixes the normalization of the UT. Moreover, this quantity is an important input parameter for various theoretical calculations. The CKM matrix element $|V_{cb}|$ is currently known with about 2% precision; performing an analysis of leptonic and hadronic moments in inclusive $b \to c\ell\bar{\nu}$ processes [66], the following value was extracted from the B-factory data [67]:

$$|V_{cb}| = (42.0 \pm 0.7) \times 10^{-3}, \tag{69}$$

which agrees with that from exclusive decays.

Let us now turn to $\bar{B} \to \pi\ell\bar{\nu}, \rho\ell\bar{\nu}$ decays, which originate from $b \to u\ell\bar{\nu}$ quark-level processes, as can be seen in Fig. 7, and provide access to $|V_{ub}|$. If we complement this CKM matrix element with $|V_{cb}|$, we may determine the UT side R_b with the help of (37). The determination of $|V_{ub}|$ is hence a very important aspect of flavour physics. Since the π and ρ are 'light' mesons, the HQET symmetry relations cannot be applied to the $\bar{B} \to \pi\ell\bar{\nu}, \rho\ell\bar{\nu}$ modes. Consequently, in order to determine $|V_{ub}|$ from these exclusive channels, the corresponding heavy-to-light form factors have to be described by models. An important alternative is provided by inclusive decays. The corresponding decay rate takes the following form:

$$\Gamma(\bar{B} \to X_u\ell\bar{\nu}) = \frac{G_{\rm F}^2|V_{ub}|^2}{192\pi^3} m_b^5 \left[1 - 2.41\frac{\alpha_s}{\pi} + \frac{\lambda_1 - 9\lambda_2}{2m_b^2} + \ldots\right], \tag{70}$$

where λ_1 and λ_2 are non-perturbative parameters, which describe the hadronic matrix elements of certain 'kinetic' and 'chromomagnetic' operators appearing within the framework of the HQET. Using the heavy-quark expansions

$$M_B = m_b + \bar{\Lambda} - \frac{\lambda_1 + 3\lambda_2}{2m_b} + \ldots, \quad M_{B^*} = m_b + \bar{\Lambda} - \frac{\lambda_1 - \lambda_2}{2m_b} + \ldots \tag{71}$$

for the $B^{(*)}$-meson masses, where $\bar{\Lambda} \sim \Lambda_{\rm QCD}$ is another non-perturbative parameter that is related to the light degrees of freedom, the parameter λ_2 can be determined from the measured values of the $M_{B^{(*)}}$. The strong dependence of (70) on m_b is a significant source of uncertainty. On the other hand, the $1/m_b^2$ corrections can be better controlled than in the exclusive case (68), where we have, moreover, to deal with $1/m_c^2$ corrections. From an experimental point of view, we have to struggle with large backgrounds, which originate from $b \to c\ell\bar{\nu}$ processes and require also a model-dependent treatment. The determination of $|V_{ub}|$ from B-meson decays caused by $b \to u\ell\bar{\nu}$ quark-level processes is therefore a very challenging issue, and the situation is less favourable than with $|V_{cb}|$ [68]. In particular, the values from inclusive and exclusive transitions differ at the $1\,\sigma$ level [69]:

$$|V_{ub}|_{\rm incl} = (4.4 \pm 0.3) \times 10^{-3}\,, \quad |V_{ub}|_{\rm excl} = (3.8 \pm 0.6) \times 10^{-3}\,, \tag{72}$$

which has to be fully settled in the future. The error on $|V_{ub}|_{\rm excl}$ is dominated by the theoretical uncertainty of lattice and light-cone sum rule calculations of $B \to \pi$ and $B \to \rho$ transition form factors [70, 71], whereas for $|V_{ub}|_{\rm incl}$ experimental and theoretical errors are at par. Using the values of $|V_{cb}|$

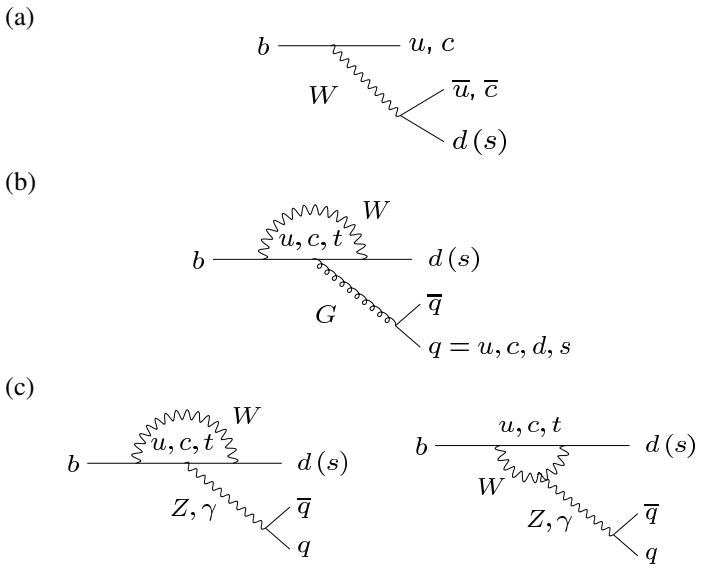

Fig. 8: Feynman diagrams of the topologies characterizing non-leptonic B-meson decays: trees (a), QCD penguins (b), and electroweak penguins (c)

and $|V_{ub}|$ given above and $\lambda = 0.225 \pm 0.001$ [72], we obtain

$$R_b^{\rm incl} = 0.45 \pm 0.03\,, \qquad R_b^{\rm excl} = 0.39 \pm 0.06\,, \tag{73}$$

where the labels 'incl' and 'excl' refer to the determinations of $|V_{ub}|$ through inclusive and exclusive $b \to u\ell\bar{\nu}_\ell$ transitions, respectively.

For a much more detailed discussion of the determinations of $|V_{cb}|$ and $|V_{ub}|$, we refer the reader to Refs. [9, 18, 63], where also the references to the vast original literature can be found.

3.3 Non-leptonic decays

3.3.1 Classification

The most complicated B decays are the non-leptonic transitions, which are mediated by $b \to q_1\,\bar{q}_2\,d\,(s)$ quark-level processes, with $q_1, q_2 \in \{u, d, c, s\}$. There are two kinds of topologies contributing to such decays: tree-diagram-like and 'penguin' topologies. The latter consist of gluonic (QCD) and electroweak (EW) penguins. In Fig. 8, the corresponding leading-order Feynman diagrams are shown. Depending on the flavour content of their final states, we may classify $b \to q_1\,\bar{q}_2\,d\,(s)$ decays as follows:

- $q_1 \neq q_2 \in \{u, c\}$: *only* tree diagrams contribute.
- $q_1 = q_2 \in \{u, c\}$: tree *and* penguin diagrams contribute.
- $q_1 = q_2 \in \{d, s\}$: *only* penguin diagrams contribute.

3.3.2 Low-energy effective Hamiltonians

In order to analyse non-leptonic B decays theoretically, we use low-energy effective Hamiltonians, which are calculated by making use of the 'operator product expansion', yielding transition matrix elements of the following structure:

$$\langle f|\mathcal{H}_{\rm eff}|i\rangle = \frac{G_{\rm F}}{\sqrt{2}}\lambda_{\rm CKM}\sum_k C_k(\mu)\langle f|Q_k(\mu)|i\rangle\,. \tag{74}$$

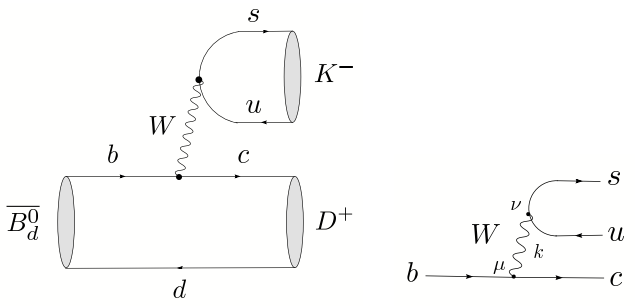

Fig. 9: Feynman diagrams contributing to the non-leptonic $\bar{B}^0_d \to D^+K^-$ decay

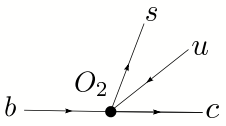

Fig. 10: The description of the $b \to d\bar{u}s$ process through the four-quark operator O_2 in the effective theory after the W boson has been integrated out

The technique of the operator product expansion allows us to separate the short-distance contributions to this transition amplitude from the long-distance ones, which are described by perturbative quantities $C_k(\mu)$ ('Wilson coefficient functions') and non-perturbative quantities $\langle f|Q_k(\mu)|i\rangle$ ('hadronic matrix elements'), respectively. As before, $G_{\rm F}$ is the Fermi constant, whereas $\lambda_{\rm CKM}$ is a CKM factor and μ denotes an appropriate renormalization scale. The Q_k are local operators, which are generated by electroweak interactions and QCD, and govern 'effectively' the decay in question. The Wilson coefficients $C_k(\mu)$ can be considered as scale-dependent couplings related to the vertices described by the Q_k.

In order to illustrate this rather abstract formalism, let us consider the decay $\bar{B}^0_d \to D^+K^-$, which allows a transparent discussion of the evaluation of the corresponding low-energy effective Hamiltonian. Since this transition originates from a $b \to c\bar{u}s$ quark-level process, it is — as we have just seen — a pure 'tree' decay, i.e. we do not have to deal with penguin topologies, which simplifies the analysis considerably. The leading-order Feynman diagram contributing to $\bar{B}^0_d \to D^+K^-$ can straightforwardly be obtained from Fig. 7 by substituting ℓ and ν_ℓ by s and u, respectively, as can be seen in Fig. 9. Consequently, the lepton current is simply replaced by a quark current, which will have important implications shown below. Evaluating the corresponding Feynman diagram yields

$$-\frac{g_2^2}{8}V^*_{us}V_{cb}\,[\bar{s}\gamma^\nu(1-\gamma_5)u]\left[\frac{g_{\nu\mu}}{k^2-M_W^2}\right][\bar{c}\gamma^\mu(1-\gamma_5)b]\,. \tag{75}$$

Because of $k^2 \sim m_b^2 \ll M_W^2$, we may — as in (55) — 'integrate out' the W boson with the help of (45), and arrive at

$$\begin{aligned}\mathcal{H}_{\rm eff} &= \frac{G_{\rm F}}{\sqrt{2}}V^*_{us}V_{cb}\,[\bar{s}_\alpha\gamma_\mu(1-\gamma_5)u_\alpha]\,[\bar{c}_\beta\gamma^\mu(1-\gamma_5)b_\beta]\\ &= \frac{G_{\rm F}}{\sqrt{2}}V^*_{us}V_{cb}(\bar{s}_\alpha u_\alpha)_{\rm V\text{–}A}(\bar{c}_\beta b_\beta)_{\rm V\text{–}A} \equiv \frac{G_{\rm F}}{\sqrt{2}}V^*_{us}V_{cb}O_2\,,\end{aligned} \tag{76}$$

where α and β denote the colour indices of the $SU(3)_{\rm C}$ gauge group of QCD. Effectively, our $b \to c\bar{u}s$ decay process is now described by the 'current–current' operator O_2, as is illustrated in Fig. 10.

So far, we have neglected QCD corrections. Their important impact is twofold: thanks to *factorizable* QCD corrections as shown in Fig. 11, the Wilson coefficient C_2 acquires a renormalization-scale

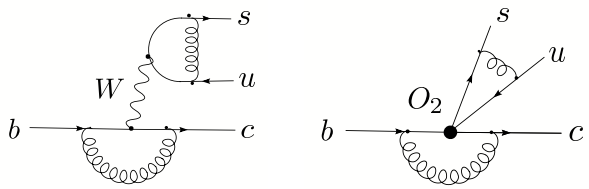

Fig. 11: Factorizable QCD corrections in the full (left panel) and effective (right panel) theories

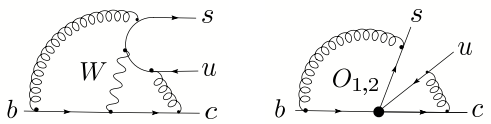

Fig. 12: Non-factorizable QCD corrections in the full (left panel) and effective (right panel) theories

dependence, i.e. $C_2(\mu) \neq 1$. On the other hand, *non-factorizable* QCD corrections as illustrated in Fig. 12 generate a second current–current operator through 'operator mixing', which is given by

$$O_1 \equiv [\bar{s}_\alpha \gamma_\mu (1-\gamma_5) u_\beta]\, [\bar{c}_\beta \gamma^\mu (1-\gamma_5) b_\alpha]\,. \tag{77}$$

Consequently, we eventually arrive at a low-energy effective Hamiltonian of the following structure:

$$\mathcal{H}_{\rm eff} = \frac{G_{\rm F}}{\sqrt{2}} V_{us}^* V_{cb}\, [C_1(\mu) O_1 + C_2(\mu) O_2]\,. \tag{78}$$

In order to evaluate the Wilson coefficients $C_1(\mu) \neq 0$ and $C_2(\mu) \neq 1$ [73], we must first calculate the QCD corrections to the decay processes both in the full theory, i.e. with W exchange, and in the effective theory, where the W is integrated out (see Figs. 11 and 12), and have then to express the QCD-corrected transition amplitude in terms of QCD-corrected matrix elements and Wilson coefficients as in (74). This procedure is called 'matching' between the full and the effective theory. The results for the $C_k(\mu)$ thus obtained contain terms of $\log(\mu/M_W)$, which become large for $\mu = \mathcal{O}(m_b)$, the scale governing the hadronic matrix elements of the O_k. Making use of the renormalization group, which exploits the fact that the transition amplitude (74) cannot depend on the chosen renormalization scale μ, we may sum up the following terms of the Wilson coefficients:

$$\alpha_s^n \left[\log\left(\frac{\mu}{M_W}\right)\right]^n \ \text{(LO)}, \quad \alpha_s^n \left[\log\left(\frac{\mu}{M_W}\right)\right]^{n-1} \ \text{(NLO)}, \quad \ldots \quad ; \tag{79}$$

detailed discussions of these rather technical aspects can be found in Ref. [74].

For the exploration of CP violation, the class of non-leptonic B decays that receives contributions both from tree and from penguin topologies plays a central rôle. In this important case, the operator basis is much larger than in our example (78), where we considered a pure 'tree' decay. If we apply the relation

$$V_{ur}^* V_{ub} + V_{cr}^* V_{cb} + V_{tr}^* V_{tb} = 0 \quad (r \in \{d, s\}), \tag{80}$$

which follows from the unitarity of the CKM matrix, and 'integrate out' the top quark (which enters through the penguin loop processes) and the W boson, we may write

$$\mathcal{H}_{\rm eff} = \frac{G_{\rm F}}{\sqrt{2}} \left[\sum_{j=u,c} V_{jr}^* V_{jb} \left\{\sum_{k=1}^{2} C_k(\mu)\, Q_k^{jr} + \sum_{k=3}^{10} C_k(\mu)\, Q_k^{r}\right\}\right]. \tag{81}$$

Here we have introduced another quark-flavour label $j \in \{u, c\}$, and the Q_k^{jr} can be divided as follows:

– Current–current operators:

$$\begin{aligned} Q_1^{jr} &= (\bar{r}_\alpha j_\beta)_{\text{V–A}}(\bar{j}_\beta b_\alpha)_{\text{V–A}} \\ Q_2^{jr} &= (\bar{r}_\alpha j_\alpha)_{\text{V–A}}(\bar{j}_\beta b_\beta)_{\text{V–A}}. \end{aligned} \tag{82}$$

– QCD penguin operators:

$$\begin{aligned} Q_3^{r} &= (\bar{r}_\alpha b_\alpha)_{\text{V–A}} \textstyle\sum_{q'}(\bar{q}'_\beta q'_\beta)_{\text{V–A}} \\ Q_4^{r} &= (\bar{r}_\alpha b_\beta)_{\text{V–A}} \textstyle\sum_{q'}(\bar{q}'_\beta q'_\alpha)_{\text{V–A}} \\ Q_5^{r} &= (\bar{r}_\alpha b_\alpha)_{\text{V–A}} \textstyle\sum_{q'}(\bar{q}'_\beta q'_\beta)_{\text{V+A}} \\ Q_6^{r} &= (\bar{r}_\alpha b_\beta)_{\text{V–A}} \textstyle\sum_{q'}(\bar{q}'_\beta q'_\alpha)_{\text{V+A}}. \end{aligned} \tag{83}$$

– EW penguin operators (the $e_{q'}$ denote the electrical quark charges):

$$\begin{aligned} Q_7^{r} &= \tfrac{3}{2}(\bar{r}_\alpha b_\alpha)_{\text{V–A}} \textstyle\sum_{q'} e_{q'}(\bar{q}'_\beta q'_\beta)_{\text{V+A}} \\ Q_8^{r} &= \tfrac{3}{2}(\bar{r}_\alpha b_\beta)_{\text{V–A}} \textstyle\sum_{q'} e_{q'}(\bar{q}'_\beta q'_\alpha)_{\text{V+A}} \\ Q_9^{r} &= \tfrac{3}{2}(\bar{r}_\alpha b_\alpha)_{\text{V–A}} \textstyle\sum_{q'} e_{q'}(\bar{q}'_\beta q'_\beta)_{\text{V–A}} \\ Q_{10}^{r} &= \tfrac{3}{2}(\bar{r}_\alpha b_\beta)_{\text{V–A}} \textstyle\sum_{q'} e_{q'}(\bar{q}'_\beta q'_\alpha)_{\text{V–A}}. \end{aligned} \tag{84}$$

The current–current, QCD and EW penguin operators are related to the tree, QCD and EW penguin processes shown in Fig. 8. At a renormalization scale $\mu = \mathcal{O}(m_b)$, the Wilson coefficients of the current–current operators are $C_1(\mu) = \mathcal{O}(10^{-1})$ and $C_2(\mu) = \mathcal{O}(1)$, whereas those of the penguin operators are $\mathcal{O}(10^{-2})$ [74]. Note that penguin topologies with internal charm- and up-quark exchanges [75] are described in this framework by penguin-like matrix elements of the corresponding current–current operators [76], and may also have important phenomenological consequences [77, 78].

Since the ratio $\alpha/\alpha_s = \mathcal{O}(10^{-2})$ of the QED and QCD couplings is very small, we would expect naïvely that EW penguins should play a minor rôle in comparison with QCD penguins. This would actually be the case if the top quark was not 'heavy'. However, since the Wilson coefficient C_9 increases strongly with m_t, we obtain interesting EW penguin effects in several B decays: $B \to K\phi$ modes are affected significantly by EW penguins, whereas $B \to \pi\phi$ and $B_s \to \pi^0\phi$ transitions are even *dominated* by such topologies [79, 80]. As we shall see in Subsection 7.2, EW penguins have also an important impact on the $B \to \pi K$ system [81, 82].

The low-energy effective Hamiltonians discussed above apply to all B decays that are caused by the same quark-level transition, i.e. they are 'universal'. Consequently, the differences between the various exclusive modes of a given decay class arise within this formalism only through the hadronic matrix elements of the relevant four-quark operators. Unfortunately, the evaluation of such matrix elements is associated with large uncertainties and is a very challenging task. In this context, 'factorization' is a widely used concept, which is our next topic.

3.3.3 Factorization of hadronic matrix elements

In order to discuss 'factorization', let us consider once more the decay $\bar{B}^0_d \to D^+K^-$. Evaluating the corresponding transition amplitude, we encounter the hadronic matrix elements of the $O_{1,2}$ operators between the $\langle K^-D^+|$ final and the $|\bar{B}^0_d\rangle$ initial states. If we use the well-known $SU(N_{\text{C}})$ colour-algebra relation

$$T^a_{\alpha\beta}T^a_{\gamma\delta} = \frac{1}{2}\left(\delta_{\alpha\delta}\delta_{\beta\gamma} - \frac{1}{N_{\text{C}}}\delta_{\alpha\beta}\delta_{\gamma\delta}\right) \tag{85}$$

to rewrite the operator O_1, we obtain

$$\begin{aligned} \langle K^-D^+|\mathcal{H}_{\text{eff}}|\bar{B}^0_d\rangle = \frac{G_{\text{F}}}{\sqrt{2}}V^*_{us}V_{cb}\Big[a_1\langle K^-D^+|(\bar{s}_\alpha u_\alpha)_{\text{V–A}}(\bar{c}_\beta b_\beta)_{\text{V–A}}|\bar{B}^0_d\rangle \\ +2\,C_1\langle K^-D^+|(\bar{s}_\alpha\, T^a_{\alpha\beta}\, u_\beta)_{\text{V–A}}(\bar{c}_\gamma\, T^a_{\gamma\delta}\, b_\delta)_{\text{V–A}}|\bar{B}^0_d\rangle\Big], \end{aligned}$$

with

$$a_1 = C_1/N_{\rm C} + C_2 \sim 1. \tag{86}$$

It is now straightforward to 'factorize' the hadronic matrix elements in (86):

$$\begin{aligned}
&\langle K^- D^+|(\bar s_\alpha u_\alpha)_{\rm V\text{-}A}(\bar c_\beta b_\beta)_{\rm V\text{-}A}|\bar B_d^0\rangle\big|_{\rm fact} \\
&\quad = \langle K^-|\,[\bar s_\alpha \gamma_\mu(1-\gamma_5)u_\alpha]\,|0\rangle\langle D^+|\,[\bar c_\beta\gamma^\mu(1-\gamma_5)b_\beta]\,|\bar B_d^0\rangle \\
&\quad = \underbrace{if_K}_{\text{decay constant}} \times \underbrace{F_0^{(BD)}(M_K^2)}_{B\to D\text{ form factor}} \times \underbrace{(M_B^2 - M_D^2)}_{\text{kinematical factor}},
\end{aligned} \tag{87}$$

$$\langle K^- D^+|(\bar s_\alpha\, T^a_{\alpha\beta}\, u_\beta)_{\rm V\text{-}A}(\bar c_\gamma\, T^a_{\gamma\delta}\, b_\delta)_{\rm V\text{-}A}|\bar B_d^0\rangle\big|_{\rm fact} = 0. \tag{88}$$

The quantity a_1 is a phenomenological 'colour factor', which governs 'colour-allowed' decays; the decay $\bar B_d^0 \to D^+K^-$ belongs to this category, since the colour indices of the K^- meson and the $\bar B_d^0$–D^+ system run independently from each other in the corresponding leading-order diagram shown in Fig. 9. On the other hand, in the case of "colour-suppressed" modes, for instance $\bar B_d^0 \to \pi^0 D^0$, where only one colour index runs through the whole diagram, we have to deal with the combination

$$a_2 = C_1 + C_2/N_{\rm C} \sim 0.25. \tag{89}$$

The concept of factorizing the hadronic matrix elements of four-quark operators into the product of hadronic matrix elements of quark currents has a long history [83], and can be justified, for example, in the large-$N_{\rm C}$ limit [84]. Interesting more recent developments are the following:

- 'QCD factorization' [85], which is in accordance with the old picture that factorization should hold for certain decays in the limit of $m_b \gg \Lambda_{\rm QCD}$ [86], provides a formalism to calculate the relevant amplitudes at the leading order of a $\Lambda_{\rm QCD}/m_b$ expansion. The resulting expression for the transition amplitudes incorporates elements both of the naïve factorization approach sketched above and of the hard-scattering picture. Let us consider a decay $\bar B \to M_1M_2$, where M_1 picks up the spectator quark. If M_1 is either a heavy (D) or a light (π, K) meson, and M_2 a light (π, K) meson, QCD factorization gives a transition amplitude of the following structure:

  $$A(\bar B \to M_1M_2) = [\text{'naïve factorization'}] \times [1 + \mathcal{O}(\alpha_s) + \mathcal{O}(\Lambda_{\rm QCD}/m_b)]\,. \tag{90}$$

  While the $\mathcal{O}(\alpha_s)$ terms, i.e. the radiative non-factorizable corrections, can be calculated systematically, the main limitation of the theoretical accuracy originates from the $\mathcal{O}(\Lambda_{\rm QCD}/m_b)$ terms.
- Another QCD approach to deal with non-leptonic B-meson decays — the 'perturbative hard-scattering approach' (PQCD) — was developed independently in Ref. [87], and differs from the QCD factorization formalism in some technical aspects.
- An interesting technique for 'factorization proofs' is provided by the framework of the 'soft collinear effective theory' (SCET) [88], which led to various applications.
- Non-leptonic B decays can also be studied within QCD light-cone sum-rule approaches [89].

A detailed presentation of these topics would be very technical and is beyond the scope of this lecture. However, for the discussion of the CP-violating effects in the B-meson system, we need only be familiar with the general structure of the non-leptonic B decay amplitudes and not enter the details of the techniques to deal with the corresponding hadronic matrix elements. Let us finally note that the B-decay data will eventually decide how well factorization and the new concepts sketched above are actually working. For example, data on the $B \to \pi\pi$ system point towards large non-factorizable corrections [90–93].

3.4 Towards studies of CP violation

As we have seen above, leptonic and semileptonic B-meson decays involve only a single weak (CKM) amplitude. On the other hand, the structure of non-leptonic transitions is considerably more complicated. Let us consider a non-leptonic decay $\bar{B} \to \bar{f}$ that is described by the low-energy effective Hamiltonian in (81). The corresponding decay amplitude is then given as follows:

$$\begin{aligned} A(\bar{B} \to \bar{f}) &= \langle \bar{f}|\mathcal{H}_{\rm eff}|\bar{B}\rangle \\ &= \frac{G_{\rm F}}{\sqrt{2}}\left[\sum_{j=u,c} V_{jr}^* V_{jb}\left\{\sum_{k=1}^{2} C_k(\mu)\langle \bar{f}|Q_k^{jr}(\mu)|\bar{B}\rangle + \sum_{k=3}^{10} C_k(\mu)\langle \bar{f}|Q_k^{r}(\mu)|\bar{B}\rangle\right\}\right]. \end{aligned} \tag{91}$$

Concerning the CP-conjugate process $B \to f$, we have

$$\begin{aligned} A(B \to f) &= \langle f|\mathcal{H}_{\rm eff}^{\dagger}|B\rangle \\ &= \frac{G_{\rm F}}{\sqrt{2}}\left[\sum_{j=u,c} V_{jr} V_{jb}^*\left\{\sum_{k=1}^{2} C_k(\mu)\langle f|Q_k^{jr\dagger}(\mu)|B\rangle + \sum_{k=3}^{10} C_k(\mu)\langle f|Q_k^{r\dagger}(\mu)|B\rangle\right\}\right]. \end{aligned} \tag{92}$$

If we use now that strong interactions are invariant under CP transformations, insert $(\mathcal{CP})^\dagger(\mathcal{CP}) = \hat{1}$ both after the $\langle f|$ and in front of the $|B\rangle$, and take the relation

$$(\mathcal{CP})Q_k^{jr\dagger}(\mathcal{CP})^\dagger = Q_k^{jr} \tag{93}$$

into account, we arrive at

$$\begin{aligned} A(B \to f) &= e^{i[\phi_{\rm CP}(B)-\phi_{\rm CP}(f)]} \\ &\times \frac{G_{\rm F}}{\sqrt{2}}\left[\sum_{j=u,c} V_{jr} V_{jb}^*\left\{\sum_{k=1}^{2} C_k(\mu)\langle \bar{f}|Q_k^{jr}(\mu)|\bar{B}\rangle + \sum_{k=3}^{10} C_k(\mu)\langle \bar{f}|Q_k^{r}(\mu)|\bar{B}\rangle\right\}\right], \end{aligned} \tag{94}$$

where the convention-dependent phases $\phi_{\rm CP}(B)$ and $\phi_{\rm CP}(f)$ are defined through

$$(\mathcal{CP})|B\rangle = e^{i\phi_{\rm CP}(B)}|\bar{B}\rangle, \quad (\mathcal{CP})|f\rangle = e^{i\phi_{\rm CP}(f)}|\bar{f}\rangle. \tag{95}$$

Consequently, we may write

$$A(\bar{B} \to \bar{f}) = e^{+i\varphi_1}|A_1|e^{i\delta_1} + e^{+i\varphi_2}|A_2|e^{i\delta_2} \tag{96}$$

$$A(B \to f) = e^{i[\phi_{\rm CP}(B)-\phi_{\rm CP}(f)]}\left[e^{-i\varphi_1}|A_1|e^{i\delta_1} + e^{-i\varphi_2}|A_2|e^{i\delta_2}\right]. \tag{97}$$

Here the CP-violating phases $\varphi_{1,2}$ originate from the CKM factors $V_{jr}^* V_{jb}$, and the CP-conserving 'strong' amplitudes $|A_{1,2}|e^{i\delta_{1,2}}$ involve the hadronic matrix elements of the four-quark operators. In fact, these expressions are the most general forms of any non-leptonic B-decay amplitude in the SM, i.e. they do not only refer to the $\Delta C = \Delta U = 0$ case described by (81). Using (96) and (97), we obtain the following CP asymmetry:

$$\begin{aligned} \mathcal{A}_{\rm CP} &\equiv \frac{\Gamma(B \to f) - \Gamma(\bar{B} \to \bar{f})}{\Gamma(B \to f) + \Gamma(\bar{B} \to \bar{f})} = \frac{|A(B \to f)|^2 - |A(\bar{B} \to \bar{f})|^2}{|A(B \to f)|^2 + |A(\bar{B} \to \bar{f})|^2} \\ &= \frac{2|A_1||A_2|\sin(\delta_1-\delta_2)\sin(\varphi_1-\varphi_2)}{|A_1|^2 + 2|A_1||A_2|\cos(\delta_1-\delta_2)\cos(\varphi_1-\varphi_2) + |A_2|^2}, \end{aligned} \tag{98}$$

where the convention-dependent phase in (97) cancels. We observe that a non-vanishing value can be generated through the interference between the two weak amplitudes, provided both a non-trivial weak

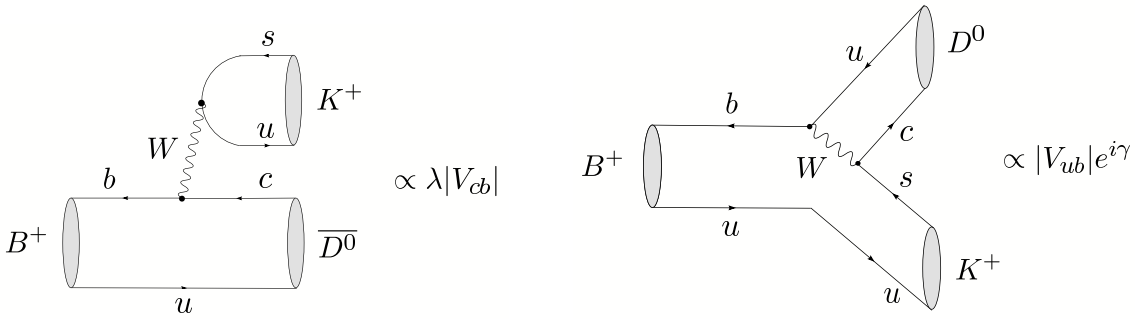

Fig. 13: Feynman diagrams contributing to $B^+ \to K^+ \bar{D}^0$ and $B^+ \to K^+ D^0$

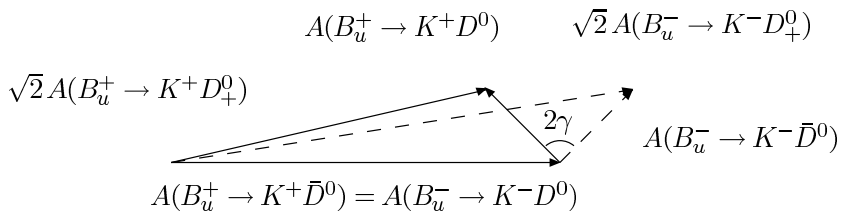

Fig. 14: The extraction of γ from $B^\pm \to K^\pm \{D^0, \bar{D}^0, D_+^0\}$ decays

phase difference $\varphi_1 - \varphi_2$ and a non-trivial strong phase difference $\delta_1 - \delta_2$ are present. This kind of CP violation is referred to as 'direct' CP violation, as it originates directly at the amplitude level of the considered decay. It is the B-meson counterpart of the effects that are probed through $\mathrm{Re}(\varepsilon'/\varepsilon)$ in the neutral kaon system,[2] and could first be established with the help of $B_d \to \pi^\mp K^\pm$ decays [94].

Since $\varphi_1 - \varphi_2$ is in general given by one of the UT angles — usually γ — the goal is to extract this quantity from the measured value of $\mathcal{A}_{\mathrm{CP}}$. Unfortunately, hadronic uncertainties affect this determination through the poorly known hadronic matrix elements in (91). In order to deal with this problem, we may proceed along one of the following two avenues:

(i) Amplitude relations can be used to eliminate the hadronic matrix elements. In these strategies, we distinguish between exact relations, using pure 'tree' decays of the kind $B^\pm \to K^\pm D$ [95, 96] or $B_c^\pm \to D_s^\pm D$ [97], and relations, which follow from the flavour symmetries of strong interactions, i.e. isospin or $SU(3)_{\mathrm{F}}$, and involve $B_{(s)} \to \pi\pi, \pi K, KK$ modes [98].

(ii) In decays of neutral B_q mesons, interference effects between B_q^0–$\bar{B}_q^0$ mixing and decay processes may induce 'mixing-induced CP violation'. If a single CKM amplitude governs the decay, the hadronic matrix elements cancel in the corresponding CP asymmetries (otherwise we have to use again amplitude relations [99]). The most important example is the decay $B_d^0 \to J/\psi K_{\mathrm{S}}$ [100].

Before discussing the features of neutral B_q mesons and B_q^0–$\bar{B}_q^0$ mixing in detail in Section 5, let us illustrate the use of amplitude relations for clean extractions of the UT angle γ from decays of charged B_u and B_c mesons.

4 Amplitude relations

4.1 $B^\pm \to K^\pm D$

The prototype of the strategies using theoretically clean amplitude relations is provided by $B^\pm \to K^\pm D$ decays [95]. Looking at Fig. 13, we observe that $B^+ \to K^+ \bar{D}^0$ and $B^+ \to K^+ D^0$ are pure 'tree'

[2] In order to calculate this quantity, an approriate low-energy effective Hamiltonian having the same structure as (81) is used. The large theoretical uncertainties mentioned in Section 1 originate from a strong cancellation between the contributions of the QCD and EW penguins (caused by the large top-quark mass) and the associated hadronic matrix elements.

decays. If we consider, in addition, the transition $B^+ \to D_+^0 K^+$, where D_+^0 denotes the CP eigenstate of the neutral D-meson system with eigenvalue $+1$,

$$|D_+^0\rangle = \frac{1}{\sqrt{2}}\left[|D^0\rangle + |\bar{D}^0\rangle\right], \tag{99}$$

we obtain interference effects, which are described by

$$\sqrt{2}A(B^+ \to K^+ D_+^0) = A(B^+ \to K^+ D^0) + A(B^+ \to K^+ \bar{D}^0) \tag{100}$$
$$\sqrt{2}A(B^- \to K^- D_+^0) = A(B^- \to K^- \bar{D}^0) + A(B^- \to K^- D^0). \tag{101}$$

These relations can be represented as two triangles in the complex plane. Since we have only to deal with tree-diagram-like topologies, we have moreover

$$A(B^+ \to K^+ \bar{D}^0) = A(B^- \to K^- D^0) \tag{102}$$
$$A(B^+ \to K^+ D^0) = A(B^- \to K^- \bar{D}^0) \times e^{2i\gamma}, \tag{103}$$

allowing a *theoretically clean* extraction of γ, as shown in Fig. 14. Unfortunately, these triangles are very squashed, since $B^+ \to K^+ D^0$ is colour-suppressed with respect to $B^+ \to K^+ \bar{D}^0$:

$$\left|\frac{A(B^+ \to K^+ D^0)}{A(B^+ \to K^+ \bar{D}^0)}\right| = \left|\frac{A(B^- \to K^- \bar{D}^0)}{A(B^- \to K^- D^0)}\right| \approx \frac{1}{\lambda}\frac{|V_{ub}|}{|V_{cb}|} \times \frac{a_2}{a_1} \approx 0.4 \times 0.3 = \mathcal{O}(0.1), \tag{104}$$

where the phenomenological 'colour' factors were introduced in Subsection 3.3.3.

Another — more subtle — problem is related to the measurement of $\mathrm{BR}(B^+ \to K^+ D^0)$. From the theoretical point of view, $D^0 \to K^- \ell^+ \nu$ would be ideal to measure this tiny branching ratio. However, because of the huge background from semileptonic B decays, we must rely on Cabibbo-allowed hadronic $D^0 \to f_{\rm NE}$ decays, such as $f_{\rm NE} = \pi^+ K^-$, $\rho^+ K^-$, ..., i.e. have to measure

$$B^+ \to K^+ D^0\,[\to f_{\rm NE}]. \tag{105}$$

Unfortunately, we then encounter another decay path into the *same* final state $K^+ f_{\rm NE}$ through

$$B^+ \to K^+ \bar{D}^0\,[\to f_{\rm NE}], \tag{106}$$

where $\mathrm{BR}(B^+ \to K^+ \bar{D}^0)$ is *larger* than $\mathrm{BR}(B^+ \to K^+ D^0)$ by a factor of $\mathcal{O}(10^2)$, while $\bar{D}^0 \to f_{\rm NE}$ is doubly Cabibbo-suppressed, i.e. the corresponding branching ratio is suppressed with respect to the one of $D^0 \to f_{\rm NE}$ by a factor of $\mathcal{O}(10^{-2})$. Consequently, we obtain interference effects of $\mathcal{O}(1)$ between the decay chains in (105) and (106). However, if two different final states $f_{\rm NE}$ are considered, γ can be extracted [96], although this determination is then more involved than the original triangle approach presented in Ref. [95].

The angle γ can actually be determined in a variety of ways through CP-violating effects in pure tree decays of type $B \to D^{(*)} K^{(*)}$ [101]. Using the present B-factory data, the following results were obtained through a combination of various methods:

$$\gamma|_{D^{(*)}K^{(*)}} = \begin{cases} (77^{+30}_{-32})^\circ & \text{(CKMfitter [44])}, \\ (88 \pm 16)^\circ & \text{(UTfit [45])}. \end{cases} \tag{107}$$

Here we have discarded a second solution given by $180^\circ + \gamma|_{D^{(*)}K^{(*)}}$ in the third quadrant of the $\bar{\rho}$–$\bar{\eta}$ plane, as it is disfavoured by the global fits of the UT, and by the data for mixing-induced CP violation in pure tree decays of type $B_d \to D^{\pm}\pi^{\mp}, D^{*\pm}\pi^{\mp}, \ldots$ [102]. A similar comment applies to the information from $B \to \pi\pi, \pi K$ modes [103].

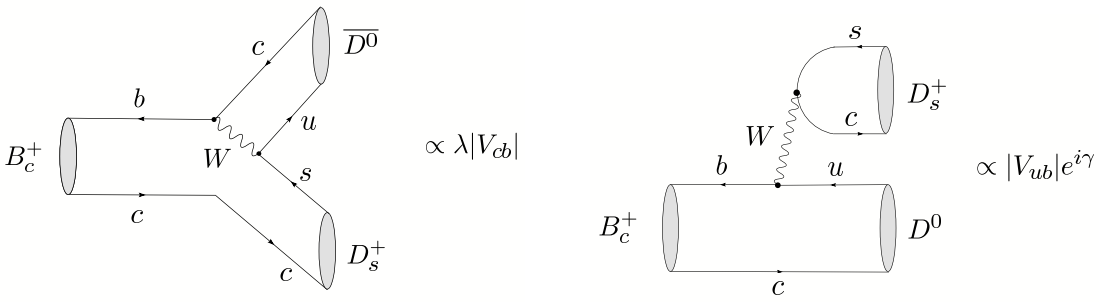

Fig. 15: Feynman diagrams contributing to $B_c^+ \to D_s^+ \bar{D}^0$ and $B^+ \to D_s^+ D^0$

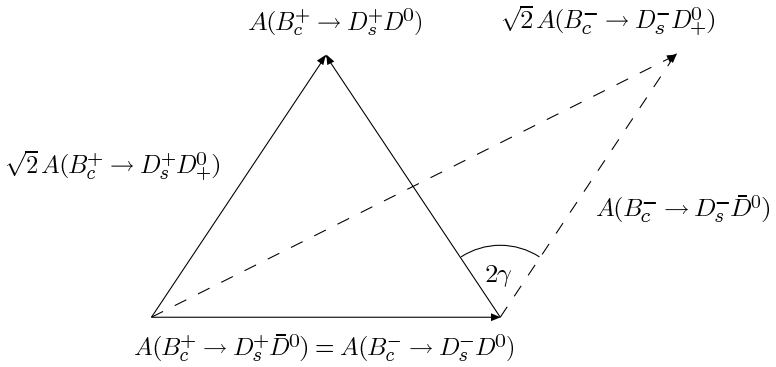

Fig. 16: The extraction of γ from $B_c^\pm \to D_s^\pm \{D^0, \bar{D}^0, D_+^0\}$ decays

4.2 $B_c^\pm \to D_s^\pm D$

In addition to the 'conventional' $B_u^\pm$ mesons, there is yet another species of charged B mesons, the B_c-meson system, which consists of $B_c^+ \sim c\bar{b}$ and $B_c^- \sim b\bar{c}$. These mesons were observed by the CDF Collaboration through their decay $B_c^+ \to J/\psi \ell^+ \nu$, with the following mass and lifetime [104]:

$$M_{B_c} = (6.40 \pm 0.39 \pm 0.13)\,\text{GeV}, \quad \tau_{B_c} = (0.46^{+0.18}_{-0.16} \pm 0.03)\,\text{ps}. \tag{108}$$

Meanwhile, the D0 Collaboration observed the $B_c^+ \to J/\psi\, \mu^+ X$ mode [105], which led to the following B_c mass and lifetime determinations:

$$M_{B_c} = (5.95^{+0.14}_{-0.13} \pm 0.34)\,\text{GeV}, \quad \tau_{B_c} = (0.448^{+0.123}_{-0.096} \pm 0.121)\,\text{ps}, \tag{109}$$

and CDF reported evidence for the $B_c^+ \to J/\psi \pi^+$ channel [106], implying

$$M_{B_c} = (6.2870 \pm 0.0048 \pm 0.0011)\,\text{GeV}. \tag{110}$$

Since a huge number of B_c mesons will be produced at the LHC, the natural question of how to explore CP violation with charged B_c decays arises, in particular whether an extraction of γ with the help of the triangle approach is possible. Such a determination is actually offered by $B_c^\pm \to D_s^\pm D$ decays, which are the B_c counterparts of the $B_u^\pm \to K^\pm D$ modes (see Fig. 15), and satisfy the following amplitude relations [107]:

$$\sqrt{2} A(B_c^+ \to D_s^+ D_+^0) = A(B_c^+ \to D_s^+ D^0) + A(B_c^+ \to D_s^+ \bar{D}^0) \tag{111}$$

$$\sqrt{2} A(B_c^- \to D_s^- D_+^0) = A(B_c^- \to D_s^- \bar{D}^0) + A(B_c^- \to D_s^- D^0), \tag{112}$$

with

$$A(B_c^+ \to D_s^+ \bar{D}^0) = A(B_c^- \to D_s^- D^0) \tag{113}$$

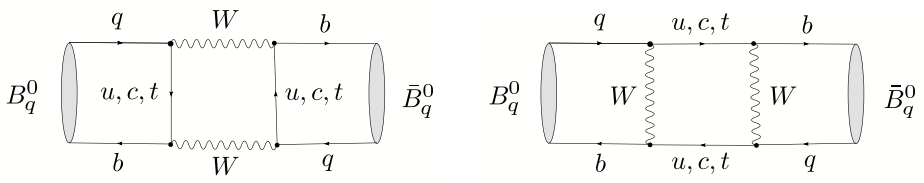

Fig. 17: Box diagrams contributing to B_q^0–$\bar{B}_q^0$ mixing in the SM ($q \in \{d, s\}$)

$$A(B_c^+ \to D_s^+ D^0) \;\; = \;\; A(B_c^- \to D_s^- \bar{D}^0) \times e^{2i\gamma}. \tag{114}$$

At first sight, everything is completely analogous to the $B_u^\pm \to K^\pm D$ case. However, there is an important difference [97], which becomes obvious by comparing the Feynman diagrams shown in Figs. 13 and 15: in the $B_c^\pm \to D_s^\pm D$ system, the amplitude with the rather small CKM matrix element V_{ub} is not colour-suppressed, while the larger element V_{cb} comes with a colour-suppression factor. Therefore, we obtain

$$\left|\frac{A(B_c^+ \to D_s^+ D^0)}{A(B_c^+ \to D_s^+ \bar{D}^0)}\right| = \left|\frac{A(B_c^- \to D_s^- \bar{D}^0)}{A(B_c^- \to D_s^- D^0)}\right| \approx \frac{1}{\lambda}\frac{|V_{ub}|}{|V_{cb}|} \times \frac{a_1}{a_2} \approx 0.4 \times 3 = \mathcal{O}(1), \tag{115}$$

and conclude that the two amplitudes are similar in size. In contrast to this favourable situation, in the decays $B_u^\pm \to K^\pm D$, the matrix element V_{ub} comes with the colour-suppression factor, resulting in a very stretched triangle. The extraction of γ from the $B_c^\pm \to D_s^\pm D$ triangles is illustrated in Fig. 16, which should be compared with the squashed $B_u^\pm \to K^\pm D$ triangles shown in Fig. 14. Another important advantage is that the interference effects arising from $D^0, \bar{D}^0 \to \pi^+ K^-$ are practically unimportant for the measurement of $\text{BR}(B_c^+ \to D_s^+ D^0)$ and $\text{BR}(B_c^+ \to D_s^+ \bar{D}^0)$ since the B_c-decay amplitudes are of the same order of magnitude. Consequently, the $B_c^\pm \to D_s^\pm D$ decays provide — from the theoretical point of view — the ideal realization of the 'triangle' approach to determine γ. However, the practical implementation at LHCb still appears to be challenging. The corresponding branching ratios were estimated in Ref. [108], with a pattern in accordance with (115).

5 The neutral B-meson system

5.1 Schrödinger equation for B_q^0–$\bar{B}_q^0$ mixing

Within the SM, B_q^0–$\bar{B}_q^0$ mixing arises from the box diagrams shown in Fig. 17. Thanks to this phenomenon, an initially, i.e. at time $t = 0$, present B_q^0-meson state evolves into a time-dependent linear combination of B_q^0 and $\bar{B}_q^0$ states:

$$|B_q(t)\rangle = a(t)|B_q^0\rangle + b(t)|\bar{B}_q^0\rangle, \tag{116}$$

where $a(t)$ and $b(t)$ are governed by a Schrödinger equation of the following form:

$$i\,\frac{\mathrm{d}}{\mathrm{d}t}\begin{pmatrix} a(t) \\ b(t) \end{pmatrix} = H \cdot \begin{pmatrix} a(t) \\ b(t) \end{pmatrix} \equiv \left[\underbrace{\begin{pmatrix} M_0^{(q)} & M_{12}^{(q)} \\ M_{12}^{(q)*} & M_0^{(q)} \end{pmatrix}}_{\text{mass matrix}} - \frac{i}{2}\underbrace{\begin{pmatrix} \Gamma_0^{(q)} & \Gamma_{12}^{(q)} \\ \Gamma_{12}^{(q)*} & \Gamma_0^{(q)} \end{pmatrix}}_{\text{decay matrix}}\right] \cdot \begin{pmatrix} a(t) \\ b(t) \end{pmatrix}.$$

The special form $H_{11} = H_{22}$ of the Hamiltonian H is an implication of the CPT theorem, i.e. of the invariance under combined CP and time-reversal (T) transformations.

It is straightforward to calculate the eigenstates $|B_\pm^{(q)}\rangle$ and eigenvalues $\lambda_\pm^{(q)}$ of (117):

$$|B_\pm^{(q)}\rangle = \frac{1}{\sqrt{1 + |\alpha_q|^2}}\left(|B_q^0\rangle \pm \alpha_q |\bar{B}_q^0\rangle\right) \tag{117}$$

$$\lambda_{\pm}^{(q)} = \left(M_0^{(q)} - \frac{i}{2}\Gamma_0^{(q)}\right) \pm \left(M_{12}^{(q)} - \frac{i}{2}\Gamma_{12}^{(q)}\right)\alpha_q, \tag{118}$$

where

$$\alpha_q e^{+i\left(\Theta_{\Gamma_{12}}^{(q)} + n'\pi\right)} = \sqrt{\frac{4|M_{12}^{(q)}|^2 e^{-i2\delta\Theta_{M/\Gamma}^{(q)}} + |\Gamma_{12}^{(q)}|^2}{4|M_{12}^{(q)}|^2 + |\Gamma_{12}^{(q)}|^2 - 4|M_{12}^{(q)}||\Gamma_{12}^{(q)}|\sin\delta\Theta_{M/\Gamma}^{(q)}}}. \tag{119}$$

Here we have written

$$M_{12}^{(q)} \equiv e^{i\Theta_{M_{12}}^{(q)}}|M_{12}^{(q)}|, \quad \Gamma_{12}^{(q)} \equiv e^{i\Theta_{\Gamma_{12}}^{(q)}}|\Gamma_{12}^{(q)}|, \quad \delta\Theta_{M/\Gamma}^{(q)} \equiv \Theta_{M_{12}}^{(q)} - \Theta_{\Gamma_{12}}^{(q)}, \tag{120}$$

and have introduced the quantity $n' \in \{0, 1\}$ to parametrize the sign of the square root in (119).

Evaluating the dispersive parts of the box diagrams shown in Fig. 17, which are dominated by internal top-quark exchanges, yields (for a more detailed discussion, see Ref. [21]):

$$M_{12}^{(q)} = \frac{G_{\rm F}^2 M_W^2}{12\pi^2}\eta_B M_{B_q} f_{B_q}^2 \hat{B}_{B_q}\left(V_{tq}^* V_{tb}\right)^2 S_0(x_t) e^{i(\pi - \phi_{\rm CP}(B_q))}, \tag{121}$$

where $\phi_{\rm CP}(B_q)$ is a convention-dependent phase, which is defined in analogy to (95). The short-distance physics is encoded in the 'Inami–Lim' function $S_0(x_t \equiv m_t^2/M_W^2)$ [109], and in the perturbative QCD correction factor η_B, which does *not* depend on $q \in \{d, s\}$, i.e. is the same for B_d and B_s mesons. On the other hand, the non-perturbative physics is described by the quantities $f_{B_q}\hat{B}_{B_q}^{1/2}$, involving — in addition to the B_q decay constant f_{B_q} — the 'bag' parameter $\hat{B}_{B_q}$, which is related to the hadronic matrix element $\langle \bar{B}_q^0|(\bar{b}q)_{\rm V-A}(\bar{b}q)_{\rm V-A}|B_q^0\rangle$. These non-perturbative parameters can be determined through QCD sum-rule calculations or lattice studies.

If we calculate also the absorptive parts of the box diagrams in Fig. 17, we obtain

$$\frac{\Gamma_{12}^{(q)}}{M_{12}^{(q)}} \approx -\frac{3\pi}{2S_0(x_t)}\left(\frac{m_b^2}{M_W^2}\right) = \mathcal{O}(m_b^2/m_t^2) \ll 1. \tag{122}$$

Consequently, we may expand (119) in $\Gamma_{12}^{(q)}/M_{12}^{(q)}$. Neglecting second-order terms, we arrive at

$$\alpha_q = \left[1 + \frac{1}{2}\left|\frac{\Gamma_{12}^{(q)}}{M_{12}^{(q)}}\right|\sin\delta\Theta_{M/\Gamma}^{(q)}\right] e^{-i\left(\Theta_{M_{12}}^{(q)} + n'\pi\right)}. \tag{123}$$

The deviation of $|\alpha_q|$ from 1 measures CP violation in B_q^0–$\bar{B}_q^0$ oscillations, and can be probed through the following 'wrong-charge' lepton asymmetries:

$$\mathcal{A}_{\rm SL}^{(q)} \equiv \frac{\Gamma(B_q^0(t) \to \ell^-\bar{\nu}X) - \Gamma(\bar{B}_q^0(t) \to \ell^+\nu X)}{\Gamma(B_q^0(t) \to \ell^-\bar{\nu}X) + \Gamma(\bar{B}_q^0(t) \to \ell^+\nu X)} = \frac{|\alpha_q|^4 - 1}{|\alpha_q|^4 + 1} \approx \left|\frac{\Gamma_{12}^{(q)}}{M_{12}^{(q)}}\right|\sin\delta\Theta_{M/\Gamma}^{(q)}. \tag{124}$$

Because of $|\Gamma_{12}^{(q)}|/|M_{12}^{(q)}| \propto m_b^2/m_t^2$ and $\sin\delta\Theta_{M/\Gamma}^{(q)} \propto m_c^2/m_b^2$, the asymmetry $\mathcal{A}_{\rm SL}^{(q)}$ is suppressed by a factor of $m_c^2/m_t^2 = \mathcal{O}(10^{-4})$ and is hence tiny in the SM. However, this observable may be enhanced through NP effects, thereby representing an interesing probe for physics beyond the SM [110, 111]. The current experimental average for the B_d-meson system compiled by the 'Heavy Flavour Averaging Group' [69] reads as follows:

$$\mathcal{A}_{\rm SL}^{(d)} = 0.0005 \pm 0.0056, \tag{125}$$

and does not indicate any non-vanishing effect.

5.2 Mixing parameters

Let us denote the masses of the eigenstates of (117) by $M_{\rm H}^{(q)}$ ('heavy') and $M_{\rm L}^{(q)}$ ('light'). It is then useful to introduce

$$M_q \equiv \frac{M_{\rm H}^{(q)} + M_{\rm L}^{(q)}}{2} = M_0^{(q)}, \tag{126}$$

as well as the mass difference

$$\Delta M_q \equiv M_{\rm H}^{(q)} - M_{\rm L}^{(q)} = 2|M_{12}^{(q)}| > 0, \tag{127}$$

which is by definition *positive*. While B_d^0–$\bar{B}_d^0$ mixing is well established and

$$\Delta M_d = (0.507 \pm 0.005)\,{\rm ps}^{-1} \tag{128}$$

known with impressive experimental accuracy [69], only lower bounds on ΔM_s were available, for many years, from the LEP (CERN) experiments and SLD (SLAC) [112]. In 2006, the value of ΔM_s was finally pinned down at the Tevatron [113]. The most recent results read as follows:

$$\Delta M_s = \begin{cases} (18.56 \pm 0.87){\rm ps}^{-1} & \text{(D0 [114])} \\ (17.77 \pm 0.10 \pm 0.07){\rm ps}^{-1} & \text{(CDF [115]).} \end{cases} \tag{129}$$

We shall return to the theoretical interpretation of these measurements in Subsection 8.1.

The decay widths $\Gamma_{\rm H}^{(q)}$ and $\Gamma_{\rm L}^{(q)}$ of the mass eigenstates, which correspond to $M_{\rm H}^{(q)}$ and $M_{\rm L}^{(q)}$, respectively, satisfy

$$\Delta\Gamma_q \equiv \Gamma_{\rm H}^{(q)} - \Gamma_{\rm L}^{(q)} = \frac{4\,{\rm Re}\left[M_{12}^{(q)}\Gamma_{12}^{(q)*}\right]}{\Delta M_q}, \tag{130}$$

whereas

$$\Gamma_q \equiv \frac{\Gamma_{\rm H}^{(q)} + \Gamma_{\rm L}^{(q)}}{2} = \Gamma_0^{(q)}. \tag{131}$$

There is the following interesting relation:

$$\frac{\Delta\Gamma_q}{\Gamma_q} \approx -\frac{3\pi}{2S_0(x_t)}\left(\frac{m_b^2}{M_W^2}\right) x_q = -\mathcal{O}(10^{-2}) \times x_q, \tag{132}$$

where

$$x_q \equiv \frac{\Delta M_q}{\Gamma_q} = \begin{cases} 0.776 \pm 0.008 & (q = d) \\ \mathcal{O}(20) & (q = s) \end{cases} \tag{133}$$

is often referred to as *the* B_q^0–$\bar{B}_q^0$ 'mixing parameter'.[3] Consequently, we observe that $\Delta\Gamma_d/\Gamma_d \sim 10^{-2}$ is negligibly small, while $\Delta\Gamma_s/\Gamma_s \sim 10^{-1}$ may be sizeable. In fact, the current state-of-the-art calculations of these quantities give the following numbers [116]:

$$\frac{|\Delta\Gamma_d|}{\Gamma_d} = (3 \pm 1.2) \times 10^{-3}, \quad \frac{|\Delta\Gamma_s|}{\Gamma_s} = 0.147 \pm 0.060. \tag{134}$$

Recently, results for $\Delta\Gamma_s$ were reported from the Tevatron, using the $B_s^0 \to J/\psi\phi$ channel [117]:

$$\Delta\Gamma_s = \begin{cases} (0.17 \pm 0.09 \pm 0.02){\rm ps}^{-1} & \text{(D0 [118])} \\ (0.076^{+0.059}_{-0.063} \pm 0.006){\rm ps}^{-1} & \text{(CDF [119]).} \end{cases} \tag{135}$$

It will be interesting to follow the evolution of these data. At LHCb, we expect a precision of $\sigma(\Delta\Gamma_s) = 0.027{\rm ps}^{-1}$ already with $0.5\,{\rm fb}^{-1}$ data, which is expected to be available by the end of 2009 [8]; ATLAS expects a relative accuracy of 13% with $30\,{\rm fb}^{-1}$ of data taken at low luminosity [120].

[3] Note that $\Delta\Gamma_q/\Gamma_q$ is negative in the SM because of the minus sign in (132).

5.3 Time-dependent decay rates

The time evolution of initially, i.e. at $t = 0$, pure B_q^0- and $\bar{B}_q^0$-meson states is given by

$$|B_q^0(t)\rangle = f_+^{(q)}(t)|B_q^0\rangle + \alpha_q f_-^{(q)}(t)|\bar{B}_q^0\rangle \tag{136}$$

and

$$|\bar{B}_q^0(t)\rangle = \frac{1}{\alpha_q} f_-^{(q)}(t)|B_q^0\rangle + f_+^{(q)}(t)|\bar{B}_q^0\rangle, \tag{137}$$

respectively, with

$$f_\pm^{(q)}(t) = \frac{1}{2}\left[e^{-i\lambda_+^{(q)}t} \pm e^{-i\lambda_-^{(q)}t}\right]. \tag{138}$$

These time-dependent state vectors allow the calculation of the corresponding transition rates. To this end, it is useful to introduce

$$|g_\pm^{(q)}(t)|^2 = \frac{1}{4}\left[e^{-\Gamma_{\rm L}^{(q)}t} + e^{-\Gamma_{\rm H}^{(q)}t} \pm 2\,e^{-\Gamma_q t}\cos(\Delta M_q t)\right] \tag{139}$$

$$g_-^{(q)}(t)\,g_+^{(q)}(t)^* = \frac{1}{4}\left[e^{-\Gamma_{\rm L}^{(q)}t} - e^{-\Gamma_{\rm H}^{(q)}t} + 2\,i\,e^{-\Gamma_q t}\sin(\Delta M_q t)\right], \tag{140}$$

as well as

$$\xi_f^{(q)} = e^{-i\Theta_{M_{12}}^{(q)}}\frac{A(\bar{B}_q^0 \to f)}{A(B_q^0 \to f)}, \quad \xi_{\bar{f}}^{(q)} = e^{-i\Theta_{M_{12}}^{(q)}}\frac{A(\bar{B}_q^0 \to \bar{f})}{A(B_q^0 \to \bar{f})}. \tag{141}$$

Looking at (121), we find

$$\Theta_{M_{12}}^{(q)} = \pi + 2{\rm arg}(V_{tq}^* V_{tb}) - \phi_{\rm CP}(B_q), \tag{142}$$

and observe that this phase depends on the chosen CKM and CP phase conventions specified in (11) and (95), respectively. However, these dependences are cancelled through the amplitude ratios in (141), so that $\xi_f^{(q)}$ and $\xi_{\bar{f}}^{(q)}$ are *convention-independent* observables. Whereas n' enters the functions in (138) through (118), the dependence on this parameter is cancelled in (139) and (140) through the introduction of the *positive* mass difference ΔM_q (see (127)). Combining the formulae listed above, we eventually arrive at the following transition rates for decays of initially, i.e. at $t = 0$, present B_q^0 or $\bar{B}_q^0$ mesons:

$$\Gamma(\overset{(-)}{B}{}_q^0\,(t) \to f) = \left[|g_\mp^{(q)}(t)|^2 + |\xi_f^{(q)}|^2|g_\pm^{(q)}(t)|^2 - 2\,{\rm Re}\left\{\xi_f^{(q)} g_\pm^{(q)}(t) g_\mp^{(q)}(t)^*\right\}\right]\tilde{\Gamma}_f, \tag{143}$$

where the time-independent rate $\tilde{\Gamma}_f$ corresponds to the 'unevolved' decay amplitude $A(B_q^0 \to f)$, and can be calculated by performing the usual phase-space integrations. The rates into the CP-conjugate final state $\bar{f}$ can straightforwardly be obtained from (143) by making the substitutions

$$\tilde{\Gamma}_f \;\to\; \tilde{\Gamma}_{\bar{f}}, \quad \xi_f^{(q)} \;\to\; \xi_{\bar{f}}^{(q)}. \tag{144}$$

5.4 'Untagged' rates

The expected sizeable width difference $\Delta\Gamma_s$ may provide interesting studies of CP violation through 'untagged' B_s rates (see Refs. [117] and [121–124]), which are defined as

$$\langle\Gamma(B_s(t) \to f)\rangle \equiv \Gamma(B_s^0(t) \to f) + \Gamma(\bar{B}_s^0(t) \to f), \tag{145}$$

and are characterized by the feature that we do not distinguish between initially, i.e. at time $t = 0$, present B_s^0 or $\bar{B}_s^0$ mesons. If we consider a final state f to which both a B_s^0 and a $\bar{B}_s^0$ may decay, and use the expressions in (143), we find

$$\langle\Gamma(B_s(t) \to f)\rangle \propto \left[\cosh(\Delta\Gamma_s t/2) - \mathcal{A}_{\Delta\Gamma}(B_s \to f)\sinh(\Delta\Gamma_s t/2)\right]e^{-\Gamma_s t}, \tag{146}$$

with

$$\mathcal{A}_{\Delta\Gamma}(B_s \to f) \equiv \frac{2\,\mathrm{Re}\,\xi_f^{(s)}}{1+\left|\xi_f^{(s)}\right|^2}. \tag{147}$$

We observe that the rapidly oscillating $\Delta M_s t$ terms cancel, and that we may obtain information about the phase structure of the observable $\xi_f^{(s)}$, thereby providing valuable insights into CP violation.

Following these lines, for instance, the untagged observables offered by the angular distribution of the $B_s \to K^{*+}K^{*-}, K^{*0}\bar{K}^{*0}$ decay products allow a determination of the UT angle γ, provided $\Delta\Gamma_s$ is actually sizeable [122]. Untagged B_s-decay rates are interesting in terms of efficiency, acceptance and purity, and are already applied for the physics analyses at the Tevatron [118, 119]. Soon they will help us to fully exploit the physics potential of the B_s-meson system at the LHC.

5.5 CP asymmetries

A particularly simple — but also very interesting — situation arises if we restrict ourselves to decays of neutral B_q mesons into final states f that are eigenstates of the CP operator, i.e. satisfy the relation

$$(\mathcal{CP})|f\rangle = \pm|f\rangle. \tag{148}$$

Consequently, we have $\xi_f^{(q)} = \xi_{\bar{f}}^{(q)}$ in this case, as can be seen in (141). Using the decay rates in (143), we find that the corresponding time-dependent CP asymmetry is given by

$$\begin{aligned}\mathcal{A}_{\mathrm{CP}}(t) &\equiv \frac{\Gamma(B_q^0(t)\to f)-\Gamma(\bar{B}_q^0(t)\to f)}{\Gamma(B_q^0(t)\to f)+\Gamma(\bar{B}_q^0(t)\to f)} \\ &= \left[\frac{\mathcal{A}_{\mathrm{CP}}^{\mathrm{dir}}(B_q\to f)\,\cos(\Delta M_q t)+\mathcal{A}_{\mathrm{CP}}^{\mathrm{mix}}(B_q\to f)\,\sin(\Delta M_q t)}{\cosh(\Delta\Gamma_q t/2)-\mathcal{A}_{\Delta\Gamma}(B_q\to f)\,\sinh(\Delta\Gamma_q t/2)}\right],\end{aligned} \tag{149}$$

with

$$\mathcal{A}_{\mathrm{CP}}^{\mathrm{dir}}(B_q\to f) \equiv \frac{1-\left|\xi_f^{(q)}\right|^2}{1+\left|\xi_f^{(q)}\right|^2}, \qquad \mathcal{A}_{\mathrm{CP}}^{\mathrm{mix}}(B_q\to f) \equiv \frac{2\,\mathrm{Im}\,\xi_f^{(q)}}{1+\left|\xi_f^{(q)}\right|^2}. \tag{150}$$

Because of the relation

$$\mathcal{A}_{\mathrm{CP}}^{\mathrm{dir}}(B_q\to f) = \frac{|A(B_q^0\to f)|^2-|A(\bar{B}_q^0\to\bar{f})|^2}{|A(B_q^0\to f)|^2+|A(\bar{B}_q^0\to\bar{f})|^2}, \tag{151}$$

this observable measures the direct CP violation in the decay $B_q \to f$, which originates from the interference between different weak amplitudes, as we have seen in (98). On the other hand, the interesting *new* aspect of (149) is due to $\mathcal{A}_{\mathrm{CP}}^{\mathrm{mix}}(B_q \to f)$, which originates from interference effects between B_q^0–$\bar{B}_q^0$ mixing and decay processes, and describes 'mixing-induced' CP violation. Finally, the width difference $\Delta\Gamma_q$, which may be sizeable in the B_s-meson system, provides access to $\mathcal{A}_{\Delta\Gamma}(B_q \to f)$ introduced in (147). However, this observable is not independent from $\mathcal{A}_{\mathrm{CP}}^{\mathrm{dir}}(B_q \to f)$ and $\mathcal{A}_{\mathrm{CP}}^{\mathrm{mix}}(B_q \to f)$, satisfying

$$\left[\mathcal{A}_{\mathrm{CP}}^{\mathrm{dir}}(B_q\to f)\right]^2+\left[\mathcal{A}_{\mathrm{CP}}^{\mathrm{mix}}(B_q\to f)\right]^2+\left[\mathcal{A}_{\Delta\Gamma}(B_q\to f)\right]^2 = 1. \tag{152}$$

In order to calculate $\xi_f^{(q)}$, we use the general expressions (96) and (97), where $e^{-i\phi_{\mathrm{CP}}(f)} = \pm 1$ because of (148), and $\phi_{\mathrm{CP}}(B) = \phi_{\mathrm{CP}}(B_q)$. If we insert these amplitude parametrizations into (141) and take (142) into account, we observe that the phase-convention-dependent quantity $\phi_{\mathrm{CP}}(B_q)$ cancels, and finally arrive at

$$\xi_f^{(q)} = \mp e^{-i\phi_q}\left[\frac{e^{+i\varphi_1}|A_1|e^{i\delta_1}+e^{+i\varphi_2}|A_2|e^{i\delta_2}}{e^{-i\varphi_1}|A_1|e^{i\delta_1}+e^{-i\varphi_2}|A_2|e^{i\delta_2}}\right], \tag{153}$$

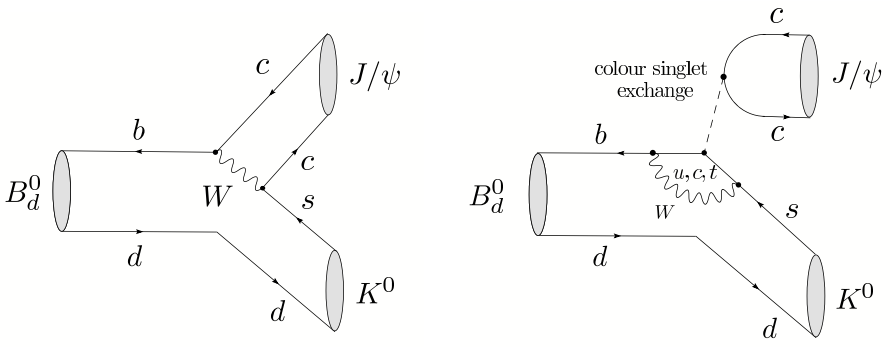

Fig. 18: Feynman diagrams contributing to the $B_d^0 \to J/\psi K^0$ decay

where

$$\phi_q \equiv 2\arg(V_{tq}^* V_{tb}) = \begin{cases} +2\beta & (q=d) \\ -2\delta\gamma & (q=s) \end{cases} \tag{154}$$

is associated with the CP-violating weak B_q^0–$\bar{B}_q^0$ mixing phase arising in the SM; β and $\delta\gamma$ refer to the corresponding angles in the unitarity triangles shown in Fig. 3.

In analogy to (98), the caclulation of $\xi_f^{(q)}$ is — in general — also affected by large hadronic uncertainties. However, if one CKM amplitude plays the dominant rôle in the $B_q \to f$ transition, we obtain

$$\xi_f^{(q)} = \mp e^{-i\phi_q}\left[\frac{e^{+i\phi_f/2}|M_f|e^{i\delta_f}}{e^{-i\phi_f/2}|M_f|e^{i\delta_f}}\right] = \mp e^{-i(\phi_q-\phi_f)}, \tag{155}$$

and observe that the hadronic matrix element $|M_f|e^{i\delta_f}$ cancels in this expression. Since the requirements for direct CP violation discussed above are then no longer satisfied, direct CP violation vanishes in this important special case, i.e. $\mathcal{A}_{\rm CP}^{\rm dir}(B_q \to f) = 0$. On the other hand, this is *not* the case for the mixing-induced CP asymmetry. In particular,

$$\mathcal{A}_{\rm CP}^{\rm mix}(B_q \to f) = \pm\sin\phi \tag{156}$$

is now governed by the CP-violating weak phase difference $\phi \equiv \phi_q - \phi_f$ and is not affected by hadronic uncertainties. The corresponding time-dependent CP asymmetry takes then the simple form

$$\left.\frac{\Gamma(B_q^0(t)\to f) - \Gamma(\bar{B}_q^0(t)\to \bar{f})}{\Gamma(B_q^0(t)\to f) + \Gamma(\bar{B}_q^0(t)\to \bar{f})}\right|_{\Delta\Gamma_q=0} = \pm\sin\phi\,\sin(\Delta M_q t), \tag{157}$$

and allows an elegant determination of $\sin\phi$.

5.6 Key application: $B_d^0 \to J/\psi K_{\rm S}$

This decay has a CP-odd final state, and originates from $\bar{b} \to \bar{c}c\bar{s}$ quark-level transitions, as can be seen in Fig. 18. Consequently, it receives contributions both from tree and from penguin topologies (see Subsection 3.3.1). In the SM, the decay amplitude can hence be written as follows [125]:

$$A(B_d^0 \to J/\psi K_{\rm S}) = \lambda_c^{(s)}\left(A_{\rm T}^{c'} + A_{\rm P}^{c'}\right) + \lambda_u^{(s)} A_{\rm P}^{u'} + \lambda_t^{(s)} A_{\rm P}^{t'}. \tag{158}$$

Here the

$$\lambda_q^{(s)} \equiv V_{qs}V_{qb}^* \tag{159}$$

are CKM factors, $A_{\rm T}^{c'}$ is the CP-conserving strong tree amplitude, while the $A_{\rm P}^{q'}$ describe the penguin topologies with internal q quarks ($q \in \{u,c,t\}$), including QCD and EW penguins; the primes remind

us that we are dealing with a $\bar{b} \to \bar{s}$ transition. If we eliminate now $\lambda_t^{(s)}$ through (80) and apply the Wolfenstein parametrization, we obtain

$$A(B_d^0 \to J/\psi K_{\rm S}) \propto \left[1 + \lambda^2 a e^{i\theta} e^{i\gamma}\right], \tag{160}$$

where

$$a e^{i\vartheta} \equiv \left(\frac{R_b}{1-\lambda^2}\right)\left[\frac{A_{\rm P}^{u'} - A_{\rm P}^{t'}}{A_{\rm T}^{c'} + A_{\rm P}^{c'} - A_{\rm P}^{t'}}\right] \tag{161}$$

is a hadronic parameter. Using now the formalism discussed in Subsection 5.5 yields

$$\xi_{\psi K_{\rm S}}^{(d)} = +e^{-i\phi_d}\left[\frac{1 + \lambda^2 a e^{i\vartheta} e^{-i\gamma}}{1 + \lambda^2 a e^{i\vartheta} e^{+i\gamma}}\right]. \tag{162}$$

Unfortunately, $a e^{i\vartheta}$, which is a measure for the ratio of the $B_d^0 \to J/\psi K_{\rm S}$ penguin to tree contributions, can only be estimated with large hadronic uncertainties. However, since this parameter enters (162) in a doubly Cabibbo-suppressed way, its impact on the CP-violating observables is practically negligible. We can put this important statement on a more quantitative basis by making the plausible assumption that $a = \mathcal{O}(\bar{\lambda}) = \mathcal{O}(0.2) = \mathcal{O}(\lambda)$, where $\bar{\lambda}$ is a 'generic' expansion parameter [126]:

$$\mathcal{A}_{\rm CP}^{\rm dir}(B_d \to J/\psi K_{\rm S}) = 0 + \mathcal{O}(\overline{\lambda}^3) \tag{163}$$

$$\mathcal{A}_{\rm CP}^{\rm mix}(B_d \to J/\psi K_{\rm S}) = -\sin\phi_d + \mathcal{O}(\overline{\lambda}^3) \stackrel{\rm SM}{=} -\sin 2\beta + \mathcal{O}(\overline{\lambda}^3). \tag{164}$$

Consequently, (164) allows an essentially *clean* determination of $\sin 2\beta$ [100].

Since the CKM fits performed within the SM pointed to a large value of $\sin 2\beta$, $B_d^0 \to J/\psi K_{\rm S}$ offered the exciting perspective of exhibiting *large* mixing-induced CP violation. In 2001, the measurement of $\mathcal{A}_{\rm CP}^{\rm mix}(B_d \to J/\psi K_{\rm S})$ allowed indeed the first observation of CP violation *outside* the K-meson system [5]. The most recent data are still not showing any signal for *direct* CP violation in $B_d^0 \to J/\psi K_{\rm S}$ within the current uncertainties, as is expected from (163), and the world average reads [69]

$$\mathcal{A}_{\rm CP}^{\rm dir}(B_d \to J/\psi K_{\rm S}) = 0.002 \pm 0.021. \tag{165}$$

As far as (164) is concerned, we have

$$(\sin 2\beta)_{\psi K_{\rm S}} \equiv -\mathcal{A}_{\rm CP}^{\rm mix}(B_d \to J/\psi K_{\rm S}) = \begin{cases} 0.714 \pm 0.032 \pm 0.018 & \text{(BaBar)} \\ 0.651 \pm 0.034 & \text{(Belle),} \end{cases} \tag{166}$$

where also other final states similar to $J/\psi K_{\rm S}$ were included [69]; the corresponding world average is then given as follows:

$$(\sin 2\beta)_{\psi K_{\rm S}} = 0.681 \pm 0.025. \tag{167}$$

In the SM, the theoretical uncertainties are generically expected to be below the 0.01 level [126]; significantly smaller effects are found in Ref. [127], whereas a fit performed in Ref. [128] yields a theoretical penguin uncertainty comparable to the present experimental systematic error. A possibility to control these uncertainties is provided by $B_s^0 \to J/\psi K_{\rm S}$ [125], which can be explored at the LHC [129].

The average in (167) yields a twofold solution for the phase $(2\beta)_{\psi K_{\rm S}}$ itself:

$$(2\beta)_{\psi K_{\rm S}} = (43 \pm 2)^\circ \quad \vee \quad (137 \pm 2)^\circ. \tag{168}$$

Here the latter solution would be in dramatic conflict with the CKM fits, and would require a large NP contribution to B_d^0–$\bar{B}_d^0$ mixing [130,131]. However, experimental information on the sign of $\cos 2\beta$ rules out a negative value of this quantity with more than 95% C.L. [101], so that we are left with the solution around 43°.

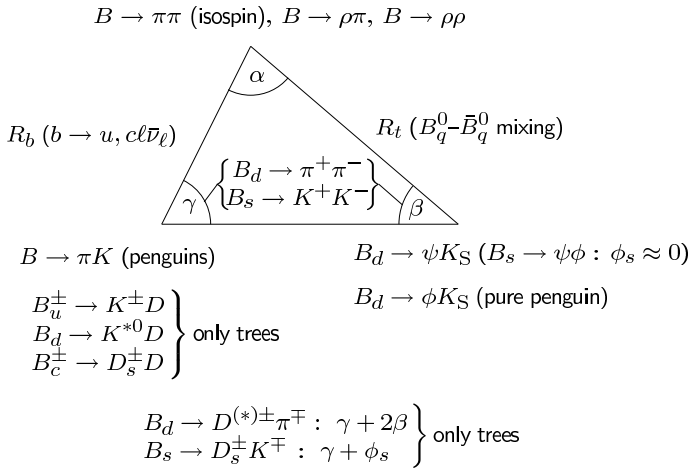

Fig. 19: A brief roadmap of B-decay strategies for the exploration of CP violation

6 Impact of new physics

6.1 General remarks

Using the concept of the low-energy effective Hamiltonians introduced in Subsection 3.3.2, we may address this important question in a systematic way [132]:

– NP may modify the 'strength' of the SM operators through new short-distance functions which depend on the NP parameters, such as the masses of charginos, squarks, charged Higgs particles and $\tan\beta \equiv v_2/v_1$ in the 'minimal supersymmetric SM' (MSSM). The NP particles may enter in box and penguin topologies, and are 'integrated out' as the W boson and top quark in the SM. Consequently, the initial conditions for the renormalization-group evolution take the following form:

$$C_k \to C_k^{\rm SM} + C_k^{\rm NP}. \tag{169}$$

It should be emphasized that the NP pieces $C_k^{\rm NP}$ may also involve new CP-violating phases which are *not* related to the CKM matrix.

– NP may enhance the operator basis:

$$\{Q_k\} \to \{Q_k^{\rm SM}, Q_l^{\rm NP}\}, \tag{170}$$

so that operators which are not present (or strongly suppressed) in the SM may actually play an important rôle. In this case, we encounter, in general, also new sources for flavour and CP violation.

Concerning model-dependent NP analyses, SUSY scenarios in particular have received a lot of attention. Examples of other fashionable NP frameworks are left–right-symmetric models, scenarios with extra dimensions, models with an extra Z', 'little Higgs' scenarios, and models with a fourth generation. For a recent overview and a guide to the literature, we refer the reader to Ref. [9].

The simplest extension of the SM is given by models with 'minimal flavour violation' (MFV) [133, 134]. Simply speaking, in this class of models, there are no new sources of flavour and CP violation, i.e. these phenomena are still governed by the CKM matrix. On account of their simplicity, the extensions of the SM with MFV show several correlations between various observables, thereby allowing for powerful tests of this scenario. A comprehensive recent discussion can be found in Ref. [9].

The B-meson system offers a variety of processes and strategies for the exploration of CP violation [18, 135], as we have illustrated in Fig. 19 through a collection of prominent examples. We see that there

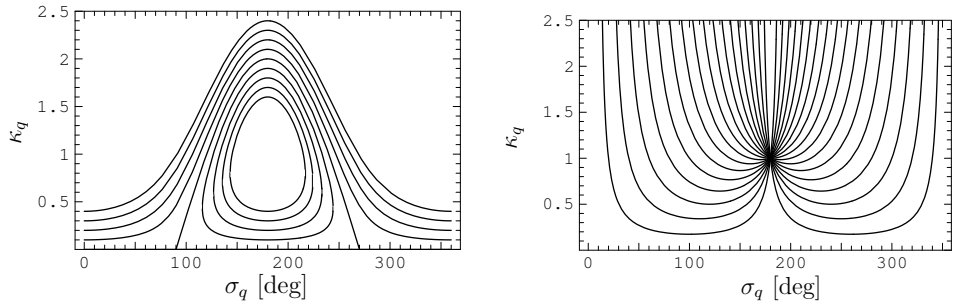

Fig. 20: Left panel: dependence of κ_q on σ_q for values of ρ_q varied in steps of 0.1 between 1.4 (upper) and 0.6 (inner curve). Right panel: dependence of κ_q on σ_q for values of $\phi_q^{\rm NP}$ varied in steps of 10° between $\pm 10^\circ$ (lower curves) and $\pm 170^\circ$; the curves for $0^\circ < \sigma_q < 180^\circ$ and $180^\circ < \sigma_q < 360^\circ$ correspond to positive and negative values of $\phi_q^{\rm NP}$, respectively.

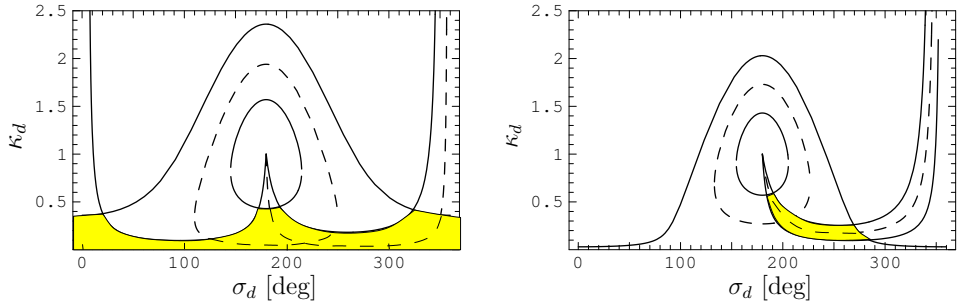

Fig. 21: Left panel: allowed region (yellow/grey) in the σ_d–κ_d plane in a scenario with the JLQCD lattice results and the 'exclusive' value of R_b in (73). Right panel: ditto for the scenario with the (HP+JL)QCD lattice results and the 'inclusive' value of R_b in (73), as discussed in the text.

are processes with a very *different* dynamics that are — in the SM — sensitive to the *same* angles of the UT. Moreover, rare B- and K-meson decays [136], which originate from loop effects in the SM, provide complementary insights into flavour physics and interesting correlations with the CP-B sector; key examples are $B \to X_s\gamma$ and the exclusive modes $B \to K^*\gamma$, $B \to \rho\gamma$, as well as $B_{s,d} \to \mu^+\mu^-$ and $K^+ \to \pi^+\nu\bar{\nu}$, $K_{\rm L} \to \pi^0\nu\bar{\nu}$. In the presence of NP in the TeV regime, discrepancies with respect to the SM picture should emerge at some level of accuracy. There are two promising avenues for NP to enter B-physics observables, as we shall discuss in the remainder of this section.

6.2 New physics in B-decay amplitudes

NP has typically a small effect if SM tree processes play the dominant rôle. However, NP could well have a significant impact on the FCNC sector: new particles may enter in penguin or box diagrams, or new FCNC contributions may even be generated at the tree level. In fact, sizeable contributions arise generically in field-theoretical estimates with $\Lambda_{\rm NP} \sim$ TeV [137], as well as in specific NP models. In Section 7, we shall have a closer look at B decays that may actually indicate NP effects at the decay-amplitude level.

In the case of the 'golden' decay $B_d^0 \to J/\psi K_{\rm S}$, NP effects have to compete with a tree contribution and are hence not expected to play a significant rôle. This is indeed signalled by a set of observables that were introduced in Ref. [126] to search for NP contributions to the $B \to J/\psi K$ decay amplitudes [138]. In the following discussion, we shall therefore assume that these NP effects are negligible.

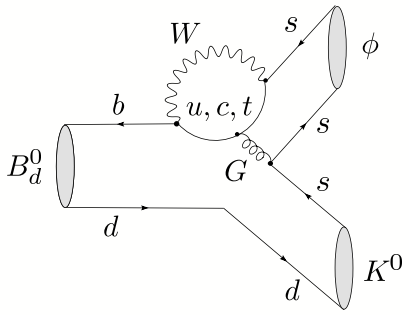

Fig. 22: Feynman diagrams contributing to the $B_d^0 \to \phi K^0$ decay

6.3 New physics in B_q^0–$\bar{B}_q^0$ mixing

Another attractive mechanism for NP to manifest itself in the B-physics landscape is offered by B_q^0–$\bar{B}_q^0$ mixing. Here NP could enter through the exchange of new particles in box diagrams, or through new contributions at the tree level. In general, we may write

$$M_{12}^{(q)} = M_{12}^{q,\mathrm{SM}} \left(1 + \kappa_q e^{i\sigma_q}\right), \tag{171}$$

where the expression for $M_{12}^{q,\mathrm{SM}}$ can be found in (121). Consequently, we obtain

$$\Delta M_q = \Delta M_q^{\mathrm{SM}} + \Delta M_q^{\mathrm{NP}} = \Delta M_q^{\mathrm{SM}} \left|1 + \kappa_q e^{i\sigma_q}\right|, \tag{172}$$

$$\phi_q = \phi_q^{\mathrm{SM}} + \phi_q^{\mathrm{NP}} = \phi_q^{\mathrm{SM}} + \arg(1 + \kappa_q e^{i\sigma_q}), \tag{173}$$

with ΔM_q^{SM} and ϕ_q^{SM} given in (127) and (154), respectively. Using dimensional arguments borrowed from effective field theory [126, 131], it can be shown that $\Delta M_q^{\mathrm{NP}}/\Delta M_q^{\mathrm{SM}} \sim 1$ and $\phi_q^{\mathrm{NP}}/\phi_q^{\mathrm{SM}} \sim 1$ could — in principle — be possible for a NP scale Λ_{NP} in the TeV regime; such a pattern may also arise in specific NP scenarios.

Introducing

$$\rho_q \equiv \left|\frac{\Delta M_q}{\Delta M_q^{\mathrm{SM}}}\right| = \sqrt{1 + 2\kappa_q \cos\sigma_q + \kappa_q^2}, \tag{174}$$

the measured values of the mass differences ΔM_q can be converted into constraints in NP parameter space through the contours shown in the left panel of Fig. 20. Further constraints are implied by the NP phases ϕ_q^{NP}, which can be probed by means of mixing-induced CP asymmetries, through the curves in the right panel of Fig. 20. Interestingly, κ_q is bounded from below for any value of $\phi_q^{\mathrm{NP}} \neq 0$. For example, even a small phase $|\phi_q^{\mathrm{NP}}| = 10^\circ$ implies a clean lower bound of $\kappa_q \geq 0.17$, i.e. NP contributions of at most 17% [68].

Consequently, using the B-factory data to measure ΔM_d and to extract the NP phase ϕ_d^{NP}, two sets of contours can be fixed in the σ_d–κ_d plane. In the former case, the SM value ΔM_d^{SM} is required. It involves the CKM parameter $|V_{td}^* V_{tb}|$, which is governed by γ in the corresponding numerical analysis if the unitarity of the CKM matrix is used. Moreover, information about the hadronic parameter $f_{B_d}\hat{B}_{B_d}^{1/2}$ which we encountered in Subsection 5.1 is needed. For the purpose of comparison, we use two benchmark sets of such results for these quantities [68]: the JLQCD results for two flavours of dynamical light Wilson quarks [139], and a combination of f_{B_d} as determined by the HPQCD Collaboration [140] for three dynamical flavours with the JLQCD result for $\hat{B}_{B_d}$ [(HP+JL)QCD] [141]. For the determination of the NP phase $\phi_d^{\mathrm{NP}} = \phi_d - \phi_d^{\mathrm{SM}}$, we use $\phi_d = (43 \pm 2)^\circ$ (see (168)), and fix the 'true' value of $\phi_d^{\mathrm{SM}} = 2\beta$ with the help of the data for tree processes. This can simply be done through the relations

$$\sin\beta = \frac{R_b \sin\gamma}{\sqrt{1 - 2R_b\cos\gamma + R_b^2}}, \quad \cos\beta = \frac{1 - R_b\cos\gamma}{\sqrt{1 - 2R_b\cos\gamma + R_b^2}} \tag{175}$$

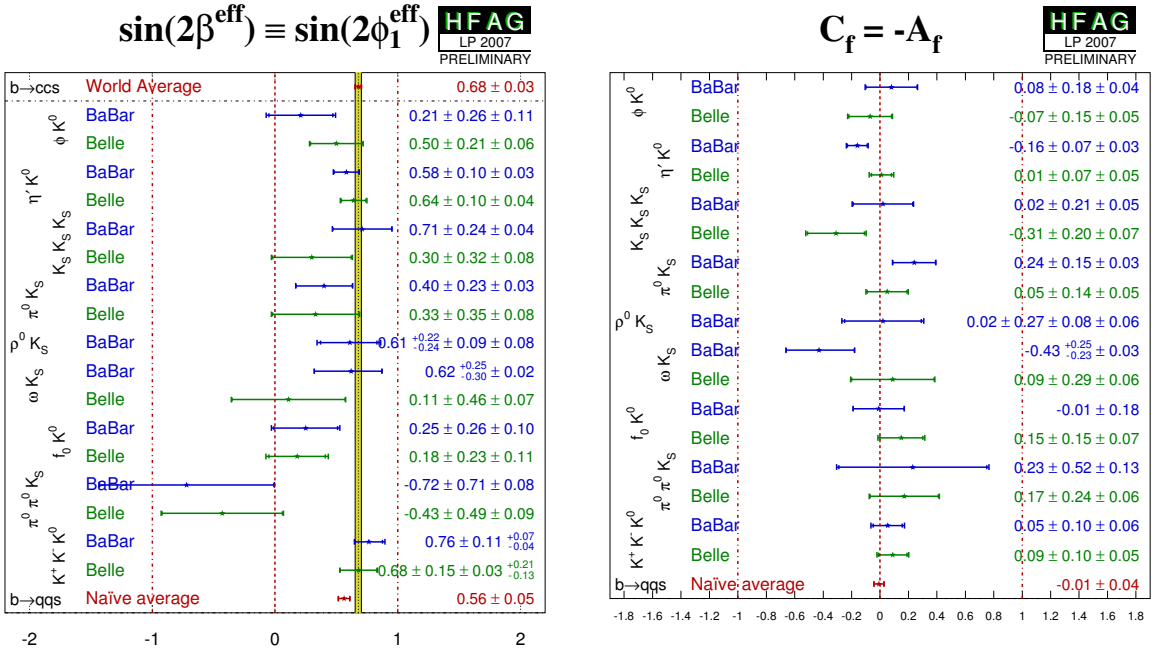

Fig. 23: Compilation of the CP violation measurements in B decays that are dominated by $b \to s$ penguin processes [69]: mixing-induced CP asymmetries (left panel), and direct CP asymmetries, where $C = \mathcal{A}_{\rm CP}^{\rm dir}$ (right panel).

between the side $R_b \propto |V_{ub}/V_{cb}|$ of the UT and its angle γ, which are determined through semileptonic $b \to u\ell\bar{\nu}_\ell$ decays and $B \to DK$ modes, respectively. A numerical analysis shows that the value of $\phi_d^{\rm NP}$ is actually governed by $R_b \propto |V_{ub}/V_{cb}|$, while $\gamma|_{D^{(*)}K^{(*)}}$, which suffers currently from large uncertainties as we saw in (107), plays only a minor rôle, in contrast to the SM analysis of ΔM_d [68]. However, the values of R_b in (73) following from the analyses of inclusive and exclusive decays differ at the $1\,\sigma$ level. We show the resulting situation in the σ_d–κ_d plane in Fig. 21, and observe that the measurement of CP violation in $B_d^0 \to J/\psi K_{\rm S}$ and similar decays has a dramatic impact on the allowed region in the NP parameter space; the right panel may indicate the presence of NP, although no definite conclusions can be drawn at the moment. It will be interesting to monitor this effect in the future. In order to detect such CP-violating NP contributions, which would immediately rule out MFV scenarios, things are much more promising in the B_s system, as we shall see in Subsection 8.2.

7 Puzzling patterns in the B-factory data

7.1 CP violation in $b \to s$ penguin modes

A particularly interesting probe of NP is offered by the decay $B_d^0 \to \phi K_{\rm S}$. As can be seen in Fig. 22, it originates from $\bar{b} \to \bar{s}s\bar{s}$ transitions and is, therefore, a pure penguin mode. This decay is described by the low-energy effective Hamiltonian in (81) with $r = s$, where the current–current operators may only contribute through penguin-like contractions, which describe penguin topologies with internal up- and charm-quark exchanges [76, 79]. The dominant rôle is played by the QCD penguin operators [142]. However, thanks to the large top-quark mass, EW penguins have a sizeable impact as well [79, 143]. In the SM, we may write

$$A(B_d^0 \to \phi K_{\rm S}) = \lambda_u^{(s)} \tilde{A}_{\rm P}^{u'} + \lambda_c^{(s)} \tilde{A}_{\rm P}^{c'} + \lambda_t^{(s)} \tilde{A}_{\rm P}^{t'}, \tag{176}$$

where we have applied the same notation as in Subsection 5.6. Eliminating the CKM factor $\lambda_t^{(s)}$ with the help of (80) yields

$$A(B_d^0 \to \phi K_{\rm S}) \propto \left[1 + \lambda^2 b e^{i\Theta} e^{i\gamma}\right], \tag{177}$$

where

$$b e^{i\Theta} \equiv \left(\frac{R_b}{1-\lambda^2}\right)\left[\frac{\tilde{A}_{\rm P}^{u'} - \tilde{A}_{\rm P}^{t'}}{\tilde{A}_{\rm P}^{c'} - \tilde{A}_{\rm P}^{t'}}\right]. \tag{178}$$

Consequently, we obtain

$$\xi_{\phi K_{\rm S}}^{(d)} = +e^{-i\phi_d}\left[\frac{1 + \lambda^2 b e^{i\Theta} e^{-i\gamma}}{1 + \lambda^2 b e^{i\Theta} e^{+i\gamma}}\right]. \tag{179}$$

The theoretical estimates of $be^{i\Theta}$ suffer from large hadronic uncertainties. However, since this parameter enters (179) in a doubly Cabibbo-suppressed way, we obtain the following expressions [144]:

$$\mathcal{A}_{\rm CP}^{\rm dir}(B_d \to \phi K_{\rm S}) = 0 + \mathcal{O}(\lambda^2) \tag{180}$$

$$\mathcal{A}_{\rm CP}^{\rm mix}(B_d \to \phi K_{\rm S}) = -\sin\phi_d + \mathcal{O}(\lambda^2), \tag{181}$$

where we made the plausible assumption that $b = \mathcal{O}(1)$. On the other hand, the mixing-induced CP asymmetry of $B_d \to J/\psi K_{\rm S}$ measures also $-\sin\phi_d$, as we saw in (164). We arrive therefore at the following relation [144, 145]:

$$-(\sin 2\beta)_{\phi K_{\rm S}} \equiv \mathcal{A}_{\rm CP}^{\rm mix}(B_d \to \phi K_{\rm S}) = \mathcal{A}_{\rm CP}^{\rm mix}(B_d \to J/\psi K_{\rm S}) + \mathcal{O}(\lambda^2), \tag{182}$$

which offers an interesting test of the SM. Since $B_d \to \phi K_{\rm S}$ is governed by penguin processes in the SM, this decay may well be affected by NP. In fact, if we assume that NP arises generically in the TeV regime, it can be shown through field-theoretical estimates that the NP contributions to $b \to s\bar{s}s$ transitions may well lead to sizeable violations of (180) and (182) [135, 137]. Moreover, this is also the case for several specific NP scenarios.

The experimental status can be summarized through the following averages [69]:

$$(\sin 2\beta)_{\phi K_{\rm S}} = 0.39 \pm 0.17, \quad \mathcal{A}_{\rm CP}^{\rm dir}(B_d \to \phi K_{\rm S}) = -0.01 \pm 0.12. \tag{183}$$

During recent years, the Belle results for $(\sin 2\beta)_{\phi K_{\rm S}}$ [146] have moved quite a bit towards the SM reference value of $(\sin 2\beta)_{\psi K_{\rm S}}$ given in (167), and are now, within the errors, in agreement with the BaBar findings [147]. Interestingly, the mixing-induced CP asymmetries of other $b \to s$ penguin modes show the same trend of having central values that are smaller than 0.681, as can be seen in Fig. 23 [69]. This feature may in fact be due to the presence of NP contributions to the corresponding decay amplitudes. However, the large uncertainties do not yet allow us to draw definite conclusions.

7.2 The $B \to \pi K$ puzzle

Another hot topic is the exploration of $B \to \pi K$ decays, which are also $b \to s$ transitions. Since tree amplitudes are suppressed by a CKM factor $\lambda^2 R_b \sim 0.02$ with respect to the penguin amplitudes, these decays are actually dominated by QCD penguins. A classification of the $B \to \pi K$ system is offered by their EW penguin contributions (see Fig. 24):

(a) In the $B_d^0 \to \pi^- K^+$ and $B^+ \to \pi^+ K^0$ decays, EW penguins contribute in colour-suppressed form and are hence expected to play a minor rôle.

(b) In the $B_d^0 \to \pi^0 K^0$ and $B^+ \to \pi^0 K^+$ decays, EW penguins contribute in colour-allowed form and have therefore a significant impact on the decay amplitude, entering at the same order of magnitude as the tree contributions, i.e. at the 20% level.

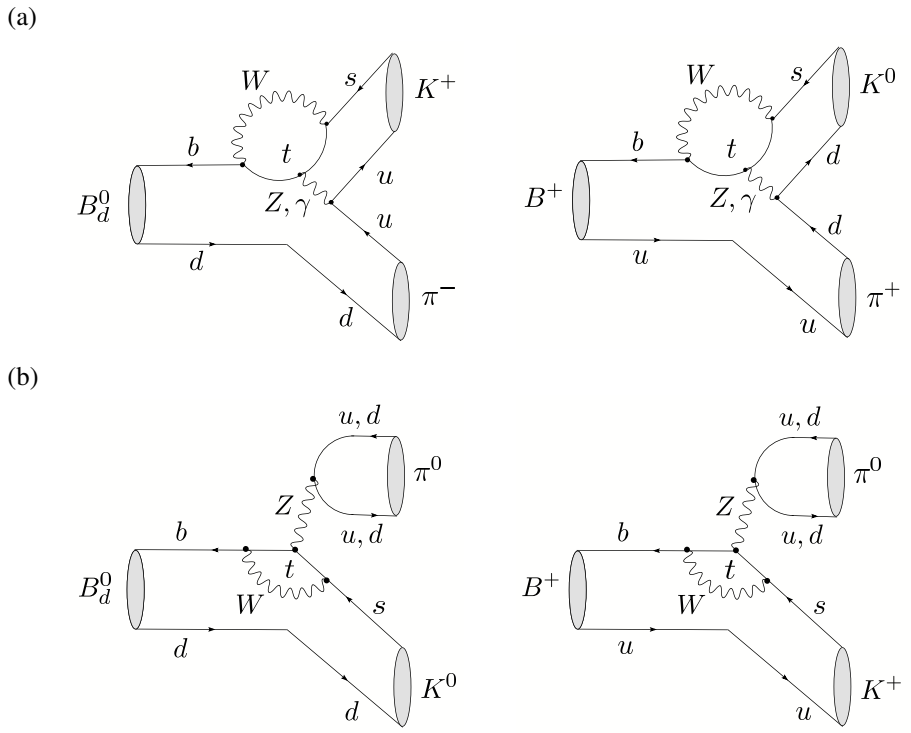

Fig. 24: Examples of the colour-suppressed (a) and colour-allowed (b) EW penguin contributions to the $B \to \pi K$ system

Interestingly, EW penguins offer an attractive avenue for NP to enter the $B \to \pi K$ system [148], and the B-factory data for decays of class (b) raise indeed the possibility of having a modified EW penguin sector through the impact of NP, which has received a lot of attention in the literature (see, e.g., Ref. [149]).

Here we shall discuss key results of the recent analysis performed in Ref. [150], following closely the strategy developed in Refs. [90, 91, 103]. The starting point is given by $B \to \pi\pi$ modes. Using the $SU(3)$ flavour symmetry of strong interactions and another plausible dynamical assumption,[4] the data for the $B \to \pi\pi$ system can be converted into the hadronic parameters of the $B \to \pi K$ modes, thereby allowing us to calculate their observables in the SM. Moreover, also γ can be extracted, with the result

$$\gamma = \left(70.0^{+3.8}_{-4.3}\right)^\circ, \tag{184}$$

which is in agreement with the SM fits of the UT [44, 45].

As far as the $B \to \pi K$ observables with tiny EW penguin contributions are concerned, perfect agreement between the SM expectation and the experimental data is found. Concerning the $B \to \pi K$ observables receiving sizeable contributions from EW penguins, we distinguish between CP-conserving and CP-violating observables. In the former case, the key quantities are given by the following ratios of CP-averaged $B \to \pi K$ branching ratios [151]:

$$R_{\rm c} \equiv 2\left[\frac{\mathrm{BR}(B^+ \to \pi^0 K^+) + \mathrm{BR}(B^- \to \pi^0 K^-)}{\mathrm{BR}(B^+ \to \pi^+ K^0) + \mathrm{BR}(B^- \to \pi^- \bar{K}^0)}\right] = 1.11 \pm 0.07 \tag{185}$$

$$R_{\rm n} \equiv \frac{1}{2}\left[\frac{\mathrm{BR}(B_d^0 \to \pi^- K^+) + \mathrm{BR}(\bar{B}_d^0 \to \pi^+ K^-)}{\mathrm{BR}(B_d^0 \to \pi^0 K^0) + \mathrm{BR}(\bar{B}_d^0 \to \pi^0 \bar{K}^0)}\right] = 0.99 \pm 0.07, \tag{186}$$

where also the experimental averages are indicated [69]. In these quantities, the EW penguin effects enter in colour-allowed form through the modes involving neutral pions, and are theoretically described by a

[4] Consistency checks of these working assumptions can be performed, which are all supported by the current data.

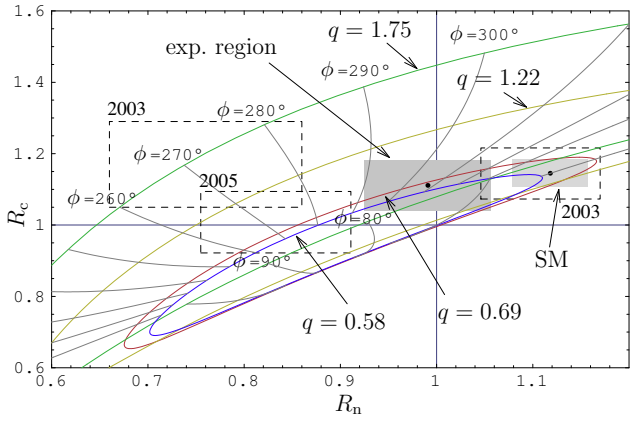

Fig. 25: The situation in the $R_{\rm n}$–$R_{\rm c}$ plane, as discussed in the text

parameter q, which measures the 'strength' of the EW penguin with respect to the tree contributions, and a CP-violating phase ϕ. In the SM, the $SU(3)$ flavour symmetry allows a prediction of $q = 0.60$ [152], and ϕ *vanishes*. However, in the case of CP-violating NP effects in the EW penguin sector, ϕ would take a value different from zero. In Fig. 25, we show the situation in the $R_{\rm n}$–$R_{\rm c}$ plane. Here the various contours correspond to different values of q, and the position on the contour is parametrized through the CP-violating phase ϕ. We observe that the SM prediction (on the right-hand side) is very stable in time, having now significantly reduced errors. On the other hand, the B-factory data have moved quite a bit towards the SM, thereby reducing the '$B \to \pi K$ puzzle' for the CP-averaged branching ratios, which emerged already in 2000 [153]. In comparison with the situation of the $B \to \pi K$ observables with tiny EW penguin contributions, the agreement between the new data for the $R_{\rm c,n}$ and their SM predictions is not as perfect. However, a case for a modified EW penguin sector cannot be made through the new measurements of these quantities.

Let us now have a closer look at the CP asymmetries of the $B^0_d \to \pi^0 K_{\rm S}$ and $B^\pm \to \pi^0 K^\pm$ channels. As can be seen in Fig. 26, SM predictions for the CP-violating observables of $B^0_d \to \pi^0 K_{\rm S}$ are obtained that are much sharper than the current B-factory data. In particular $\mathcal{A}_{\rm CP}^{\rm mix}(B_d \to \pi^0 K_{\rm S})$ offers a very interesting quantity. We also see that the experimental central values can be reached for large *positive* values of ϕ. For the new input data, the non-vanishing difference

$$\Delta A \equiv \mathcal{A}_{\rm CP}^{\rm dir}(B^\pm \to \pi^0 K^\pm) - \mathcal{A}_{\rm CP}^{\rm dir}(B_d \to \pi^\mp K^\pm) \stackrel{\rm exp}{=} -0.140 \pm 0.030 \tag{187}$$

is likely to be generated through hadronic effects, i.e. not through the impact of physics beyond the SM. A similar conclusion was drawn in Ref. [154], where it was also noted that the measured values of $R_{\rm c}$ and $R_{\rm n}$ are now in accordance with the SM.

Performing, finally, a simultaneous fit to $R_{\rm n}$, $R_{\rm c}$ and the CP-violating $B_d \to \pi^0 K_{\rm S}$ asymmetries yields the following result:

$$q = 1.7^{+0.5}_{-1.3}, \quad \phi = +\left(73^{+6}_{-18}\right)^\circ . \tag{188}$$

Interestingly, these parameters — in particular the large *positive* phase — would also allow us to accommodate the experimental values of $(\sin 2\beta)_{\phi K_{\rm S}}$ and the CP asymmetries of other $b \to s$ penguin modes with central values smaller than $(\sin 2\beta)_{\psi K_{\rm S}}$. The large central value of q would be excluded by constraints from rare decays in simple scenarios where NP enters only through Z penguins, but could still be accommodated in other scenarios, e.g. in models with leptophobic Z' bosons.

7.3 Prospects for LHCb

Unfortunately, it is unlikely that the current B factories will allow us to establish — or rule out — the tantalizing option of having NP in the $b \to s$ penguin processes. However, at LHCb, this exciting topic

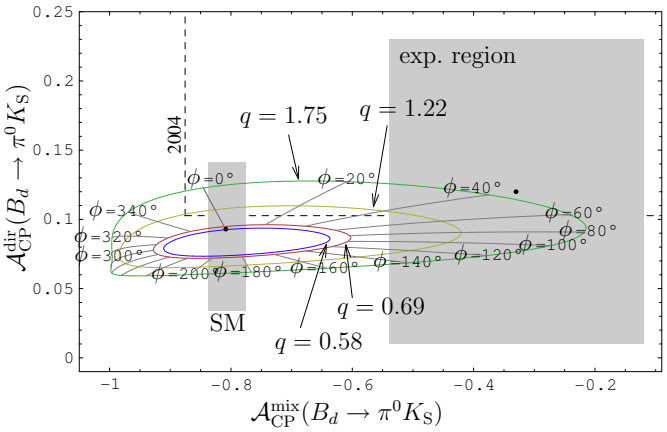

Fig. 26: The situation in the $\mathcal{A}_{\rm CP}^{\rm mix}(B_d \to \pi^0 K_{\rm S})$–$\mathcal{A}_{\rm CP}^{\rm dir}(B_d \to \pi^0 K_{\rm S})$ plane, as discussed in the text

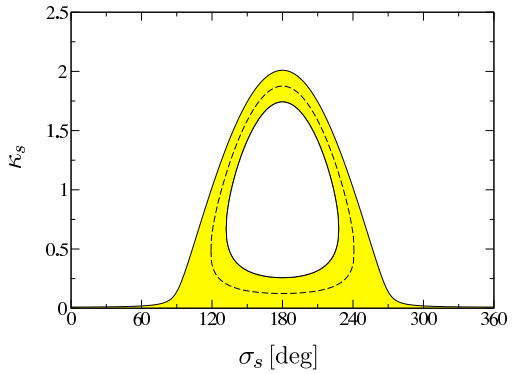

Fig. 27: The allowed region in the σ_s–κ_s plane of NP parameters for B_s^0–$\bar{B}_s^0$ mixing

can be explored with the help of the decay $B_s^0 \to \phi\phi$ [155]. A handful of events were observed in this mode a few years ago by the CDF Collaboration at the Tevatron, corresponding to a branching ratio of $(14^{+6}_{-5} \pm 6) \times 10^{-6}$ [156]. A proposal for studying time and angular dependence in this decay mode has been made by the LHCb Collaboration [157]. The proposal is based on an estimated sample of about 3100 events collected in one year of running. In order to control hadronic uncertainties, the decay mode $B_s \to \phi\phi$ may be related through the $SU(3)$ flavour symmetry to $B_s \to \phi\bar{K}^{*0}$ and plausible dynamical assumptions, which can be checked through experimental control channels [155]. The current B-factory data on the CP asymmetries of the $b \to s$ penguin modes leave ample space for NP phenomena in the $B_s^0 \to \phi\phi$ decay to be discovered at LHCb. Let us next have a closer look at other key targets of the physics programme of this experiment.

8 Highlights of B-physics at the LHC

Since the current e^+e^- B factories run at the $\Upsilon(4S)$ resonance, which decays into $B_{u,d}$, but not into B_s mesons, the B_s system cannot be explored by the BaBar and Belle experiments.[5] However, plenty of B_s mesons are produced at hadron colliders, i.e. at the Tevatron and soon at the LHC. The B-decay programme at the LHC is characterized by its high statistics and the complementarity to the studies at the e^+e^- B factories; in particular, the physics potential of the B_s-meson system, which offers various powerful strategies for the exploration of CP violation, can be fully exploited.

[5]The asymmetric e^+e^- KEKB collider was recently also operated at the $\Upsilon(5S)$ resonance, allowing the Belle experiment to take first B_s data [7].

8.1 In Pursuit of new physics with ΔM_s

As we discussed in Subsection 5.2, the mass difference ΔM_s of the B_s-meson system was recently measured at the Tevatron, with the results summarized in (129). On the other hand, the HPQCD Collaboration has reported the following lattice QCD prediction [158]:

$$\Delta M_s^{\rm SM} = 20.3(3.0)(0.8)\,{\rm ps}^{-1}. \tag{189}$$

In contrast to the case of ΔM_d discussed in Subsection 6.3, the CKM factor entering this SM value does not require information on γ and $|V_{ub}/V_{cb}|$, as

$$|V_{ts}^* V_{tb}| = |V_{cb}| \left[1 + \mathcal{O}(\lambda^2)\right], \tag{190}$$

which is an important advantage. Using (174), we may convert the experimental value of ΔM_s into the allowed region in the σ_s–κ_s plane shown in Fig. 27 [68]. We see that the measurement of ΔM_s leaves ample space for the NP parameters σ_s and κ_s, which can also be accommodated in specific scenarios (e.g. SUSY, extra Z' and little Higgs models). It should be noted that the experimental errors are already significantly smaller than the theoretical lattice QCD uncertainties. The experimental results on ΔM_s have immediately triggered a lot of theoretical activity (see, e.g., [68, 159, 160]).

As in the case of the B_d-meson system, the allowed region in the σ_s–κ_s plane will be dramatically reduced as soon as measurements of CP violation in the B_s-meson system become available. The 'golden' channel in this respect is $B_s^0 \to J/\psi\phi$, our next topic.

8.2 The decay $B_s^0 \to J/\psi\phi$

This mode is the counterpart of the $B_d^0 \to J/\psi K_{\rm S}$ transition, where we have just to replace the down quark by a strange quark. The structures of the corresponding decay amplitudes are completely analogous to each other. However, there is also an important difference with respect to $B_d^0 \to J/\psi K_{\rm S}$, since the final state of $B_s^0 \to J/\psi\phi$ contains two vector mesons and is, hence, an admixture of different CP eigenstates. Using the angular distribution of the $J/\psi[\to \ell^+\ell^-]\phi[\to\ K^+K^-]$ decay products, the CP eigenstates can be disentangled [161] and the time-dependent decay rates calculated [117, 124]. As in the case of $B_d^0 \to J/\psi K_{\rm S}$, the hadronic matrix elements cancel then in the mixing-induced observables. For the practical implementation, a set of three linear polarization amplitudes is usually used: $A_0(t)$ and $A_\parallel(t)$ correspond to CP-even final-state configurations, whereas $A_\perp(t)$ describes a CP-odd final-state configuration.

It is instructive to illustrate how this works by having a closer look at the one-angle distribution, which takes the following form [117, 124]:

$$\frac{d\Gamma(B_s^0(t) \to J/\psi\phi)}{d\cos\Theta} \propto \left(|A_0(t)|^2 + |A_\parallel(t)|^2\right)\frac{3}{8}\left(1+\cos^2\Theta\right) + |A_\perp(t)|^2\frac{3}{4}\sin^2\Theta. \tag{191}$$

Here Θ is defined as the angle between the momentum of the ℓ^+ and the normal to the decay plane of the K^+K^- system in the J/ψ rest frame. The time-dependent measurement of the angular dependence allows us to extract the following observables:

$$P_+(t) \equiv |A_0(t)|^2 + |A_\parallel(t)|^2, \quad P_-(t) \equiv |A_\perp(t)|^2, \tag{192}$$

where $P_+(t)$ and $P_-(t)$ refer to the CP-even and CP-odd final-state configurations, respectively. If we consider the case of having an initially, i.e. at time $t = 0$, present $\bar{B}_s^0$ meson, the CP-conjugate quantities $\bar{P}_\pm(t)$ can be extracted as well. Using an *untagged* data sample, the untagged rates

$$P_\pm(t) + \overline{P}_\pm(t) \propto \left[(1 \pm \cos\phi_s)e^{-\Gamma_{\rm L}t} + (1 \mp \cos\phi_s)e^{-\Gamma_{\rm H}t}\right] \tag{193}$$

can be determined, while a *tagged* data sample allows us to measure the CP-violating asymmetries

$$\frac{P_\pm(t)-\overline{P}_\pm(t)}{P_\pm(t)+\overline{P}_\pm(t)}=\pm\left[\frac{2\,\sin(\Delta M_s t)\sin\phi_s}{(1\pm\cos\phi_s)e^{+\Delta\Gamma_s t/2}+(1\mp\cos\phi_s)e^{-\Delta\Gamma_s t/2}}\right]. \tag{194}$$

In the presence of CP-violating NP contributions to B_s^0–$\bar{B}_s^0$ mixing, we obtain

$$\phi_s=-2\lambda^2\eta+\phi_s^{\rm NP}\approx-2^\circ+\phi_s^{\rm NP}\approx\phi_s^{\rm NP}. \tag{195}$$

Consequently, NP of this kind would be indicated by the following features:

- The *untagged* observables depend on *two* exponentials;
- *sizeable* values of the CP-violating asymmetries.

These general features hold also for the full three-angle distribution [117, 124]: it is much more involved than the one-angle case, but provides also additional information through interference terms of the form

$$\mathrm{Re}\{A_0^*(t)A_\parallel(t)\},\quad \mathrm{Im}\{A_f^*(t)A_\perp(t)\}\,(f\in\{0,\parallel\}). \tag{196}$$

From an experimental point of view, there is no experimental draw-back with respect to the one-angle case. Following these lines, $\Delta\Gamma_s$ (see (135)) and ϕ_s can be extracted. Recently, the D0 Collaboration reported first results for the measurement of ϕ_s through the untagged, time-dependent three-angle $B_s^0\to J/\psi\phi$ distribution [162]:

$$\phi_s=-0.79\pm0.56\,(\mathrm{stat.})^{+0.14}_{-0.01}\,(\mathrm{syst.})=-(45\pm32^{+1}_{-8})^\circ, \tag{197}$$

which is complemented by three additional mirror solutions. This phase is therefore not yet stringently constrained. Using (173), we then obtain the curves in the σ_s–κ_s plane shown in the left panel of Fig. 28. Very recently, CDF reported first bounds on ϕ_s from flavour-tagged $B_s^0\to J/\psi\phi$ decays [163].

Fortunately, ϕ_s will be very accessible at LHCb, where already the initial $0.5\,\mathrm{fb}^{-1}$ of data will give an uncertainty of $\sigma(\phi_s)=0.046=2.6^\circ$ by the end of 2009, which will be significantly improved further thanks to the $2\,\mathrm{fb}^{-1}$ that should be available by the end of 2010 [8]. At some point, also in view of LHCb upgrade plans [164], we have to include hadronic penguin uncertainties. This can be done with the help of the $B_d^0\to J/\psi\rho^0$ decay [165]. In order to illustrate the impact of the measurement of CP violation in $B_s^0\to J/\psi\phi$, we show in the right panel of Fig. 28 the case corresponding to $(\sin\phi_s)_{\rm exp}=-0.20\pm0.02$. Such a measurement would give a NP signal at the $10\,\sigma$ level, which would immediately rule out MFV models, and demonstrates the power of the B_s system to search for NP [68]. It should be emphasized that the contour following from the measurement of ϕ_s would be essentially clean, in contrast to the shaded region representing the constraint from the measured value of ΔM_s, which suffers from lattice QCD uncertainties.

8.3 Further benchmark decays for LHCb

This experiment has a very rich physics programme. Besides many other interesting aspects, there are two major lines of research:

1. Precision measurements of γ:
   On the one hand, there are strategies using tree decays: $B_s^0\to D_s^\mp K^\pm$ [$\sigma_\gamma\sim5^\circ$], $B_d^0\to D^0K^*$ [$\sigma_\gamma\sim8^\circ$], $B^\pm\to D^0K^\pm$ [$\sigma_\gamma\sim5^\circ$], where we have also indicated the expected sensitivities for $10\,\mathrm{fb}^{-1}$; by 2013, a LHCb tree determination of γ with $\sigma_\gamma=2^\circ\sim3^\circ$ should be available [8]. This very impressive situation should be compared with the current B-factory data, yielding the results summarized in (107). These extractions are essentially unaffected by NP effects. On the other hand, γ can also be determined through B decays with penguin contributions: $B_s^0\to K^+K^-$ and $B_d^0\to\pi^+\pi^-$ [$\sigma_\gamma\sim5^\circ$], $B_s^0\to D_s^+D_s^-$ and $B_d^0\to D_d^+D_d^-$. The key question is whether discrepancies will arise in these determinations.

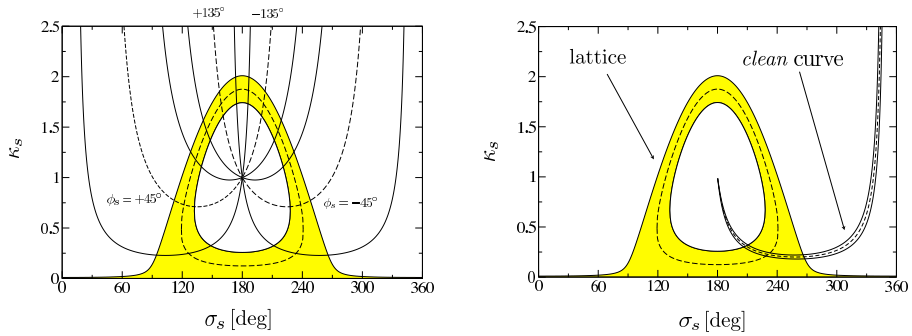

Fig. 28: Impact of the measurement of CP violation in $B_s^0 \to J/\psi\phi$: current D0 data (left panel), and a NP scenario with $(\sin\phi_s)_{\rm exp} = -0.20 \pm 0.02$ (right panel)

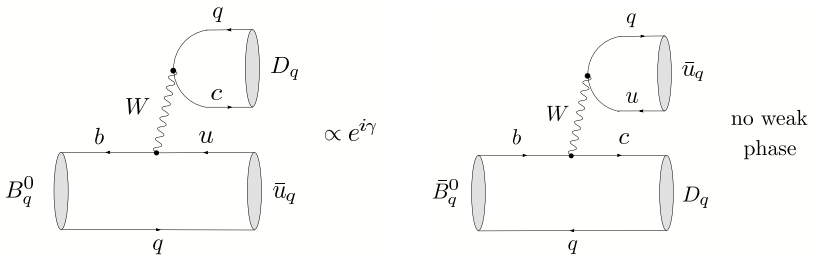

Fig. 29: Feynman diagrams contributing to $B_q^0 \to D_q\bar{u}_q$ and $\bar{B}_q^0 \to D_q\bar{u}_q$ decays

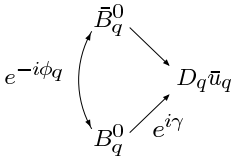

Fig. 30: Interference effects between $B_q^0 \to D_q\bar{u}_q$ and $\bar{B}_q^0 \to D_q\bar{u}_q$ decays

2. Analyses of rare decays, which are absent at the SM tree level: prominent examples are $B_{s,d}^0 \to \mu^+\mu^-$, $B_d^0 \to K^{*0}\mu^+\mu^-$ and $B_s^0 \to \phi\mu^+\mu^-$. In order to complement the studies of CP violation in $b \to s$ penguin modes at the B factories, $B_s^0 \to \phi\phi$ is a very interesting mode for LHCb, as we noted in Subsection 7.3.

Let us next have a closer look at some of these decays.

8.3.1 $B_s \to D_s^\pm K^\mp$ and $B_d \to D^\pm\pi^\mp$

The decays $B_s \to D_s^\pm K^\mp$ [166] and $B_d \to D^\pm\pi^\mp$ [167] can be treated on the same theoretical basis, and provide new strategies to determine γ [102]. Following this paper, we write these modes, which are pure 'tree' decays according to the classification of Subsection 3.3.1, generically as $B_q \to D_q\bar{u}_q$. As can be seen from the Feynman diagrams in Fig. 29, their characteristic feature is that both a B_q^0 and a $\bar{B}_q^0$ meson may decay into the same final state $D_q\bar{u}_q$. Consequently, as illustrated in Fig. 30, interference effects between B_q^0–$\bar{B}_q^0$ mixing and decay processes arise, which allow us to probe the weak phase $\phi_q+\gamma$ through measurements of the corresponding time-dependent decay rates.

In the case of $q = s$, i.e. $D_s \in \{D_s^+, D_s^{*+}, ...\}$ and $u_s \in \{K^+, K^{*+}, ...\}$, these interference effects are governed by a hadronic parameter $X_s e^{i\delta_s} \propto R_b \approx 0.4$, where $R_b \propto |V_{ub}/V_{cb}|$ is the usual UT side, and hence are large. On the other hand, for $q = d$, i.e. $D_d \in \{D^+, D^{*+}, ...\}$ and $u_d \in \{\pi^+, \rho^+, ...\}$, the

interference effects are described by $X_d e^{i\delta_d} \propto -\lambda^2 R_b \approx -0.02$, and hence are tiny.

Measuring the $\cos(\Delta M_q t)$ and $\sin(\Delta M_q t)$ terms of the time-dependent $B_q \to D_q \bar{u}_q$ rates, a theoretically clean determination of $\phi_q + \gamma$ is possible [166, 167]. Since the ϕ_q can be determined separately, as we saw above, γ can be extracted. However, in the practical implementation, there are problems: we encounter an eightfold discrete ambiguity for $\phi_q + \gamma$, which is very disturbing for the search of NP, and in the $q = d$ case, an additional input is required to extract X_d since $\mathcal{O}(X_d^2)$ interference effects would otherwise have to be resolved, which is impossible. Performing a combined analysis of the $B_s^0 \to D_s^+ K^-$ and $B_d^0 \to D^+ \pi^-$ decays, these problems can be solved [102]. This strategy exploits the fact that these transitions are related to each other through the U-spin symmetry of strong interactions,[6] allowing us to simplify the hadronic sector. Following these lines, an unambiguous value of γ can be extracted from the observables. To this end, X_d has actually not to be fixed, and X_s may only enter through a $1 + X_s^2$ correction, which is determined through untagged B_s rates. The first studies for LHCb are very promising, and are currently being further refined [168].

8.3.2 The $B_s \to K^+K^-$, $B_d \to \pi^+\pi^-$ system

As can be seen in Fig. 31, the decay $B_s^0 \to K^+K^-$ is a $\bar{b} \to \bar{s}$ transition that involves tree and penguin contributions. In analogy to the $B \to \pi K$ case discussed in Subsection 7.2, the latter topologies actually play the dominant rôle in $B_s^0 \to K^+K^-$. If we replace the strange quarks in Fig. 31 through down quarks, we obtain the decay topologies for the $B_d^0 \to \pi^+\pi^-$ channel shown in Fig. 32. However, because of the different CKM structure, the tree topologies play the dominant rôle in $B_d^0 \to \pi^+\pi^-$, although the QCD penguins have an important impact as well. Following the discussion of Subsections 5.6 and 7.1, we may write the corresponding decay amplitudes in the SM as follows [99]:

$$A(B_d^0 \to \pi^+\pi^-) \propto \left[e^{i\gamma} - de^{i\theta}\right] \tag{198}$$

$$A(B_s^0 \to K^+K^-) \propto \left[e^{i\gamma} + \left(\frac{1-\lambda^2}{\lambda^2}\right) d' e^{i\theta'}\right], \tag{199}$$

where the CP-conserving hadronic parameters $de^{i\theta}$ and $d'e^{i\theta'}$ describe — sloppily speaking — the ratios of penguin to tree contributions. The direct and mixing-induced CP asymmetries take then the following general form:

$$\mathcal{A}_{\rm CP}^{\rm dir}(B_d \to \pi^+\pi^-) = G_1(d, \theta; \gamma), \quad \mathcal{A}_{\rm CP}^{\rm mix}(B_d \to \pi^+\pi^-) = G_2(d, \theta; \gamma, \phi_d) \tag{200}$$

$$\mathcal{A}_{\rm CP}^{\rm dir}(B_s \to K^+K^-) = G_1'(d', \theta'; \gamma), \quad \mathcal{A}_{\rm CP}^{\rm mix}(B_s \to K^+K^-) = G_2'(d', \theta'; \gamma, \phi_s). \tag{201}$$

Since ϕ_d is already known and ϕ_s is negligibly small in the SM — or can be determined with the help of $B_s^0 \to J/\psi\phi$ should CP-violating NP contributions to B_s^0–$\bar{B}_s^0$ mixing make it sizeable — we may convert the measured values of $\mathcal{A}_{\rm CP}^{\rm dir}(B_d \to \pi^+\pi^-)$, $\mathcal{A}_{\rm CP}^{\rm mix}(B_d \to \pi^+\pi^-)$ and $\mathcal{A}_{\rm CP}^{\rm dir}(B_s \to K^+K^-)$, $\mathcal{A}_{\rm CP}^{\rm mix}(B_s \to K^+K^-)$ into *theoretically clean* contours in the γ–d and γ–d' planes, respectively. In Fig. 33, we show these contours (solid and dot-dashed) for an example, which is inspired by the current B-factory data.

Looking at the Feynman diagrams shown in Figs. 31 and 32, we see that $B_d^0 \to \pi^+\pi^-$ is actually related to $B_s^0 \to K^+K^-$ through the interchange of all down and strange quarks. Consequently, each decay topology contributing to $B_d^0 \to \pi^+\pi^-$ has a counterpart in $B_s^0 \to K^+K^-$ and vice versa, and the corresponding hadronic parameters can be related to each other with the help of the U-spin flavour symmetry of strong interactions, implying the following relations [99]:

$$d' = d, \quad \theta' = \theta. \tag{202}$$

[6] The U-spin symmerty is an $SU(2)$ subgroup of the $SU(3)_{\rm F}$ flavour-symmetry group of QCD, connecting d and s quarks in analogy to the isospin symmetry, which relates d and u quarks to each other.

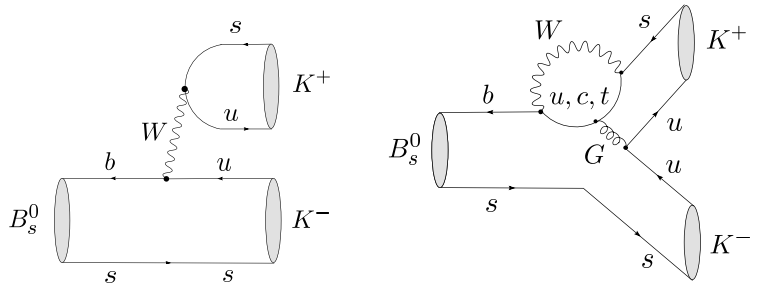

Fig. 31: Feynman diagrams contributing to the $B_s^0 \to K^+K^-$ decay

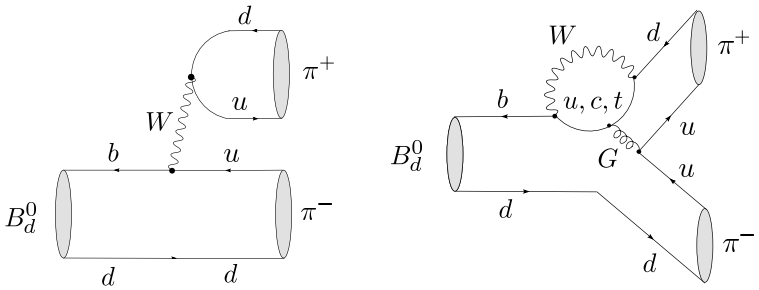

Fig. 32: Feynman diagrams contributing to the $B_d^0 \to \pi^+\pi^-$ decay

Applying the former, we may extract γ and d through the intersections of the theoretically clean γ–d and γ–d' contours. In the example of Fig. 33, a twofold ambiguity arises from the solid and dot-dashed curves. However, as discussed in Ref. [99], it can be resolved with the help of the dotted contour, thereby leaving us with the 'true' solution of $\gamma = 70^\circ$ in this case. Moreover, we may determine θ and θ', which allow an interesting internal consistency check of the second U-spin relation in (202).

This strategy is very promising from an experimental point of view for LHCb, where an accuracy for γ of a few degrees can be achieved [169]. As far as possible U-spin-breaking corrections to $d' = d$ are concerned, they enter the determination of γ through a relative shift of the γ–d and γ–d' contours; their impact on the extracted value of γ therefore depends on the form of these curves, which is fixed through the measured observables. In the examples discussed in Ref. [99] and Fig. 33, the extracted value of γ would be very stable with respect to such effects. It should also be noted that the U-spin relations in (202) are particularly robust since they involve only ratios of hadronic amplitudes, where all $SU(3)$-breaking decay constants and form factors cancel in factorization and also chirally enhanced terms would not lead to U-spin-breaking corrections [99].

A detailed analysis of the status and prospects of the $B_{s,d} \to \pi\pi, \pi K, KK$ system in view of the first results on the B_s modes from the Tevatron [170] was recently performed in Ref. [171]. Interestingly, the data for the $B_d \to \pi^+\pi^-$, $B_s \to K^+K^-$ system favour the BaBar measurement of the direct CP violation in $B_d \to \pi^+\pi^-$, which results in a fortunate situation for the extraction of γ, yielding $\gamma = (66.6^{+4.3+4.0}_{-5.0-3.0})^\circ$, where the latter errors correspond to an estimate of U-spin-breaking effects. An important further step will be the measurement of the mixing-induced CP violation in $B_s \to K^+K^-$, which is predicted in the SM as $\mathcal{A}_{\rm CP}^{\rm mix}(B_s \to K^+K^-) = -0.246^{+0.036+0.052}_{-0.030-0.024}$, where the second errors illustrate the impact of large non-factorizable U-spin-breaking corrections. In the case of CP-violating NP contributions to B_s^0–$\bar{B}_s^0$ mixing also this observable would be sensitively affected, as can be seen in Fig. 34, and allows an unambiguous determination of the B_s^0–$\bar{B}_s^0$ mixing phase with the help of $B_s \to J/\psi\phi$ at LHCb. Finally, the measurement of the direct CP violation in the $B_s \to K^+K^-$ channel will make the full exploitation of the physics potential of the $B_{s,d} \to \pi\pi, \pi K, KK$ modes possible.

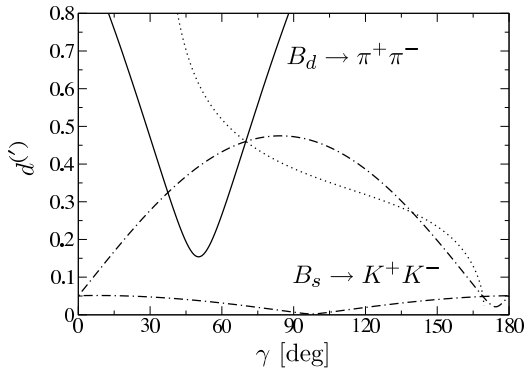

Fig. 33: The contours in the γ–$d^{(\prime)}$ plane for an example corresponding to the CP asymmetries $\mathcal{A}_{\rm CP}^{\rm dir}(B_d \to \pi^+\pi^-) = -0.24$ and $\mathcal{A}_{\rm CP}^{\rm mix}(B_d \to \pi^+\pi^-) = +0.59$, as well as $\mathcal{A}_{\rm CP}^{\rm dir}(B_s \to K^+K^-) = +0.09$ and $\mathcal{A}_{\rm CP}^{\rm mix}(B_s \to K^+K^-) = -0.23$

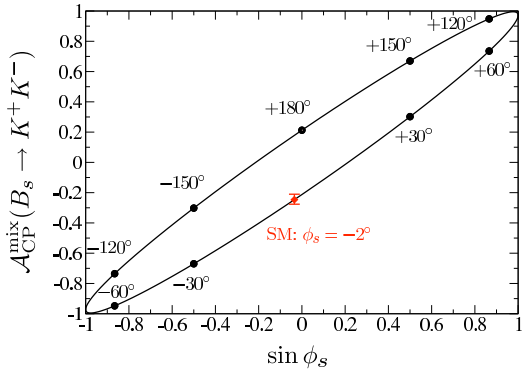

Fig. 34: The correlation between $\sin\phi_s$, which can be determined through mixing-induced CP violation in $B_s^0 \to J/\psi\phi$, and $\mathcal{A}_{\rm CP}^{\rm mix}(B_s \to K^+K^-)$. Each point on the curve corresponds to a given value of ϕ_s, as indicated by the numerical values [171].

8.3.3 The rare decays $B_s^0 \to \mu^+\mu^-$ and $B_d^0 \to \mu^+\mu^-$

As can be seen in Fig. 35, these decays originate from Z^0-penguin and box diagrams in the SM. The corresponding low-energy effective Hamiltonian is given as follows [74]:

$$\mathcal{H}_{\rm eff} = -\frac{G_{\rm F}}{\sqrt{2}}\left[\frac{\alpha}{2\pi\sin^2\Theta_{\rm W}}\right] V_{tb}^* V_{tq}\, \eta_Y Y_0(x_t)\, (\bar{b}q)_{\rm V-A}(\bar{\mu}\mu)_{\rm V-A} \;+\; \text{h.c.}, \tag{203}$$

where α denotes the QED coupling and $\Theta_{\rm W}$ is the Weinberg angle. The short-distance physics is described by $Y(x_t) \equiv \eta_Y Y_0(x_t)$, where $\eta_Y = 1.012$ is a perturbative QCD correction, and the Inami–Lim function $Y_0(x_t)$ describes the top-quark mass dependence. We observe that only the matrix element $\langle 0|(\bar{b}q)_{\rm V-A}|B_q^0\rangle$ is required. Since here the vector-current piece vanishes, as the B_q^0 is a pseudoscalar meson, this matrix element is simply given by the decay constant f_{B_q}. Consequently, we arrive at a very favourable situation with respect to the hadronic matrix elements. Since, moreover, NLO QCD corrections were calculated, and long-distance contributions are expected to play a negligible rôle [172], the $B_q^0 \to \mu^+\mu^-$ modes belong to the cleanest rare B decays.

Using also the data for the mass differences ΔM_q to reduce the hadronic uncertainties,[7] the following SM predictions were obtained in Ref. [160]:

$$\text{BR}(B_s \to \mu^+\mu^-) \;=\; (3.35 \pm 0.32) \times 10^{-9} \tag{204}$$

[7] This input allows us to replace the decay constants f_{B_q} through the bag parameters $\hat{B}_{B_q}$.

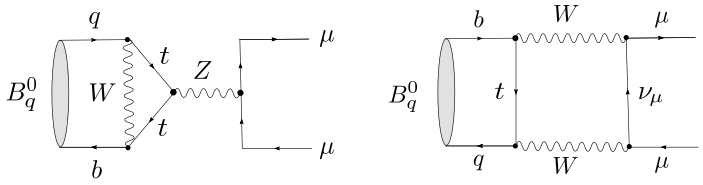

Fig. 35: Feynman diagrams contributing to $B_q^0 \to \mu^+\mu^-$ ($q \in \{s, d\}$) decays

$$\text{BR}(B_d \to \mu^+\mu^-) \quad = \quad (1.03 \pm 0.09) \times 10^{-10}. \tag{205}$$

Consequently, these branching ratios are extremely tiny. But things could actually be much more exciting, as NP effects may significantly enhance $\text{BR}(B_s \to \mu^+\mu^-)$ [9]. The current upper bounds (95% C.L.) from the CDF Collaboration read as follows [173]:

$$\text{BR}(B_s \to \mu^+\mu^-) < 5.8 \times 10^{-8}, \quad \text{BR}(B_d \to \mu^+\mu^-) < 1.8 \times 10^{-8}, \tag{206}$$

while the D0 Collaboration finds the following 90% C.L. (95% C.L.) upper limit [174]:

$$\text{BR}(B_s \to \mu^+\mu^-) < 7.5\ (9.3) \times 10^{-8}. \tag{207}$$

Consequently, there is still a long way to go within the SM. However, by the end of 2009, with $0.5\,\text{fb}^{-1}$ data, LHCb can exclude or discover a NP contribution to $B_s \to \mu^+\mu^-$ at the level of the SM [8]. This decay is also very interesting for ATLAS and CMS, where detailed signal and background studies are currently in progress [120].

8.3.4 The rare decay $B_d^0 \to K^{*0}\mu^+\mu^-$

The key observable for NP searches through this channel is the following forward–backward asymmetry:

$$A_{\rm FB}(\hat{s}) = \frac{1}{{\rm d}\Gamma/{\rm d}\hat{s}} \left[\int_0^{+1} {\rm d}(\cos\theta) \frac{{\rm d}^2\Gamma}{{\rm d}\hat{s}\,{\rm d}(\cos\theta)} - \int_{-1}^{0} {\rm d}(\cos\theta) \frac{{\rm d}^2\Gamma}{{\rm d}\hat{s}\,{\rm d}(\cos\theta)}\right]. \tag{208}$$

Here θ is the angle between the B_d^0 momentum and that of the μ^+ in the dilepton centre-of-mass system, and $\hat{s} \equiv s/M_B^2$ with $s = (p_{\mu^+} + p_{\mu^-})^2$. A particularly interesting kinematical point is characterized by

$$A_{\rm FB}(\hat{s}_0)|_{\rm SM} = 0, \tag{209}$$

as $\hat{s}_0$ is quite robust with respect to hadronic uncertainties (see, e.g., Ref. [175]). In SUSY extensions of the SM, $A_{\rm FB}(\hat{s})$ could take opposite sign or take a dependence on $\hat{s}$ without a zero point [176]. The current B-factory data for the inclusive $b \to s\ell^+\ell^-$ branching ratios and the integrated forward–backward asymmetries are in accordance with the SM, but suffer still from large uncertainties. This situation will improve dramatically at the LHC. Here LHCb will measure the zero crossing point by $\sim$ 2013 with $10\,\text{fb}^{-1}$ with $\sigma(s_0) = 0.27(\text{GeV}/c^2)^2$, corresponding to 19k events [8]. For other interesting observables provided by $B_d^0 \to K^{*0}\mu^+\mu^-$, see Ref. [177]. Also alternative $b \to s\mu^+\mu^-$ modes are currently under study, such as $B_s^0 \to \phi\mu^+\mu^-$ and $\Lambda_b \to \Lambda\mu^+\mu^-$ [8, 120].

9 Conclusions and outlook

In this decade, we have seen tremendous progress in the exploration of the phenomenology of flavour physics and CP violation that was made possible through a fruitful interplay between theory and experiment. Altogether, the e^+e^- B factories have already produced $\mathcal{O}(10^9)$ $B\bar{B}$ pairs, and the Tevatron has recently succeeded in observing B_s^0–$\bar{B}_s^0$ mixing. Thanks to these efforts, CP violation is now well

established in the B-meson system, thereby complementing the neutral K-meson system, where this unexpected effect was discovered almost 45 years ago. The B-factory data agree globally with the KM mechanism of CP violation in an impressive way, but we have also hints for possible discrepancies, which could be the first footprints of NP in the quark-flavour sector. Unfortunately, definite conclusions cannot yet be drawn as the uncertainties are still too large.

Exciting new perspectives for B physics and the exploration of CP violation will arise in the summer of 2008 through the start of the LHC, with its dedicated B-decay experiment LHCb. Thanks to the large statistics that can be collected there and the full exploitation of the physics potential of the B_s-meson system, we shall be able to enter a new territory in the investigation of CP violation. The golden channel for the search of CP-violating NP contributions to B_s^0–$\bar{B}_s^0$ mixing is $B_s^0 \to J/\psi\phi$, where the recent measurement of ΔM_s still leaves ample space for such effects both in terms of the general NP parameters and in specific extensions of the SM. In contrast to the theoretical interpretation of ΔM_s, the corresponding CP asymmetries have not to rely on non-perturbative lattice QCD calculations. Moreover, it will be very interesting to search for CP-violating NP effects in $b \to s$ penguin processes through the $B_s^0 \to \phi\phi$ channel. These measurements will be complemented by other key ingredients for the search of NP: precision measurements of the UT angle γ by means of various processes with a very different dynamics, and powerful analyses of rare B decays.

In addition to B physics, which was the focus of this lecture, there are other important flavour probes. An outstanding example is charm physics, where evidence for D^0–$\bar{D}^0$ mixing was found at the B factories in the spring of 2007 [178], and very recently also at CDF [179]. The mixing parameters are measured in the ball park of the SM predictions, which are unfortunately affected by large long-distance effects. A striking NP signal would be given by CP-violating effects (for recent theoretical analyses, see, e.g. Ref. [180]). There is also a powerful charm-physics programme at LHCb. As far as kaon physics is concerned, the future lies on the extremely rare decays $K^+ \to \pi^+\nu\bar{\nu}$ and $K_{\rm L} \to \pi^0\nu\bar{\nu}$: these are very clean from the theoretical point of view, but unfortunately hard to measure. Nevertheless, there is a proposal to take this challenge and to measure the former channel at the CERN SPS, and efforts to explore the latter — even more difficult decay — at J-PARC in Japan. Moreover, interesting flavour probes are offered by top physics and the flavour violation in the neutrino and charged lepton sectors; regarding the latter (for a recent overview, see Ref. [181]), an experimental investigation of the lepton flavour violating decay $\mu \to e\gamma$ is the target of the MEG experiment at PSI, and studies of $\mu \to e$ conversion are proposed at FNAL and J-PARC. Further studies in this direction using τ decays at the LHC and at a possible future super-B factory will be important. Finally, continued searches of electric dipole moments and measurements of the anomalous magnetic moment of the muon are essential parts of the future experimental programme, providing also a strong interplay with theory.

In view of the quickly approaching start of the LHC, there is a burning question: what is the synergy between the plenty of information following from analyses of the flavour sector with the high-Q^2 programme of ATLAS and CMS? The main goal of these experiments is to explore electroweak symmetry breaking, in particular the question of whether this is actually caused by the Higgs mechanism, to produce and observe new particles, which could themselves be the mediators of new flavour- and CP-violating interactions, and then to go back to the deep questions of particle physics, such as the origin of dark matter and the baryon asymmetry of the Universe. It is obvious that there should be a very fruitful interplay between these 'direct' studies of NP and the 'indirect' information provided by flavour physics [182]. I have no doubts that the next few years will be extremely exciting!

Acknowledgements

I would like to thank the students for their interest in my lectures, the discussion leaders for their efforts to complement them in the discussion sessions, and the local organizers — in particular Claudio Dib — for hosting this exciting school in Viña del Mar.

References

[1] J.H. Christenson *et al.*, Phys. Rev. Lett. **13** (1964) 138.

[2] V. Fanti *et al.* [NA48 Collaboration], Phys. Lett. **B465** (1999) 335;
A. Alavi-Harati *et al.* [KTeV Collaboration], Phys. Rev. Lett. **83** (1999) 22.

[3] J.R. Batley *et al.* [NA48 Collaboration], Phys. Lett. **B544** (2002) 97.

[4] A. Alavi-Harati *et al.* [KTeV Collaboration], Phys. Rev. **D67** (2003) 012005.

[5] B. Aubert *et al.* [BaBar Collaboration], Phys. Rev. Lett. **87** (2001) 091801;
K. Abe *et al.* [Belle Collaboration], Phys. Rev. Lett. **87** (2001) 091802.

[6] M. Bona *et al.*, arXiv:0709.0451 [hep-ex]; A. G. Akeroyd *et al.*, arXiv:hep-ex/0406071.

[7] K. Abe *et al.* [Belle Collaboration], hep-ex/0610003;
J. Wicht *et al.* [Belle Collaboration], arXiv:0712.2659 [hep-ex].

[8] T. Nakada, talk at 2nd Workshop on Flavour Dynamics, Albufeira, Portugal, 3–10 November 2007 [http://www.theorie.physik.uni-muenchen.de/lsfritzsch/albufeira/].

[9] G. Buchalla *et al.*, arXiv:0801.1833 [hep-ph], Report of Working Group 2 of the CERN Workshop "Flavour in the era of the LHC", Geneva, Switzerland, November 2005 – March 2007.

[10] C. Wagner, lecture given at this school.

[11] G. Barenboim, lecture given at this school.

[12] J. Ellis, lecture given at this school.

[13] A.D. Sakharov, JETP Lett. **5** (1967) 24.

[14] V.A. Rubakov and M.E. Shaposhnikov, Usp. Fiz. Nauk **166** (1996) 493; Phys. Usp. **39** (1996) 461;
A. Riotto and M. Trodden, Annu. Rev. Nucl. Part. Sci. **49** (1999) 35.

[15] For a recent review, see W. Buchmüller, R.D. Peccei and T. Yanagida, Annu. Rev. Nucl. Part. Sci. **55** (2005) 311.

[16] N. Cabibbo, Phys. Rev. Lett. **10** (1963) 531.

[17] M. Kobayashi and T. Maskawa, Prog. Theor. Phys. **49** (1973) 652.

[18] M. Battaglia *et al.*, CERN 2003-002-corr, *The CKM matrix and the unitarity triangle* (CERN, Geneva, 2003) [hep-ph/0304132].

[19] For a recent review, see A.J. Buras and M. Jamin, JHEP **0401** (2004) 048.

[20] L. Wolfenstein, Phys. Rev. Lett. **13** (1964) 562.

[21] A.J. Buras and R. Fleischer, Adv. Ser. Direct. High Energy Phys. **15** (1998) 65.

[22] G. Branco, L. Lavoura and J. Silva, *CP Violation*, International Series of Monographs on Physics 103, Oxford Science Publications (Clarendon Press, Oxford, 1999).

[23] I.I. Bigi and A.I. Sanda, *CP Violation*, Cambridge Monographs on Particle Physics, Nuclear Physics and Cosmology (Cambridge University Press, Cambridge, 2000).

[24] T. Mannel, Springer Tracts Mod. Phys. **203** (2004) 1.

[25] A.J. Buras, lectures given at 2004 European School of High-Energy Physics, Sant Feliu de Guixols, Barcelona, Spain, 30 May – 12 June 2004, R. Fleischer (ed.), CERN-2006-003 [hep-ph/0505175].

[26] I.I. Bigi, lectures given at 2006 European School of High-Energy Physics, Aronsborg, Sweden, 18 June – 1 July 2006, R. Fleischer (ed.), CERN-2007-005 [hep-ph/0701273].

[27] Y. Nir, arXiv:0708.1872 [hep-ph], lectures given at 2nd Workshop on Monte Carlo Tools for Beyond the Standard Model Physics (MC4BSM), Princeton, New Jersy, 23–24 March 2007 and at the 2nd Joint Fermilab–CERN Hadron Collider Physics Summer School, CERN, Geneva, Switzerland, 6–15 June 2007.

[28] A. Ali, arXiv:0712.1022 [hep-ph].

[29] M. Gronau, Int. J. Mod. Phys. **A22** (2007) 1953.

[30] A. Höcker and Z. Ligeti, Annu. Rev. Nucl. Part. Sci. **56** (2006) 501.

[31] S.L. Glashow, Nucl. Phys. **22** (1961) 579;
S. Weinberg, Phys. Rev. Lett. **19** (1967) 1264;
A. Salam, in *Elementary Particle Theory*, ed. N. Svartholm (Almqvist and Wiksell, Stockholm, 1968).

[32] A. Pich, lecture given at this school, arXiv:0705.4264 [hep-ph].

[33] S.L. Glashow, J. Iliopoulos and L. Maiani, Phys. Rev. **D2** (1970) 1285.

[34] S. Eidelman *et al.* [Particle Data Group], Phys. Lett. **B592** (2004) 1.

[35] C. Jarlskog, Phys. Rev. Lett. **55** (1985) 1039; Z. Phys. **C29** (1985) 491.

[36] J. Bernabeu, G. Branco and M. Gronau, Phys. Lett. **B169** (1986) 243.

[37] W.M. Yao *et al.* [Particle Data Group], J. Phys. **G33** (2006) 1.

[38] L. Wolfenstein, Phys. Rev. Lett. **51** (1983) 1945.

[39] A.J. Buras, M.E. Lautenbacher and G. Ostermaier, Phys. Rev. **D50** (1994) 3433.

[40] A.J. Buras, hep-ph/0101336, lectures given at Erice International School of Subnuclear Physics: Theory and Experiment Heading for New Physics, Erice, Italy, 27 August – 5 September 2000.

[41] R. Aleksan, B. Kayser and D. London, Phys. Rev. Lett. **73** (1994) 18.

[42] C. Jarlskog and R. Stora, Phys. Lett. **B208** (1988) 268.

[43] L.L. Chau and W.-Y. Keung, Phys. Rev. Lett. **53** (1984) 1802.

[44] J. Charles *et al.* [CKMfitter Group], Eur. Phys. J. C **41** (2005) 1; for the most recent updates, see http://ckmfitter.in2p3.fr/.

[45] M. Bona *et al.* [UTfit Collaboration], JHEP **0507** (2005) 028; for the most recent updates, see http://utfit.roma1.infn.it/.

[46] B. Kopeliovich, lectures given at this school.

[47] A. Khodjamirian, lectures given at the 2003 European School on High-Energy Physics, Tsakhkadzor, Armenia, 24 August – 6 September 2003, A.G. Olshevskii (ed.), CERN-2005-007 [hep-ph/0403145].

[48] M. Lüscher, Annales Henri Poincare **4** (2003) S197 [hep-ph/0211220]; PoS **LAT2005** (2006) 002.

[49] C.T. Sachrajda, AIP Conf. Proc. **842** (2006) 198.

[50] M. Della Morte, PoS **LAT2007**, 008 (2007).

[51] F. De Fazio, hep-ph/0010007.

[52] K. Ikado *et al.*, Phys. Rev. Lett. **97** (2006) 251802.

[53] B. Aubert *et al.* [BaBar Collaboration], hep-ex/0608019.

[54] W.S. Hou, Phys. Rev. **D48** (1993) 2342.

[55] T.E. Browder, Nucl. Phys. Proc. Suppl. **163** (2007) 117.

[56] D.G. Cassel, eConf **C0304052** (2003) WG501 [hep-ex/0307038].

[57] C. Davies, plenary talk at HEP2005 Europhysics Conference, Lisbon, Portugal, 21–27 July 2005, http://www.lip.pt/events/2005/hep2005/.

[58] C. Aubin *et al.*, Phys. Rev. Lett. **95** (2005) 122002.

[59] M. Artuso *et al.* [CLEO Collaboration], Phys. Rev. Lett. **95** (2005) 251801.

[60] J.L. Rosner and S. Stone, arXiv:0802.1043 [hep-ex].

[61] N. Isgur and M.B. Wise, Phys. Lett. **B232** (1989) 113 and **B237** (1990) 527.

[62] M. Neubert, Phys. Rep. **245** (1994) 259.

[63] *The BaBar Physics Book*, eds. P. Harrison and H.R. Quinn, SLAC-R-504 (1998).

[64] M. Neubert, Phys. Lett. **B264** (1991) 455.

[65] M.E. Luke, Phys. Lett. **B252** (1990) 447.

[66] P. Gambino and N. Uraltsev, Eur. Phys. J. **C34** (2004) 181.

[67] O. Buchmüller and H. Flächer, Phys. Rev. **D73** (2006) 073008.

[68] P. Ball and R. Fleischer, Eur. Phys. J. **C48** (2006) 413.

[69] Heavy Flavour Averaging Group [E. Barberio *et al.*], arXiv:0704.3575 [hep-ex]; for online updates, see http://www.slac.stanford.edu/xorg/hfag.

[70] M. Okamoto *et al.*, Nucl. Phys. Proc. Suppl. **140** (2005) 461;
E. Gulez *et al.*, Phys. Rev. **D73** (2006) 074502.

[71] A. Khodjamirian *et al.*, Phys. Rev. **D62** (2000) 114002;
P. Ball and R. Zwicky, JHEP **0110** (2001) 019; Phys. Rev. **D71** (2005) 014015; Phys. Rev. **D71** (2005) 014029; Phys. Lett. **B625** (2005) 225.

[72] E. Blucher *et al.*, hep-ph/0512039.

[73] F.J. Gilman and M.B. Wise, Phys. Rev. **D20** (1979) 2392;
G. Altarelli, G. Curci, G. Martinelli and S. Petrarca, Phys. Lett. **B99** (1981) 141;
A.J. Buras and P.H. Weisz, Nucl. Phys. **B333** (1990) 66.

[74] G. Buchalla, A.J. Buras and M.E. Lautenbacher, Rev. Mod. Phys. **68** (1996) 1125.

[75] M. Bander, D. Silverman and A. Soni, Phys. Rev. Lett. **43** (1979) 242.

[76] R. Fleischer, Z. Phys. **C58** (1993) 483.

[77] A.J. Buras and R. Fleischer, Phys. Lett. **B341** (1995) 379.

[78] M. Ciuchini, E. Franco, G. Martinelli, M. Pierini and L. Silvestrini, Phys. Lett. **B515** (2001) 33;
C. Isola, M. Ladisa, G. Nardulli, T.N. Pham and P. Santorelli, Phys. Rev. **D65** (2002) 094005;
C.W. Bauer, D. Pirjol, I.Z. Rothstein and I.W. Stewart, Phys. Rev. **D70** (2004) 054015.

[79] R. Fleischer, Z. Phys. **C62** (1994) 81; Phys. Lett. **B321** (1994) 259 and **B332** (1994) 419.

[80] R. Fleischer, Int. J. Mod. Phys. **A12** (1997) 2459.

[81] N.G. Deshpande and X.-G. He, Phys. Rev. Lett. **74** (1995) 26 [E: ibid., p. 4099];
M. Gronau, O.F. Hernandez, D. London and J.L. Rosner, Phys. Rev. **D52** (1995) 6374.

[82] R. Fleischer, Phys. Lett. **B365** (1996) 399.

[83] M. Neubert, B. Stech, Adv. Ser. Direct. High Energy Phys. **15** (1998) 294, and references therein.

[84] A.J. Buras and J.-M. Gérard, Nucl. Phys. **B264** (1986) 371;
A.J. Buras, J.-M. Gérard and R. Rückl, Nucl. Phys. **B268** (1986) 16.

[85] M. Beneke, G. Buchalla, M. Neubert and C. Sachrajda, Phys. Rev. Lett. **83** (1999) 1914; Nucl. Phys. **B591** (2000) 313; Nucl. Phys. **B606** (2001) 245.

[86] J.D. Bjorken, Nucl. Phys. (Proc. Suppl.) **B11** (1989) 325;
M. Dugan and B. Grinstein, Phys. Lett. **B255** (1991) 583;
H.D. Politzer and M.B. Wise, Phys. Lett. **B257** (1991) 399.

[87] H.-n. Li and H.L. Yu, Phys. Rev. **D53** (1996) 2480;
Y.Y. Keum, H.-n. Li and A.I. Sanda, Phys. Lett. **B504** (2001) 6;
Y.Y. Keum and H.-n. Li, Phys. Rev. **D63** (2001) 074006;
A. Ali *et al.*, Phys. Rev. **D76** (2007) 074018.

[88] C.W. Bauer, D. Pirjol and I.W. Stewart, Phys. Rev. Lett. **87** (2001) 201806;
C.W. Bauer, B. Grinstein, D. Pirjol and I.W. Stewart, Phys. Rev. **D67** (2003) 014010.

[89] A. Khodjamirian, Nucl. Phys. **B605** (2001) 558;
A. Khodjamirian, T. Mannel and B. Melic, Phys. Lett. **B571** (2003) 75.

[90] A.J. Buras, R. Fleischer, S. Recksiegel and F. Schwab, Phys. Rev. Lett. **92** (2004) 101804.

[91] A.J. Buras, R. Fleischer, S. Recksiegel and F. Schwab, Nucl. Phys. **B697** (2004) 133.

[92] A. Ali, E. Lunghi and A.Y. Parkhomenko, Eur. Phys. J. **C36** (2004) 183.

[93] C.W. Chiang, M. Gronau, J.L. Rosner and D.A. Suprun, Phys. Rev. **D70** (2004) 034020.

[94] B. Aubert *et al.* [BaBar Collaboration], Phys. Rev. Lett. **93** (2004) 131801;
Y. Chao *et al.* [Belle Collaboration], Phys. Rev. Lett. **93** (2004) 191802.

[95] M. Gronau and D. Wyler, Phys. Lett. **B265** (1991) 172.

[96] D. Atwood, I. Dunietz, A. Soni, Phys. Rev. Lett. **78** (1997) 3257; Phys. Rev. **D63** (2001) 036005.

[97] R. Fleischer and D. Wyler, Phys. Rev. **D62** (2000) 057503.

[98] M. Gronau, J.L. Rosner and D. London, Phys. Rev. Lett. **73** (1994) 21;
M. Gronau, O.F. Hernandez, D. London and J.L. Rosner, Phys. Rev. **D50** (1994) 4529.

[99] R. Fleischer, Phys. Lett. **B459** (1999) 306.

[100] A.B. Carter and A.I. Sanda, Phys. Rev. Lett. **45** (1980) 952; Phys. Rev. **D23** (1981) 1567;
I.I. Bigi and A.I. Sanda, Nucl. Phys. **B193** (1981) 85.

[101] G. Cavoto, R. Fleischer, K. Trabelsi and J. Zupan, arXiv:0706.4227 [hep-ph].

[102] R. Fleischer, Nucl. Phys. **B671** (2003) 459.

[103] A.J. Buras, R. Fleischer, S. Recksiegel and F. Schwab, Eur. Phys. J. **C45** (2006) 701.

[104] F. Abe *et al.* [CDF Collaboration], Phys. Rev. Lett. **81** (1998) 2432.

[105] D0 Collaboration, D0 Note 4539-CONF (August 2004).

[106] D. Acosta *et al.* [CDF Collaboration], Phys. Rev. Lett. **96** (2006) 082002.

[107] M. Masetti, Phys. Lett. **B286** (1992) 160.

[108] M.A. Ivanov, J.G. Körner and O.N. Pakhomova, Phys. Lett. **B555** (2003) 189.

[109] T. Inami and C.S. Lim, Prog. Theor. Phys. **65** (1981) 297 [E: ibid., p. 1772].

[110] S. Laplace, Z. Ligeti, Y. Nir and G. Perez, Phys. Rev. **D65** (2002) 094040.

[111] M. Beneke, G. Buchalla, A. Lenz and U. Nierste, Phys. Lett. **B576** (2003) 173;
M. Ciuchini, E. Franco, V. Lubicz, F. Mescia and C. Tarantino, JHEP **0308** (2003) 031.

[112] B Oscillations Working Group: `http://lepbosc.web.cern.ch/LEPBOSC/`.

[113] V.M. Abazov *et al.* [D0 Collaboration], Phys. Rev. Lett. **97** (2006) 021802;
A. Abulencia *et al.* [CDF Collaboration], Phys. Rev. Lett. **97** (2006) 062003.

[114] The D0 Collaboration, D0 Note 5474-conf (2007) [http://www-d0.fnal.gov].

[115] A. Abulencia *et al.* [CDF Collaboration], Phys. Rev. Lett. **97** (2006) 242003.

[116] A. Lenz, arXiv:0710.0940 [hep-ph].

[117] A.S. Dighe, I. Dunietz and R. Fleischer, Eur. Phys. J. **C6** (1999) 647.

[118] V.M. Abazov *et al.* [D0 Collaboration], Phys. Rev. Lett. **98** (2007) 121801.

[119] T. Aaltonen *et al.* [CDF Collaboration], arXiv:0712.2348 [hep-ex].

[120] A. Krasznahorkay, "Outlook for B physics at the LHC in ATLAS and CMS," in the proceedings of DIS 2007, Munich, Germany, 16–20 April 2007.

[121] I. Dunietz, Phys. Rev. **D52** (1995) 3048.

[122] R. Fleischer and I. Dunietz, Phys. Rev. **D55** (1997) 259.

[123] R. Fleischer and I. Dunietz, Phys. Lett. **B387** (1996) 361.

[124] I. Dunietz, R. Fleischer and U. Nierste, Phys. Rev. **D63** (2001) 114015.

[125] R. Fleischer, Eur. Phys. J. **C10** (1999) 299.

[126] R. Fleischer and T. Mannel, Phys. Lett. **B506** (2001) 311.

[127] H. Boos, T. Mannel and J. Reuter, Phys. Rev. **D70** (2004) 036006.

[128] M. Ciuchini, M. Pierini and L. Silvestrini, Phys. Rev. Lett. **95** (2005) 221804.

[129] P. Ball *et al.*, hep-ph/0003238, in *CERN Workshop on Standard Model physics (and more) at the LHC*, 25–26 May 1999, CERN-2000-004 (CERN, Geneva, 2000), p. 305.

[130] R. Fleischer and J. Matias, Phys. Rev. **D66** (2002) 054009.

[131] R. Fleischer, G. Isidori and J. Matias, JHEP **0305** (2003) 053.

[132] A.J. Buras, Springer Proc. Phys. **98** (2005) 315.

[133] A.J. Buras, P. Gambino, M. Gorbahn, S. Jäger and L. Silvestrini, Phys. Lett. **B500** (2001) 161.

[134] G. D'Ambrosio, G.F. Giudice, G. Isidori and A. Strumia, Nucl. Phys. **B645** (2002) 155.

[135] R. Fleischer, Phys. Rep. **370** (2002) 537.

[136] For reviews, see, for instance, A. Ali, hep-ph/0412128;
G. Isidori, AIP Conf. Proc. **722** (2004) 181;
M. Misiak, Acta Phys. Polon. **B34** (2003) 4397;
T. Hurth, Rev. Mod. Phys. **75** (2003) 1159.

[137] R. Fleischer and T. Mannel, Phys. Lett. **B511** (2001) 240.

[138] R. Fleischer, J. Phys. **G32** (2006) R71.

[139] S. Aoki *et al.* [JLQCD Collaboration], Phys. Rev. Lett. **91** (2003) 212001.

[140] A. Gray *et al.* [HPQCD Collaboration], Phys. Rev. Lett. **95** (2005) 212001.

[141] M. Okamoto, PoS **LAT2005** (2005) 013.

[142] D. London and R.D. Peccei, Phys. Lett. **B223** (1989) 257;
N.G. Deshpande and J. Trampetic, Phys. Rev. **D41** (1990) 895 and 2926;
J.-M. Gérard and W.-S. Hou, Phys. Rev. **D43** (1991) 2909; Phys. Lett. **B253** (1991) 478.

[143] N.G. Deshpande and X.-G. He, Phys. Lett. **B336** (1994) 471.

[144] R. Fleischer, Int. J. Mod. Phys. **A12** (1997) 2459.

[145] Y. Grossman and M.P. Worah, Phys. Lett. **B395** (1997) 241.

[146] K.F. Chen *et al.* [Belle Collaboration], Phys. Rev. Lett. **98** (2007) 031802.

[147] B. Aubert *et al.* [BaBar Collaboration], Phys. Rev. Lett. **99** (2007) 161802.

[148] R. Fleischer and T. Mannel, hep-ph/9706261;
Y. Grossman, M. Neubert and A.L. Kagan, JHEP **9910** (1999) 029.

[149] T. Yoshikawa, Phys. Rev. **D68** (2003) 054023;
M. Gronau and J.L. Rosner, Phys. Lett. **B572** (2003) 43;
M. Beneke and M. Neubert, Nucl. Phys. **B675** (2003) 333;
V. Barger, C.W. Chiang, P. Langacker and H.S. Lee, Phys. Lett. **B598** (2004) 218;
Y.L. Wu and Y.F. Zhou, Phys. Rev. **D72** (2005) 034037.

[150] R. Fleischer, S. Recksiegel and F. Schwab, Eur. Phys. J. **C51** (2007) 55.

[151] A.J. Buras and R. Fleischer, Eur. Phys. J. **C11** (1999) 93.

[152] M. Neubert and J.L. Rosner, Phys. Rev. Lett. **81** (1998) 5076.

[153] A.J. Buras and R. Fleischer, Eur. Phys. J. **C16** (2000) 97.

[154] M. Gronau and J.L. Rosner, Phys. Rev. **D74** (2006) 057503; Phys. Lett. **B644** (2007) 237.

[155] R. Fleischer and M. Gronau, Phys. Lett. **B660** (2008) 212.

[156] D. Acosta *et al.* [CDF Collaboration], Phys. Rev. Lett. **95** (2005) 031801.

[157] S. Amato *et al.*, CERN-LHCb-2007-047.

[158] E. Dalgic *et al.* [HPQCD Collaboration], Phys. Rev. **D76** (2007) 011501.

[159] M. Carena *et al.*, Phys. Rev. **D74** (2006) 015009;
M. Ciuchini and L. Silvestrini, Phys. Rev. Lett. **97** (2006) 021803;
M. Endo and S. Mishima, Phys. Lett. **B640** (2006) 205;
Z. Ligeti, M. Papucci and G. Perez, Phys. Rev. Lett. **97** (2006) 101801;
J. Foster, K.I. Okumura and L. Roszkowski, Phys. Lett. **B641** (2006) 452;
Y. Grossman, Y. Nir and G. Raz, Phys. Rev. Lett. **97** (2006) 151801;
S. Baek, J.H. Jeon and C.S. Kim, Phys. Lett. **B641** (2006) 183;

M. Blanke and A.J. Buras, JHEP **0705** (2007) 061.

[160] M. Blanke, A.J. Buras, D. Guadagnoli and C. Tarantino, JHEP **0610** (2006) 003.

[161] A.S. Dighe, I. Dunietz, H. Lipkin and J.L. Rosner, Phys. Lett. **B369** (1996) 144.

[162] V. M. Abazov *et al.* [D0 Collaboration], Phys. Rev. Lett. **98** (2007) 121801.

[163] T. Aaltonen *et al.* [CDF Collaboration], arXiv:0712.2397 [hep-ex].

[164] F. Muheim, Nucl. Phys. Proc. Suppl. **170** (2007) 317.

[165] R. Fleischer, Phys. Rev. **D60** (1999) 073008.

[166] R. Aleksan, I. Dunietz and B. Kayser, Z. Phys. **C54** (1992) 653.

[167] I. Dunietz and R.G. Sachs, Phys. Rev. **D37** (1988) 3186 [E: **D39** (1989) 3515];
I. Dunietz, Phys. Lett. **B427** (1998) 179;
D.A. Suprun, C.W. Chiang and J.L. Rosner, Phys. Rev. **D65** (2002) 054025.

[168] G. Wilkinson, in G. Cavoto *et al.*, Proceedings of CKM 2005 (WG5), San Diego, California, 15–18 March 2005 [hep-ph/0603019]; V. Gligorov and G. Wilkinson, work in progress.

[169] G. Balbi *et al.*, CERN-LHCb/2003-123 and 124; R. Antunes Nobrega *et al.* [LHCb Collaboration], *Reoptimized LHCb Detector, Design and Performance*, Technical Design Report 9, CERN/LHCC 2003-030; A. Carbone, J. Nardulli, S. Pennazzi, A. Sarti and V. Vagnoni, CERN-LHCb-2007-059.

[170] A. Abulencia *et al.* [CDF Collaboration], Phys. Rev. Lett. **97** (2006) 211802; CDF Note 8579 (2006).

[171] R. Fleischer, Eur. Phys. J. **C52** (2007) 267.

[172] G. Buchalla and A.J. Buras, Nucl. Phys. **B400** (1993) 225 and **B548** (1999) 309;
M. Misiak and J. Urban, Phys. Lett. **B451** (1999) 161.

[173] T. Aaltonen *et al.* [CDF Collaboration], arXiv:0712.1708 [hep-ex].

[174] D0 Collaboration, D0 Note 5344-CONF (2007) [http://www-d0.fnal.gov].

[175] G. Burdman, Phys. Rev. **D57** (1998) 4254;
M. Beneke, T. Feldmann and D. Seidel, Eur. Phys. J. **C41** (2005) 173;
A. Ali, G. Kramer and G. h. Zhu, Eur. Phys. J. C **47** (2006) 625.

[176] A. Ali, P. Ball, L.T. Handoko and G. Hiller, Phys. Rev. **D61** (2000) 074024.

[177] F. Krüger and J. Matias, Phys. Rev. **D71** (2005) 094009;
E. Lunghi and J. Matias, JHEP **0704** (2007) 058.

[178] B. Aubert *et al.* [BABAR Collaboration], Phys. Rev. Lett. **98** (2007) 211802;
M. Staric *et al.* [Belle Collaboration], Phys. Rev. Lett. **98** (2007) 211803.

[179] T. Aaltonen *et al.* [CDF Collaboration], arXiv:0712.1567 [hep-ex].

[180] Y. Nir, JHEP **0705** (2007) 102 (2007);
E. Golowich, J. Hewett, S. Pakvasa and A.A. Petrov, Phys. Rev. **D76** (2007) 095009.

[181] M. Raidal *et al.*, arXiv:0801.1826 [hep-ph], Report of Working Group 3 of the CERN Workshop "Flavour in the era of the LHC", Geneva, Switzerland, November 2005 – March 2007.

[182] These topics were addressed at the CERN Workshop "Flavour in the era of the LHC", November 2005 – March 2007 [http://flavlhc.web.cern.ch/flavlhc/].